SEMMELWEIS EGYETEM

DOKTORI ISKOLA

Ph.D. értekezések

3222.

NARIMAN ESSMAT MOHAMED ABDELTAWAB GOMAA

Experimentális és klinikai farmakológia

című program

Programvezető: Dr. Szökő Éva, egyetemi tanár

Témavezető: Dr. Al-Khrasani Mahmoud, egyetemi docens

TOLPERISONE-PREGABALIN-BASED APPROACH FOR NEUROPATHIC PAIN MANAGEMENT AND MORPHINE TOLERANCE

Ph.D. thesis

Nariman Essmat Mohamed Abdeltawab Gomaa

Pharmaceutical Sciences and Health Technologies Division

Semmelweis University

Supervisor: Mahmoud Al-Khrasani, Pharm.D., Ph.D.
Official reviewers: Zupkó István, Pharm.D., D.Sc.
Papp Noémi, Pharm.D., Ph.D.

Head of Complex Examination Committee: Benyó Zoltán, MD, DSc.
Members of Complex Examination Committee: Miklya Ildikó, Pharm.D., Ph.D.
Kitka Tamás, Ph.D.

Budapest
2025

List of Abbreviations

AMPA: Amino-3- hydroxy-5-methyl-4-isoxazole propionate

b.l.: Baseline

CaM-KII: Calcium calmodulin-dependent protein kinase II

cAMP: Cyclic adenosine monophosphate

CBZ: Carbamazepine

CGRP: Calcitonin gene-related peptide

CNS: Central nervous system

CREB: Cyclic adenosine monophosphate response element binding protein

CSF: Cerebrospinal fluid

CYP: Cytochrome P450

DH: Dorsal horn

DPA: Dynamic plantar esthesiometer

DRG: Dorsal root ganglia

DR-VRP: Dorsal root stimulation-evoked ventral root potentials

DUL: Duloxetine

ERK: Extracellular signal-regulated kinase

GABA: Gamma-aminobutyric Acid

GI: Gastrointestinal

IASP: International Association for the Study of Pain

MAPK) Mitogen-activated protein kinase pathway

Mg^{2+}: Magnesium

mGluR: Metabotropic (G-protein coupled) glutamate receptor

Morph: Morphine

MORs: μ-opioid receptors

MPE: Maximum possible effect

MVD: Mouse vas deferens

NK1: Neurokinin 1

nM: Nanomolar

NMDA: N-methyl-D-aspartate

NNT: Number needed to treat

NP: Neuropathic pain

PAG: Ventrolateral periaqueductal gray

PDPN: Painful diabetic polyneuropathy

PGB: Pregabalin

PI3K: Phosphatidylinositol-3-kinase

PKA: Protein kinase A

PKC: Protein kinase C

pSNL: Partial sciatic nerve ligation

PWTs: Paw withdrawal thresholds

R: Right

RVM: Rostral ventromedial medulla

s.c.: Subcutaneous

S.E.M.: Standard error of means

SNRI: serotonin and norepinephrine reuptake inhibitor

STZ: Streptozotocin

TCAs: Tricyclic antidepressants

TOLP: Tolperisone

TrkB: Tyrosine receptor kinase B

TRPV1: Transient receptor potential cation channel subfamily V member 1

VGCCs: Voltage-gated calcium channels

VGSCs: Voltage-gated sodium channels

1. Introduction

1.1. Neuropathic Pain

Pain can be physiological in nature, acting as an early warning system to protect our bodies from various harmful stimuli. Inflammatory pain is the term used to describe pain that accompanies tissue damage surrounding the nociceptors. It has adaptive and protective properties, but responds to a low pain threshold. On the other hand, pain resulting from damage or dysfunction in the somatosensory system is called neuropathic pain (NP), a type of pathological pain that is maladaptive rather than protective (1). NP is a debilitating disease, and its treatment has not been fully solved thus far. The International Association for the Study of Pain (IASP) defined NP as pain resulting from damage or diseases affecting the somatosensory nervous system at the peripheral or central nervous system (CNS) or both (2). NP presents with a variety of symptoms, including two distinct manifestations: allodynia and hyperalgesia (3). According to the definition issued by IASP, allodynia is pain due to a stimulus that does not normally provoke pain. For instance, a light touch or gentle pressure may be perceived as painful. Hyperalgesia refers to an increased sensitivity to pain. In this case, stimuli that are usually painful are experienced as being even more intense (4). According to estimates, the incidence of NP varies between 7% and 10% worldwide. However, this prevalence rises to approximately 20% to 30% in diabetic patients (5). In general, chronic pain affects 20% of the European population and 100 million American citizens (6,7). This prevalence even outpaces the number of individuals with diabetes mellitus, heart disease, or cancer. The treatment options that are currently being used by healthcare to manage NP are unfortunately severely limited by their poor efficacy and tolerability (8). In this regard, less than 50% of patients respond to the current medications, leaving about 40% of patients inadequately treated and about 30% with no relief at all (9–12). NP is classified into peripheral and central types or mixed (13). Peripheral NP conditions encompass peripheral nerve injury-induced NP, postherpetic neuralgia, trigeminal neuralgia, painful radiculopathy, chemotherapy-induced peripheral neuropathy, and NP caused by carpal tunnel syndrome (13,14). Central NP includes pain associated with spinal cord injury, brain injury, post-stroke pain, and pain associated with multiple sclerosis (13,14). Peripheral NP is further classified into mono- and poly-neuropathic pain types. Mononeuropathy affects one peripheral nerve and is caused by compression or trauma,

such as carpal tunnel syndrome, radial nerve palsy, or peroneal nerve palsy (15). Polyneuropathy affects many nerves where up to 50% of cases are idiopathic or may be induced by disease or toxin such as diabetes mellitus, alcohol abuse, human immunodeficiency viruses, porphyria, amyloidosis, vitamin B12 or folate deficiency, Guillain-Barré syndrome, and chemotherapeutic agents as cisplatin or oxaliplatin, among others (15).

With respect to painful diabetic polyneuropathy (PDPN), it affects 30%–50% of patients where pain is caused by dysfunction of the somatosensory system attributed to diabetes mellitus (16). Recent data issued by the International Diabetes Federation have reported that 537 million people are currently suffering from diabetes, and the situation is even worse as it is predicted that this estimate will increase to 643 and 783 million by 2030 and 2045, respectively. Based on that, as many as 270 million people with diabetes worldwide may be affected by PDPN (17). NP treatment is challenging due to complex symptoms, poor outcomes, and difficult treatment decisions. It significantly reduces patients' quality of life, which is reflected by a decrease in the productivity of the patients that contributes largely to socio-economic cost, yet the need for more medications and frequent healthcare visits further exacerbates the social burden (18). Therefore, developing non-addictive novel medications and treatment approaches or repurposing existing medications with adequate analgesia of fast onset and tolerable side effects is a profound challenge in pain research.

1.2. Molecular Mechanisms Attributed to Neuropathic Pain Development

Peripheral and central molecular mechanisms are implicated in the development of NP. Peripheral neuropathy is developed as a result of damage to the peripheral pain-sensing neurons, causing changes in pain transduction, amplification, and conduction. Not to mention that afferent primary sensory neurons are exposed to inflammatory mediators and medications or toxins that are circulating in the blood due to their location. With respect to central neuropathy, the implication of both spinal and supraspinal targets is well established (19,20). Functional changes were observed in central targets that have been reported to govern the ascending and descending pain processing pathways. The pain pathway is a complex process influenced by neuronal, hormonal, and immunological factors, highlighting its multifaceted nature. Pain stimuli are transmitted by primary afferent sensory neurons, unmyelinated C fibers, and small myelinated Aδ. The C fibers

host polymodal nociceptors responding to thermal, mechanical, and chemical noxious stimuli and carry pain of different stimuli (heat, chemicals, mechanical), whereas the later convey pain of high-threshold mechanoreceptors and cold from the peripheral sensory receptors to the dorsal part of spinal cord, specifically Rexed's laminae I and II (21). As a matter of fact, diseases or nerve injury can be associated with changes in pain perception and processing that enter the dorsal horn (DH) of the spinal cord and travel up to the brainstem, thalamus, somatosensory cortex, insular cortex, and anterior cingulate cortex, among other supraspinal structures (22–24). It is worth noting that, under NP, two fundamental structural, functional, and chemical changes take place, namely peripheral and central sensitization. These states contribute to the generation of pain in response to normally innocuous stimuli. In fact, despite superficial similarities, the molecular mechanisms behind central sensitization and its manifestation are significantly different from those of peripheral sensitization. Peripheral sensitization involves increased excitability of sensory neurons, typically triggered by peripheral nerve injury, tissue damage, or inflammation. This process is driven by the release of pro-nociceptive mediators from immune cells like macrophages and mast cells, as well as from adjacent nerve endings. These mediators, including prostaglandins, histamine, bradykinin, serotonin, substance P, extracellular ATP, protons, growth factors, cytokines, chemokines, and peptides, interact with specific receptors and ion channels or alter their sensitivity to stimuli (25–27). Glutamate, the primary excitatory neurotransmitter at central synapses, also contributes to peripheral sensitization through non-synaptic mechanisms. It binds to amino-3-hydroxy-5-methyl-4-isoxazole propionate (AMPA) receptors and N-methyl-D-aspartate (NMDA) receptors located at peripheral nerve endings. This interaction supports peripheral cell-to-cell communication (e.g., upon release from immune cells) or autocrine regulation, as seen when glutamate is released from sensory nerve terminals following calcium influx mediated by transient receptor potential cation channel subfamily V member 1 (TRPV1) (28). Upon nerve injury, literature data have shed light on an increase in the expression of voltage-gated sodium channels (VGSCs) at the injury site and in the dorsal root ganglia (DRG), which significantly contributes to abnormal neuronal discharge (29). Various VGSCs, such as NaV 1.1, NaV 1.6, NaV 1.7, NaV 1.8, and NaV 1.9, are found in the sensory neurons, which are essential for neuronal excitability. Nav1.7 initiates an action potential that transmits nociceptive signals from

the peripheral nervous system to the CNS. At rest, the ion-conducting pores of most Na^+ channels remain closed. When a stimulus is applied, these channels open, allowing Na^+ influx, which leads to depolarization and the generation of an action potential that propagates to the DH of the spinal cord. Changes in VGSC expression and/or function can modify the firing behaviour of sensory primary afferent neurons as well as central neurons. Injury to sensory primary afferent neurons frequently leads to abnormal discharges or an increased response to subsequent sensory input, playing a role in the development of chronic inflammation and NP (30). The importance of VGSC in NP is recognized by administering lamotrigine and carbamazepine (CBZ), which are known as VGSC blockers, to manage NP (31,32). In addition, in diabetic neuropathy, there is a variation in the gene encoding NaV 1.7 (33). Another study reported that knocking down the VGSC NaV 1.6 encoding gene alleviated NP in mice (34). Furthermore, several studies have shown an elevated expression of NaV 1.8 channels in neuromas. These findings were also found for NaV 1.6 in another preclinical study in mice (34). The increased expression of VGSC leads to a lowered threshold and causes ectopic firing of nerve fibers (35,36). The recent discovery of suzetrigine, a selective inhibitor of NaV 1.8 which is distributed in the peripheral pain-sensing neurons, further opens research avenues for developing drugs that are acting peripherally and are supposed to have a diminished CNS side effect owing to the absence of this sodium channel subtype in this region (37). Journavx (suzetrigine, oral tablets) was approved by the U.S. Food and Drug Administration, presenting the first-in-class non-opioid analgesic for the management of moderate to severe acute pain in adults (38–40). Ultimately, suzetrigine is also being evaluated in a phase 2, randomized, double-blind study in patients with PDPN (41).

Central sensitization occurs when the central nociceptive neurons become hypersensitive to neuronal afferent input (42). This central sensitization becomes maladaptive in the case of peripheral NP, with continuous painful signals (43,44). Normally, the NMDAR channel is blocked by a magnesium (Mg^{2+}) ion that resides in the receptor pore (45). Prolonged release of glutamate by nociceptors leads to membrane depolarization, which displaces Mg^{2+} from the NMDAR pore, enabling glutamate to bind to the receptor and generate an inward current (45). Glutamate is the main fast excitatory neurotransmitter in the DH of the spinal cord, released by primary afferent neurons following a noxious stimulus and activating postsynaptic glutamate receptors on the spinal DH neurons, including AMPA,

NMDA, and Kainate receptors and several metabotropic (G-protein coupled) glutamate receptor subtypes (mGluR) (46). Indeed, increased glutamatergic signaling in NP has been proven in several preclinical studies (47,48). In a rat model of chronic sciatic nerve ligation-induced NP, a high glutamate level was reported in the DH of the spinal cord (49). Additionally, an elevated glutamate concentration in the cerebrospinal fluid (CSF) was also found in nerve-ligated neuropathic rats, which may be attributed to an overflow resulting from excessive glutamate release at the spinal nerve endings (50).

In addition to glutamate, other molecules such as substance P, calcitonin gene-related peptide (CGRP), and brain-derived neurotrophic factor are released. These bind to neurokinin 1 (NK1), CGRP1, and tyrosine receptor kinase B (TrkB) receptors, respectively, to promote central sensitization and enhance the ascending transmission of painful stimuli. Moreover, bradykinin can contribute to central sensitization by activating bradykinin B2 receptors, which leads to the potentiation of glutamatergic synaptic transmission (51). Similarly, the activation of nitric oxide receptors by nitric oxide leads to changes in neuronal excitability and synaptic strength by acting on both pre- and postsynaptic sites. Activation of NMDAR and mGluR causes a rapid increase in calcium, which activates intracellular kinases such as protein kinase C (PKC), calcium calmodulin-dependent protein kinase II (CaM-KII), protein kinase A (PKA), and extracellular signal-regulated kinase (ERK). These kinases then phosphorylate several key residues on the C-terminus of ionotropic NMDA and AMPA glutamate receptors, resulting in functional changes that contribute to central sensitization (52,53). Stimulation of AMPAR and group I mGluRs, alongside NMDAR, contributes to the activation of intracellular pathways such as PLC/PKC (54,55), phosphatidylinositol-3-kinase (PI3K) and the mitogen-activated protein kinase (MAPK) pathways that maintain central sensitization. These pathways activate ERK1/2 and the cyclic adenosine monophosphate response element binding protein (CREB) (46). An increase in intracellular calcium can activate ERK and CREB by initiating a calmodulin-dependent stimulation of adenylyl cyclases 1 and 8. This activation leads to the production of cyclic adenosine monophosphate (cAMP), which then activates PKA and initiates subsequent cascades. The transcriptional changes driven by CREB activation and other transcription factors promote the expression of genes such as c-Fos, NK1, TrkB, and Cox-2, resulting in a long-lasting strengthening of the synapse (46).

Based on the crucial role that these molecular and cellular alterations play in maintaining NP, targeting them is a potential treatment approach. Chronic pain can be reduced by dampening the increased neuronal excitability and adjusting the activity of certain receptors, ion channels, and neurotransmitter systems implicated in central sensitization. Potential therapeutic targets to inhibit central sensitization include using NMDA receptor blockers, which block excitatory glutamatergic transmission, and gamma-aminobutyric acid (GABA) agonists, which enhance inhibitory control within the spinal cord, though no medications that affect $GABA_A$ receptors are utilized to manage NP. Nevertheless, data on the effect of $GABA_B$ agonists in NP conditions have been reported (56), which is overviewed below. Several preclinical studies in rodents with peripheral nerve injuries have examined the antinociceptive impact of NMDAR antagonists. Ketamine, MK-801, memantine, and dextrorphan have been found to alleviate or prevent allodynia and hyperalgesia, particularly following injuries such as sciatic nerve constriction and spinal nerve ligation (61–63). Additionally, the intrathecal administration of amino-5-phosphonopentanoate, an NMDAR antagonist, relieves mechanical allodynia evoked by spinal cord injury (64). Mechanical and thermal hyperalgesia, but not sciatic nerve injury-evoked tactile allodynia, were alleviated by nor-ketamine with minimal side effects (65). Memantine and neramexane have faster unblocking rates and exhibit greater voltage dependence. This makes them promising for targeting continuous NMDAR activity in NP conditions with fewer adverse effects. When administered for two weeks, both memantine and neramexane provide sustained relief from mechanical hyperalgesia and allodynia in diabetic NP rats (66).

It is worth addressing that targeting voltage-gated calcium channels (VGCCs) and VGSCs, which are essential for neuronal excitability, has also demonstrated potential for lowering pain signals. As was already noted, one factor that leads to the development of NP is VGCC dysfunction. The VGCC can be classified as L, N, P/Q, R, and T types. Animal studies of NP reveal significant changes in the levels and structure of N-type calcium channels. These channels are important targets for new pain-relief drugs. Notably, mice without N-type channels show reduced sensitivity to pain compared to normal mice (67). The calcium channel blocker ziconotide has demonstrated clinical effectiveness in treating pain following intrathecal injection (68). Omega-conotoxin MVIIA alleviates NP after spinal cord injury by inhibiting N-type VGCCs on the spinal

DH (69). In addition, in sensory neurons, nifedipine, an L-type blocker, inhibits substance P release induced by inflammation, which indicates its involvement in nociception (70). Additionally, anticonvulsant drugs, such as gabapentinoids like pregabalin (PGB) and gabapentin, are considered first-line treatments for NP. They work by binding to the α_2-δ subunits of VGCC in the DH of the spinal cord, which reduces the release of excitatory neurotransmitters like glutamate, substance P, and CGRP, thereby decreasing central sensitization and providing pain relief (71,72). In NP conditions, PGB was demonstrated to alleviate NP entities in several studies (73,74).

At the DH part of the spinal cord, under NP conditions, convincing evidence has shed light on the existence of an imbalance between excitatory and inhibitory systems of pain control. In the descending inhibitory pathway, neuronal inhibition is mediated by GABAergic, glycinergic, and opioid neurons; these neurons release GABA, glycine, and endogenous opioids, respectively, which bind to their respective receptors: GABA, glycine, and opioid receptors, causing inhibition in the postsynaptic potentials (75,76). The binding of GABA to the GABA receptors on postsynaptic membranes exerts antinociceptive effects, which indicates the pivotal role of GABA receptors' activity in NP. In rat models of chronic constriction injury, activating $GABA_A$ receptors with muscimol reduces pain sensitivity caused by peripheral nerve damage (77). Likewise, spinal delivery of muscimol or baclofen, a $GABA_B$ receptor agonist, lessens both mechanical hypersensitivity and neuronal overactivity in chronic dorsal root ganglion compression (78). Despite these findings, GABA receptors have not yet been validated as effective drug targets for NP. On the other hand, increasing evidence from preclinical studies highlights glycine transporter inhibitors as promising candidates for pain relief in NP conditions (21,50). Alongside GABA and the glycinergic system, the opioid system plays an important role in the descending inhibitory pathway. Most opioid analgesics, such as morphine, methadone, fentanyl, and oxycodone, exert their effects by targeting μ-opioid receptors (MORs). MORs are G-protein-coupled receptors that activate inhibitory Gi/o proteins, leading to intracellular signaling changes and modulation of ion channels. They are found in crucial areas like the periaqueductal gray (PAG), rostral ventromedial medulla (RVM), and the dorsal part of the spinal cord, all of which play important roles in the antinociceptive actions of opioids (79,80). At the level of the midbrain, next to Morph treatment, Morph binds to presynaptic MORs. It inhibits VGCC

via $G_{\beta}\gamma$ proteins yet activates Gi/o proteins, which results in the inhibition of adenylyl cyclase and decreases cAMP production, whereas binding to postsynaptic MORs activates potassium channels via Gα proteins, resulting in an increase in potassium ion conductance that results in neuronal hyperpolarization. As a result, GABA release is blocked, which suppresses inhibition and enhances the output of the PAG neurons projecting to the RVM, which excite glutamate projections to off cells, which are GABAergic, thus inhibiting pain responses in the DH (80). Long-term opioid analgesic use develops opioid analgesic tolerance in patients, which remains an unresolved issue in clinical practice. Dose escalation is required to restore analgesic efficacy, which causes intolerable side effects (including overdose, opioid use disorders, constipation, opioid-induced hyperalgesia, and others) (81).

1.3. Current Approaches for Neuropathic Pain Management

The currently available medication approaches for NP management include different pharmacological agents with different mechanisms of action. Antidepressants, gabapentinoids, and topical lidocaine are the first-line therapies for NP. Tricyclic antidepressants (TCAs) such as amitriptyline are also among the first-line antidepressants in the treatment of NP, which act by inhibiting the major monoamine neurotransmitters' (serotonin, norepinephrine, and dopamine) reuptake, in addition to blocking VGSCs, which has also been proposed as a mechanism (82,83). Duloxetine (DUL) is a serotonin and norepinephrine reuptake inhibitor (SNRI) that was originally developed as an antidepressant. It facilitates the descending inhibitory pain pathway by inhibiting the reuptake of serotonin and norepinephrine to induce pain relief (84). Gabapentinoids (PGB and gabapentin) are anticonvulsants that act by binding to α_2-δ subunits of VGCCs located in the DH of the spinal cord, thereby decreasing excitatory neurotransmitters release such as glutamate, substance P, and CGRP, so reducing central sensitization, decreasing neuronal excitability, and causing subsequent pain relief (71,72).

Topical lidocaine is a VGSC blocker that causes local pain relief (71,85). Its use is limited to local allodynia due to its low bioavailability. Thus, it is not noteworthy to be administered orally (86). Lidocaine is the prototype of a class I/B antidysrhythmics drug. Because of high first-pass metabolism, lidocaine is administered intravenously (87–89), but systemic metabolism is still an obstacle factor to giving lidocaine. In addition, in long-

term treatment, the intravenous route of administration and the side effects are not favourable to patients.

Moreover, preclinical studies carried out in dogs and rats that utilized both oral and intravenous lidocaine to evaluate its antiarrhythmic or antiallodynic effects have shown that the oral dose is much larger than the intravenous one (90,91). In the context of NP, the translation of the applied doses in rats (15 mg/kg, intravenous) (91) to humans reveals that a much higher dose is required to obtain an antiallodynic effect in humans (2.4 mg/kg, intravenous) (92), which can be toxic without monitoring. On the other hand, topical lidocaine has been approved for the management of NP, specifically post-herpetic neuralgia (93). Studies have also shown some degree of efficacy and safety in the treatment of diabetic peripheral neuropathy, postsurgical pain, chronic lower back pain, carpal tunnel syndrome, and osteoarthritis (94). Also, a previous study reported that lidocaine induced antiallodynic and antihyperalgesic effects after local or systemic (intraplantar or intraperitoneal, respectively) administration in diabetic neuropathic rats (95).

Most anticonvulsants that are used to alleviate NP are VGSC blockers, such as CBZ, phenytoin, valproic acid, and lamotrigine. CBZ is considered a third-line medication for NP treatment that blocks VGSCs; however, it's a first choice for treating primary trigeminal neuralgia, which is not the object of the present work (96). Antiarrhythmic agents are also effective in relieving pain. Mexiletine, an oral VGSC belonging to the I/B type antiarrhythmic class that is indicated for ventricular arrhythmias (86). All the previously mentioned VGSC blockers (local anesthetics, TCAs, antiarrhythmics, anticonvulsants) have therapeutic potential in NP management, which indicates that VGSCs are a crucial target for NP management (86). Opioids act as second (tramadol and tapentadol)- or third-line (Morph and oxycodone) treatments for NP (8). Tramadol and tapentadol have a dual mode of action that combines MOR agonism and serotonin and/or norepinephrine reuptake inhibition (24). Tramadol is used in peripheral NPs (24), whereas tapentadol is effective in diabetic peripheral neuropathy and chronic low back pain (97).

Current monotherapies for NP develop several side effects, which may make them intolerable to the patients. Antidepressants such as TCAs have anticholinergic adverse effects, such as constipation and xerostomia, in addition to weight gain, somnolence, and dizziness (71), whereas SNRI as DUL can induce dizziness, somnolence, nausea, dry

mouth, and constipation (98). Gabapentinoids cause central side effects, such as somnolence, lightheadedness, and cognitive impairment, as well as peripheral side effects, like nausea and vomiting. Also, they can induce peripheral edema (rare), weight gain, fatigue, headache, and xerostomia, among others (99). Topical lidocaine can cause local skin reactions like irritation, tingling, and numbness in the application site (100). Weak opioids such as tramadol and tapentadol can cause gastrointestinal (GI) side effects such as constipation, where the risk is lower with tapentadol. Also, they have a lower risk of abuse compared to strong opioids (101,102). Strong opioid agonists, such as Morph, are effective in acute and chronic pain upon initiating therapy. However, they develop opioid analgesic tolerance, which emerges upon chronic administration demanding dose escalation. This dose increase can lead to serious side effects such as constipation and opioid use disorder, among others (81).

All the previously mentioned approaches include various drugs of different targets, which indicate that NP has different etiologies and complex underlying mechanisms (23,103); however, a relatively large number of patients, about 35%, continued to experience pain. Indeed, dose escalation could further reduce the pain but is associated with the risk and cost of several side effects, which makes it intolerable to patients. As a result, the management of NPs is still a big challenge for clinicians. Therefore, satisfactory treatment has not yet been fulfilled.

1.4. The Standpoint Hypothesis of the Present Thesis

Tolperisone (TOLP) was originally used as a skeletal muscle relaxant and acts within the CNS. Several clinical trials have approved its efficacy in relieving post-stroke spasticity, painful reflex muscle spasms, and muscle-related pain (104). Similar to lidocaine, TOLP has the ability to block ion channels, the VGSC isoform Nav1.7 in particular; this paves the way to its potential use in the treatment of NP as the inhibition of the excitatory pain pathway is an important target for NP management (30). Our previous study has shown the acute antiallodynic effect of TOLP in a rat model of partial sciatic nerve ligation (pSNL)-induced NP. A single oral dose of TOLP significantly reduced allodynia as measured by the Randall-Selitto test. These results were similar to that of PGB, which was used as a positive control. TOLP was also effective in decreasing glutamate release from rat brain synaptosomes (74). As previously stated, medications that block the

glutamatergic pathway have demonstrated antiallodynic effects in a variety of NP conditions (57,62,63).

Preclinical studies are largely based on pain-related behaviours to quantify NP. To do this, the animals are subject to various types of pain stimuli, such as dynamic or static stimuli that gently stroke or press the affected paws, respectively. For the assessment of the former pain condition von Frey test, and for the later one the Randall-Selitto paw pressure test are used. These two assays are utilized to measure tactile allodynia (mechanical allodynia) or mechanical hyperalgesia, respectively (105). The effects of TOLP on tactile allodynia have not been investigated thus far. Nevertheless, in both preclinical and clinical contexts, medications with a pharmacological profile similar to TOLP, specifically VGSC blockage, have been demonstrated to attenuate tactile allodynia (71,86,95).

Next, using multimodal analgesia containing two or more drugs at the sub-analgesic doses may increase efficacy and decrease side effects compared to using single-drug therapy (106). This strategy was followed in several clinical studies, to name just a few; gabapentinoids were combined with TCAs, such as nortriptyline or opioid analgesics, to relieve post-herpetic neuralgia or PDPN (107–109). The findings from these studies showed that the combination achieved a higher analgesic effect than every single drug. However, using anticholinergic and opioid agonists in these combination therapies increased the side effects, such as constipation and dry mouth, compared to the use of gabapentinoids alone (110). In another clinical study, treating diabetic neuropathic patients with an oxycodone/gabapentin combination showed no deterioration in the typical opioid-induced side effects, indicating that this combination is safe to use for managing NP (111). With respect to the analgesic effect of oxycodone/PGB, inconsistent results have been reported. In patients with either painful diabetic neuropathy or post-herpetic neuralgia, oxycodone in a small dose has not been shown to improve PGB's ability to reduce pain (112). Several animal studies evaluated the impact of applying a combinational therapy for NP management. In 2002, Matthews and Dickenson carried out an animal model of spinal nerve ligation to induce NP. The study found that, unlike morphine, gabapentin enhanced the suppression of DH neuronal activity after being administered systemically (113), although the effect of Morph was abolished. Thus, based on the combination strategies described above, we postulated that various combinational

therapies comprising TOLP and additional medications with distinct mechanisms of action, like PGB, DUL, or Morph, are promising analgesics for NP.

Acute or chronic administration of the combination of TOLP and Morph to treat pain has not yet been evaluated. Opioid analgesic tolerance is a barrier to continuing opioid treatment in the context of long-term treatment. To circumvent it requires dose escalation, which is associated with worsening opioid analgesics' side effects. Previous studies have shown that VGSC blockers could delay the development of Morph antinociceptive tolerance. CBZ, a VGSC blocker, potentially reduces the upregulated sodium channels in Morph-dependent rats, thereby diminishing Morph tolerance development and enhancing the duration of Morph analgesia post-operatively (114). Moreover, Jun et al., 2009 reported that intrathecal Morph administration for 7 days developed tolerance to the Morph antinociceptive effect. Intrathecal co-administration of oxcarbazepine with Morph blocked the development of antinociceptive tolerance assessed by tail-flick assay in rats (115). Similarly, intrathecal co-injection of lamotrigine with Morph delayed antinociceptive Morph tolerance in rats (116). Lidocaine, a commonly used local anesthetic, efficiently mitigates Morph tolerance. Intrathecally administered lidocaine potentiated an anti-nociceptive effect of Morph and attenuated chronic antinociceptive tolerance through the inhibition of neuroinflammation in mice assessed by the tail-flick assay as reported by Zhang et al., 2017 (117). On the other hand, a continuous intrathecal infusion of lidocaine with Morph in rats did not delay the development of Morph tolerance as previously reported (118). The aforementioned data provide justification for assessing TOLP's impact on the development of opioid antinociceptive tolerance.

2. Objectives

1- To assess the antiallodynic effects of oral acute and long-term treatment with the following drugs: TOLP, CBZ, PGB, and DUL in rats with mono-neuropathic pain induced by pSNL and manifested by tactile allodynia.

2- To evaluate the acute antiallodynic effects of the following combinations: sub-analgesic doses of oral TOLP with oral PGB or DUL, or with subcutaneous (s.c.) Morph in pSNL-induced mono-neuropathic pain and manifested by tactile allodynia in rats.

3- To further investigate the acute antiallodynic effect of the promising combination in rat mono-neuropathic pain in another pain model, type 1 diabetes-induced polyneuropathic pain in rats (induced by streptozotocin (STZ)).

4- To assess the impact of TOLP compared to PGB in the development of Morph antinociceptive tolerance in the rat tail-flick test.

5- To assess the impact of the promising combination (TOLP/PGB) on motor function and GI transit in rats.

6- To decipher how the potential combination and its constituent drugs produce their antiallodynic effect. In this regard, the following measurements were made:

6.a. Quantifying glutamate content in CSF of rats with mono-neuropathic pain evoked by pSNL and treated with TOLP, PGB, vehicle, or TOLP/PGB combination.

6.b. Evaluation of the effect of TOLP, PGB, or their combination on glutamate release from rat brain synaptosomes induced by 4-aminopyridine.

6.c. Determining MOR protein levels in spinal cord tissue from diabetic neuropathic rats by Western blot.

6.d. Determining D-serine and glycine levels in CSF samples from tolerant rats by capillary electrophoresis.

6.e. Assessing the efficacy (E_{max}) of the TOLP, PGB, and reference compounds (DAMGO, a highly MOR selective peptide, and Morph) in vitro in the mouse vas deferens (MVD) assay.

6.f. Assessing the effect of TOLP and PGB or Morph combinations in MVD.

6.g. Assessing the impact of TOLP or PGB on MVD developing tolerance to Morph.

3. Materials and Methods

3.1. Animals

In the present work of the thesis, male Wistar rats were used in studies designed to evoke a mono-neuropathic pain model by pSNL. The weight of the animals was 120-150 g at the operation time, and their weight ranged from 200–285 g at the time of acute and chronic drug testing. For the rat tail-flick, rotarod, and charcoal meal tests, 170–200 g male Wistar rats were used. In the polyneuropathic pain model, STZ-induced type 1 diabetes mellitus, male Wistar rats weighing 200–230 g were used. In this set of test, rats were kept in a mesh-bottomed cage (type IV cage) according to the EU's regulations. For the MVD assay, male NMRI mice (35–45 g) were used. The mice and rats were bought from Toxi-Coop Zrt., Budapest, Hungary. Animals were kept in standard cages designed for 4 or 5 animals, depending on their weights, and housed in the local animal house at the Department of Pharmacology and Pharmacotherapy, Semmelweis University (Budapest, Hungary). Animals were maintained at a controlled temperature (20 ± 2 °C), light/dark cycle (12/12 h), with free access to food and water. All procedures and housing conditions were performed in accordance with the European Communities Council Directives (2010/63/EU), the Hungarian Act for the Protection of Animals in Research (XXVIII.tv.32.§), and the local animal care committee (PEI/001/276-4/2013 and PE/EA/619-8/2018).

3.2. Chemicals

TOLP and PGB were obtained from Meditop Pharmaceuticals Ltd. (Budapest, Hungary). Morph-HCl was purchased from Alkaloida Chemical Company Zrt. (Tiszavasvári, Hungary). STZ, DUL, and CBZ were obtained from Sigma–Aldrich (St. Louis, MO, USA). For glutamate release measurement, glutamate oxidase, horseradish peroxidase, and Amplex Red, as well as hydroxyethyl cellulose, were purchased from Sigma–Aldrich (St. Louis, MO, USA). The constituents of Krebs solution were obtained from REANAL labor, Budapest, Hungary. All compounds were stored and used according to manufacturing procedures.

3.3. Experimental Protocols of the Animal Study

The experimental schedule of the mono-neuropathic pain models is summarized in experimental schemes 1 and 2. First, animals´ paw withdrawal thresholds (PWTs) were measured before the operation using dynamic plantar esthesiometer 37450 (DPA) purchased from Ugo Basil, Gemonio, Italy, expressed in gram (g). These measurements were considered as the baseline then the surgery was done as described in the next Section (3.4). To determine the development of tactile allodynia, PWTs were measured again 7 days post-operation, and neuropathic animals were selected and allocated randomly to different groups administered either oral vehicle or drugs. After acute oral treatment, PWTs were measured again at three time points (60, 120, and 180 min) to evaluate the acute antiallodynic effect of the administered drugs. After that, treatment was continued for 2 weeks/twice daily to investigate the chronic antiallodynic effects of the tested drugs. On days 14 and 21 post-operation, DPA measurements were repeated to assess the chronic effect of the tested compounds after 1 and 2 weeks of chronic administration, respectively (see Experimental Schedule 1). In another group of animals, baseline PWTs were measured, the surgery was done, PWTs were measured again two weeks post-operation, and treatments were given orally to the neuropathic rats to test the acute antiallodynic effect on day 14 post-surgery. In these experiments, subsequent to oral administration, tactile allodynia was assessed again at 60, 120, and 180 min to evaluate the acute antiallodynic impact of the tested drugs and their combinations as shown in Experimental Schedule 2.

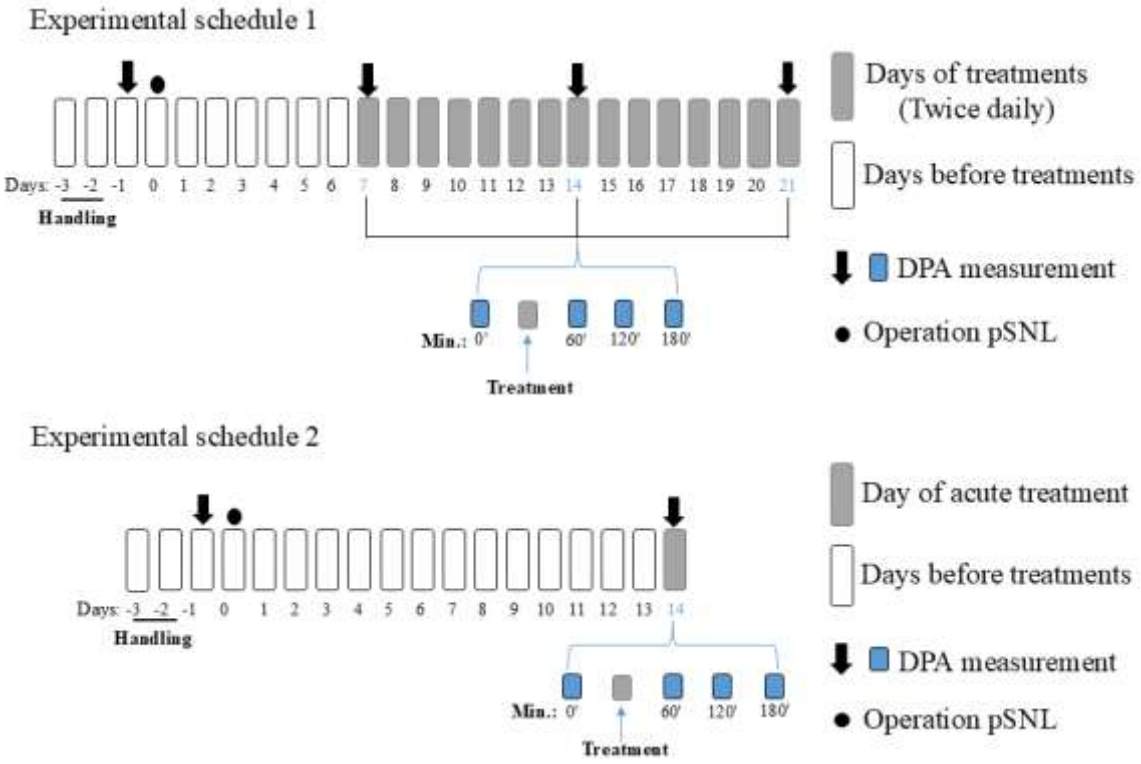

Experimental Schedule 1. illustrates the acute and chronic effects of PGB and TOLP (both at 25, 50, and 100 mg/kg), CBZ (16.25, 32.5, and 65 mg/kg), and DUL (10 and 20 mg/kg) on tactile allodynia induced by pSNL in rats. Tactile allodynia was tested by DPA. Also, the treatment schedule and days for DPA measurements are indicated.

Experimental Schedule 2. illustrates the acute antiallodynic effects of PGB, TOLP (both at 25, 50, and 100 mg/kg), their combination (both at 25 mg/kg), CBZ (16.25, 32.5, and 65 mg/kg), DUL (10 and 20 mg/kg), the TOLP/DUL combination (25 mg/kg + 20 mg/kg), and TOLP/Morph combination (25 mg/kg + 3.22 mg/kg). Tactile allodynia was tested by DPA. Also, the day for treatment and DPA measurement is indicated.

3.4. Partial Sciatic Nerve Ligation

The pSNL was carried out as previously mentioned (119,120). In short, rats were anesthetized using a single intraperitoneal dose of pentobarbital 60 mg/kg, given in a volume of 2.5 mL/kg. After anesthesia, animals were kept on a warm mat at 30° C, and the fur covering the right paws' and thighs' dorsal skin was shaved. After that, in an aseptic condition, an incision was created to expose the sciatic nerve that was tightly ligated at the dorsal 1/3 to 1/2 of the nerve thickness at the thigh level using polypropylene wire

(size 7-0). Then, two stitches were used to seal the wound. In the sham-operated rats (controls), the sciatic nerve was exposed without ligation.

3.5. Assessment of Static Tactile Mechanical Allodynia

Based on the previous investigations, DPA was used to assess the development of tactile allodynia, which is the main symptom of NP (79,119). Two days before starting the experiment, animals were handled by placing them in the DPA chambers once a day for acclimatization to the experimental procedures. On the day of the operation, animals' PWTs were measured after 5 min acclimatization and expressed in g; then, a small metal filament (0.5 mm in diameter) was directed to the rat's hind paws alternately (incrementation: 10 g/s, maximal force: 50 g) 3 times for each paw, and then the measurements were averaged. Rat was considered allodynic if the average PWT value of the right operated paw was decreased by 20% compared to the left unoperated paw (79,121). Measurements were done according to instructions in Section 3.3 and experimental schedules 1 and 2.

3.6. Treatment of Mono-neuropathic Animals

On the 7-day post-operation, the PWTs were measured, and the neuropathic rats were chosen and allocated randomly to different treatment groups. Drugs used in the study are PGB and TOLP, which were given at the same doses (25, 50, and 100 mg/kg), DUL at (10 and 20 mg/kg), and CBZ at (16.25, 32.5, and 65 mg/kg). All drugs were administered orally, and then the allodynia was assessed again 60, 120, and 180 min post administration. On the same animals, treatments were given continuously for 2 weeks/ twice a day, and the effect of chronic treatment was checked on days 14 and 21 post-operation. On another set of animals, on day 14 after pSNL, the acute effects of PGB and TOLP (both at 25, 50, and 100 mg/kg), DUL (10 and 20 mg/kg), CBZ (16.25, 32.5, and 65 mg/kg), the TOLP/PGB combination (both at 25 mg/kg), and the TOLP/DUL combination (25 mg/kg + 20 mg/kg), as well as TOLP/Morph combination (25 mg/kg + 3.22 mg/kg) were tested after acute oral treatment, except Morph that was given subcutaneously 30 min before the measurements. In a 1% hydroxyethyl cellulose solution, CBZ was suspended; however, the other drugs were dissolved in 0.9% saline and given in a volume of 5 mL/kg using an orogastric gavage, except morphine was given in a volume of 2.5 mL/kg.

3.7. Capillary Electrophoresis Analysis of Cerebrospinal Fluid Glutamate Content

The CSF glutamate level was measured using a capillary electrophoresis laser-induced fluorescence technique developed in our lab (122). Two weeks after surgery, rats were euthanized with isoflurane, and CSF samples were obtained from both control and neuropathic rats by puncturing the cisterna magna. Samples were first centrifuged (2000 × g for 10 min at 4 °C) and deproteinized by adding two volumes of cold acetonitrile. A second centrifugation was then performed (20,000 × g for 10 min at 4 °C). The resulting supernatants were derivatized with 1 mg/mL NBD-F in 20 mM borate buffer (pH 8.5) for 20 min at 65 °C, with 1 μM L-cysteic acid serving as an internal standard. For analysis of the derivatized compounds, a P/ACE MDQ Plus capillary electrophoresis system equipped with a laser-induced fluorescence detector (SCIEX, Framingham, MA, USA) was used, with excitation and emission wavelengths set to 488 nm and 520 nm, respectively. Separation was carried out in polyacrylamide-coated fused silica capillaries (i.d.: 75 μm, effective/total length: 40/50 cm) at 15 °C, applying a constant voltage of -27 kV in a 50 mM HEPES buffer at pH 7.0 containing 6 mM 6-monodeoxy-6-mono (3-hydroxy) propylamino-β-cyclodextrin.

3.8. Glutamate Release from Synaptosomes

The impact of TOLP, PGB, or their combination on depolarization-induced glutamate release was tested using rat brain synaptosomes that were prepared in accordance with a modified Modi et al. method (123). In short, animals were sacrificed, their brain was taken quickly, and in 0.32 M sucrose and 4 mM HEPES (pH 7.4) solution, homogenization was done. Then, homogenate was centrifuged (2 × 10 min, 1500 × g, at 4 °C), and the supernatants were collected and centrifuged again (2 × 10 min, 20,000 × g, at 4 °C). After that, the pellet was collected and resuspended using a buffer solution composed of 4 mM HEPES, 0.32 M sucrose, 10% fetal bovine serum, and 10% dimethyl sulfoxide and stored at -80 °C to be used later.

As previously described in our earlier study (74), glutamate release was measured as follows: The stored synaptosomal suspensions were thawed on the day of the experiment, and centrifugation was done (10 min, 20,000 × g, at 4 °C); then the pellet was resuspended using 10 mM HE-PES buffer composed of 5.4 mM KCl, 130 mM NaCl, 0.9 mM MgCl2, 1.3 mM CaCl2, and 5.5 mM glucose (pH 7.4). Synaptosomal suspensions (10 mg) were

used to collect the supernatant that was centrifuged thereafter to an 8-well strip plate (15 min, 2500 × g, at 4 °C). Equilibrium of synaptosomes was done for 2 × 10 min at 37 °C before stimulation in HEPES buffer containing 40 μM of DL-TBOA (a competitive, non-transportable blocker of excitatory amino acid transporters) (124), to prevent glutamate reuptake. During the equilibration, tested drugs were added as a pretreatment. After the equilibration period, 1 mM 4-aminopyridine was used as a stimulation buffer to initiate depolarization and subsequent release of glutamate. After that, aliquots were taken at 8 min and kept at -20 °C until the analysis with enzyme-linked fluorescent assay to be done.

3.9. Enzyme-Linked Fluorescent Assay of Glutamate Released from Synaptosomes

From Sigma–Aldrich (St. Louis, MO, USA), a Glutamate Oxidase Assay Kit was purchased, and glutamate release was determined using an enzyme-linked fluorescent assay. In brief, a working solution containing glutamate oxidase (0.04 U/mL), horseradish peroxidase (0.125 U/mL), and Amplex Red (50 μM) (final concentrations) was prepared and then mixed with the samples. Fluorescent readings were carried out after 30 min incubation at 37 °C. Fluorescence was measured at 488 and 520 nm excitation and emission wavelengths, respectively.

3.10. Animal Model of Type 1 Diabetes-Induced Polyneuropathic Pain

In accordance with the EU's regulations, rats were kept in a mesh-bottomed cage (type IV cage). Type 1 diabetes was induced by intraperitoneal injection of a single large dose of STZ (60 mg/kg) that was freshly prepared using cold distilled water (1–3 °C) just before injection to avoid drug degradation (125,126). Using the Dcont Etalon blood glucose meter obtained from Roche Diagnostics GmbH, Mannheim, Germany, blood glucose level was measured 3 days later from tail vein blood, and those animals with blood glucose levels higher than >14 mmol/L were considered diabetic. The glucometer can determine blood glucose up to 33.3 mmol/L (127). The PWTs for the left and right paws were measured 3 times alternatively for each paw, assessed every 3 weeks, and expressed in g. After that, the average PWT values for each animal's two paws were calculated. Control rats were used, including age-matched non-diabetic animals of the same age as diabetic ones, and vehicle-treated animals. Tactile allodynia is determined by a 20% reduction in the average PWTs of the diabetic rats compared with the age-matched non-diabetic rats (121). After 9 weeks, diabetic neuropathic rats were selected

and allocated randomly into different groups to receive either the vehicle or the drugs (25 mg/kg PGB, 25 mg/kg TOLP, or their combination) to assess their acute antiallodynic effect measured at 60 and 120 min post single oral administration (see Experimental Schedule 3).

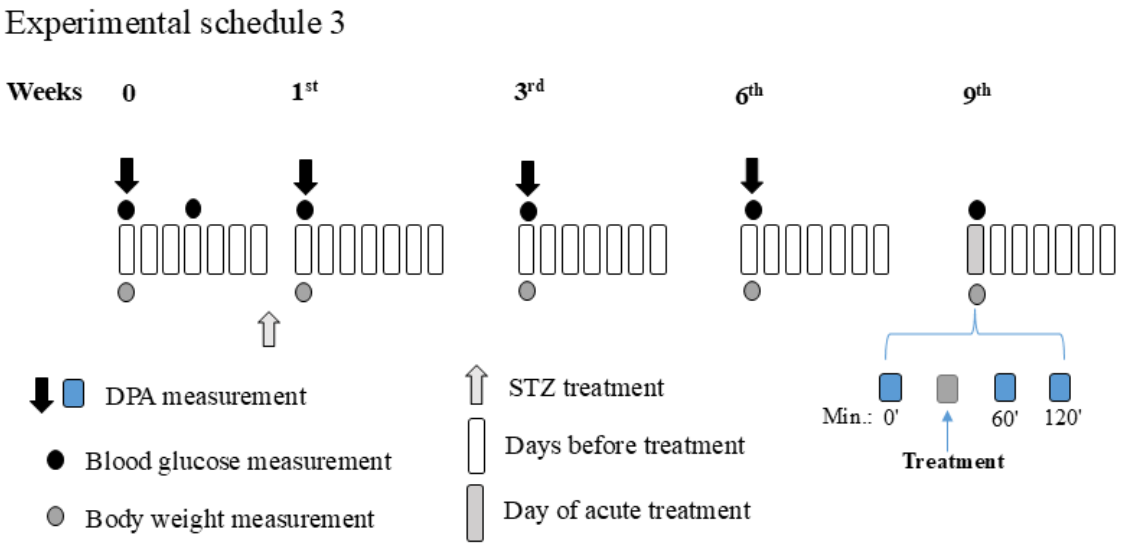

Experimental Schedule 3. shows a schematic representation of the study design applied to type 1 diabetes-induced polyneuropathic pain. The scheme indicates the timeline of the blood glucose, body weight, DPA measurements, and the treatment day.

3.11. Western Blot Analysis

Using a TissueLyser (Qiagen, Venlo, Netherlands), spinal cord tissues were homogenized in lysis buffer containing a protease inhibitor cocktail (complete ULTRA Tablets, Roche, Basel, Switzerland) and PMSF (Sigma, St. Louis, MO, USA). After two rounds of centrifugation at 1500 × g for 15 min at 4 °C, the supernatants were collected. Protein concentrations were quantified using the bicinchoninic acid assay (BCA, Thermo Fisher Scientific, Waltham, MA, USA). Thirty-five micrograms of protein were mixed with a reducing loading buffer (Pierce Lane Marker, Thermo Fisher Scientific, Waltham, MA, USA), loaded, and separated in a 4%–20% precast Tris-glycine SDS polyacrylamide gel (BioRad, Hercules, CA, USA). Proteins were transferred overnight at 200 mA to a polyvinylidene difluoride membrane (BioRad, Hercules, CA, USA) which was blocked for 1 hr at room temperature with 5% non-fat dry milk (BioRad, Hercules, CA, USA) in Tris-buffered saline with 0.05% Tween-20 (0.05% TBS-T; Sigma, St. Louis, MO, USA). Following blocking, membranes were incubated overnight at 4 °C with a primary

antibody against MOR (ABIN617908, 1:1500) (antibodies-online GmbH, Aachen, Germany), then with the corresponding secondary antibody for 2 hr at room temperature. To control for sample loading and protein transfer and to normalize the content of the target protein, GAPDH (D16H11, 1:10000, Cell Signaling Technology, Danvers, MA, USA) was used. Each assay was repeated at least three times. To detect signals, a chemiluminescence kit was used (BioRad, Hercules, CA, USA) by Chemidoc XRS+ (BioRad, Hercules, CA, USA) (128).

3.12. Morph Antinociceptive-Tolerance Model

The rat tail-flick test (ITC Life Sciences equipment) was used to evaluate the effect of co-administering oral doses of 100 mg/kg of TOLP or PGB on the development of morph antinociceptive tolerance evoked by s.c. dose of 10 mg/kg of morph. Handling was done to acclimatize the animals to the experimental conditions. All drugs were prepared in 0.9% saline and administered twice daily for 10 days in a volume of 5 mL/kg for oral administration and 2.5 mL/kg for s.c. injections (under the skin over the neck). The tail-flick test was performed as previously described (129,130). In brief, a beam of radiant heat was directed to the dorsum of the lower third of the rat tail, and then the time when rats flicked their tail was recorded as the latency time before (baseline) and 30, 60, 120, and 180 min after the drug administration to test the antinociceptive effect of the test compounds. Next, the latency time was calculated as a percentage of maximum possible effect (% MPE) = (post-drug latency−baseline latency) / (cut-off time−baseline latency) ×100 (131). To avoid tissue damage, the cut-off time was set to 8 s. The treatment schedule and the Morph dose used to induce Morph antinociceptive tolerance were selected as described by our group (132) and are shown in Experimental Schedule 4.

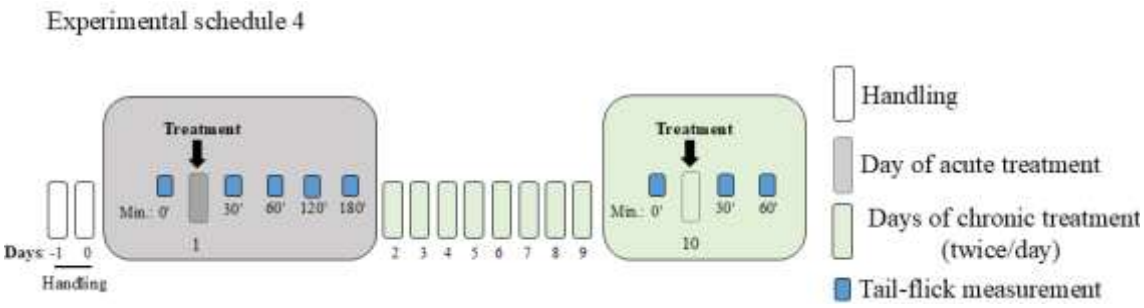

Experimental Schedule 4. shows the study design applied to induce Morph antinociceptive tolerance. The scheme indicates the timeline of the treatment and tail-flick measurement.

3.13. Capillary Electrophoresis Analysis of Cerebrospinal Fluid D-serine and Glycine Content

After 10 days of TOLP, Morph, Morph/TOLP, Morph/PGB, or vehicle treatment, CSF samples were collected to detect D-serine and glycine levels as detailed in section 3.7.

3.14. Isolated Mouse Vas Deferens Assay

All procedures were performed as reported by Lacko et al. (2012), with minor modifications (133). In brief, MVD experiments used 35-45 g male NMRI mice of 6-10 weeks of age. Vasa deferentia were separated, taken out of their sheaths, and put in 5 ml organ baths containing Krebs solution aerated with a mixture of 95% O_2+ 5% CO_2 right away. They were then suspended between two electrodes; the lower one is straight, while the upper one is ring-shaped. The Krebs solution used contained the following components: 118.0 mM NaCl, 25.0 mM $NaHCO_3$, 4.7 mM KCl, 1.2 mM KH_2PO_4, 11.0 mM glucose, 2.5 mM $CaCl_2$, and 1.2 mM $MgSO_4$. The organ's upper part was connected to a computer through a transducer and an amplifier. The resting tension was adjusted to 0.1 g. Electrical stimulation consisted of 10 Hz trains, each containing 10 rectangular pulses lasting 1 ms, delivered at 9 V/cm (supramaximal intensity), and repeated every 10 seconds (0.1 Hz) using a Stimulator 88 (Grass Medical Instruments, Quincy, MA, USA). Prior to drug administration, organs underwent a 50-60 min equilibration period under electrical field stimulation and were washed with Krebs solution every 5 min. After the equilibrium, concentration-response curves of drugs were constructed in a cumulative manner with 2 min of drug exposure. Applied concentration ranges were in nM: 10-100,000; 10-1,000,000; 1.56-6,400; and 3.125-800 for TOLP, PGB, Morph, and DAMGO, respectively.

3.15. Procedures and Assessment of Morph Tolerance in Isolated Mouse Vas Deferens Assay

In this set of experiments, MVD was used to induce an ex vivo Morph tolerance model. A high concentration of Morph (1000 nM) was used, which is 4 times the EC_{50} (218.9) calculated from Morph concentration-response curves obtained from the previous experiments (see section 3.14). After the organ was isolated and prepared as described above, 1000 nM Morph was added into the organ bath with 5 min drug exposure followed by quick washing. This treatment form was repeated 3 times. Next, extensive washing

was done to regain at least 80% of the height of contractions, and then 500 nM Morph was injected into the organ bath. To evaluate the effect of PGB and TOLP on Morph tolerance, the organs were treated 3 times with the combination of 1000 nM Morph and PGB or TOLP. As a control, the vehicle was used instead of 1000 nM Morph. Finally, the effect of 500 nM Morph was assessed on Morph, Morph/PGB, Morph/TOLP, or vehicle-treated organs (134).

3.16. Motor Function Test in Naïve Rats

In naïve male Wistar rats, the effect of test drugs on motor function was tested using the rotarod test (Rat Rotarod, Model 7750; Ugo Basile, Gemonio, Italy). At 16 rpm, the speed of the rotating rod of the instrument was fixed, and rats were trained to stay on it for 180 s (cut-off time) 24 hours before the experiment. On the next day, different drugs were given orally, including TOLP (100 and 150 mg/kg), PGB (25, 50, and 100 mg/kg), and the TOLP/PGB combination (both at 25 mg/kg), or vehicle, and their acute effect were evaluated at 60 and 120 min after acute oral treatment. The fall-off time, or the latency time, was used to indicate motor coordination (50,135).

3.17. Determination of Gastrointestinal Peristalsis in Naïve Rats

The effect of tested drugs on GI transit was evaluated in naïve male Wistar rats using the charcoal meal test (136). In short, after 18 hours of fasting, TOLP (25 and 50 mg/kg), PGB (25 and 50 mg/kg), or the TOLP/PGB combination both at 25 mg/kg were given orally. An oral charcoal suspension was prepared (10% charcoal in 5% gum Arabic) and given via oral gavage 30 min post-oral drug administration in a volume of 2 mL/animal. After another 30 min, animals were sacrificed, and the whole small intestines were taken. Then, the charcoal travel distance was measured and compared with the whole small intestinal length.

3.18. Statistical Analysis

Data were statistically analyzed using GraphPad Prism 8.0 Software (San Diego, CA, USA). Values were presented as mean ± standard error of means (S.E.M.). Data were analyzed by one-way or two-way ANOVA followed by Dunnett's or Tukey's post-hoc test for multiple comparisons. Data were analyzed by unpaired t-test for Figure 9, panels (a-c, e). Significant differences were considered if $p < 0.05$. ROUT analysis was done to find outliers, with a Q value = 0.5%.

4. Results

4.1. Oral TOLP and PGB Produce Significant Anti-tactile Allodynic Effects Only After Chronic Treatment in Rats with Mono-neuropathic Pain Induced by pSNL

This section shows the results related to the effect of a single oral treatment of TOLP and PGB at day 7 post-operation and the chronic effect measured after 1 and 2 weeks of chronic oral treatment at days 14 and 21, respectively (Figures 1 and 2). The anti-tactile allodynic effects of TOLP and PGB were tested at 3 different doses (25, 50, and 100 mg/kg). Tactile allodynia was evoked by pSNL and measured by DPA. Allodynia was evidenced by a decrease in the rat PWT. The effect of the test drugs was evaluated at 60, 120, and 180 min after oral administration as described in Experimental Schedule (1).

TOLP was ineffective in restoring the developed allodynia either after a single dose or 1 week of chronic administration at all given doses, as presented in Figures 1a and b, respectively. On the other hand, the results depicted in Figure 1c indicate that TOLP treatment at 100 mg/kg dose produced a significant anti-tactile allodynic effect that was obtained at 60 min following 2 weeks of chronic treatment compared to the vehicle-treated group (two-way ANOVA: F (treatment group; 4, 45) = 25.41, $p < 0.0001$, Dunnett's post-hoc test: $p = 0.0260$). Similarly, after a single dose or 1 week of chronic administration, PGB in all tested doses failed to alleviate the developed allodynia (Figures 2a, b). In addition, Figure 2c indicates that PGB treatment at 50 mg/kg dose can also exert a significant anti-tactile allodynic effect that was obtained at 60 min after 2 weeks of chronic treatment compared to the vehicle-treated group (two-way ANOVA: F (treatment group; 4, 39) = 23.91, $p < 0.0001$, Dunnett's post-hoc test: $p = 0.0080$).

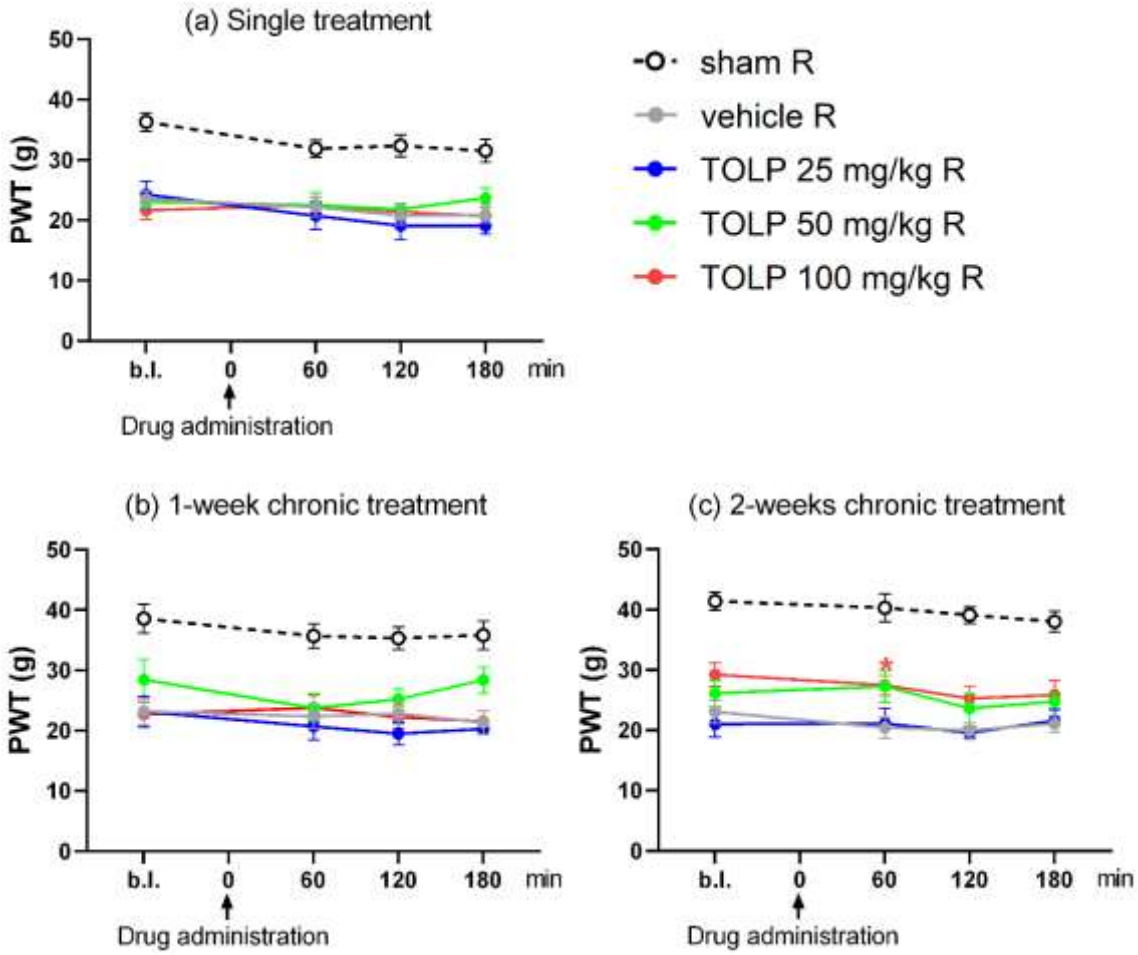

Figure 1. shows the antiallodynic effect of TOLP on tactile allodynia induced by pSNL in rats. On day 7 post-operation, the PWTs were measured before and after a single administration (panel a). Also, on days 14 and 21 post-operation, PWTs were measured after 1 and 2 weeks of chronic administration, as shown in panels b and c, respectively. After oral treatment, tactile allodynia was assessed at 60, 120, and 180 min by DPA. Values are presented as the mean ± SEM of 8-13 animals/group. Data were analyzed by two-way ANOVA and Dunnett's post-hoc test. *P < 0.05 means statistical significance versus the vehicle's right (R) operated paw at the indicated time points after administration. PWTs measured before the first administration are called baseline (b.l.), whereas single treatment indicates the PWTs measured after a single oral administration on day 7 post-operation.

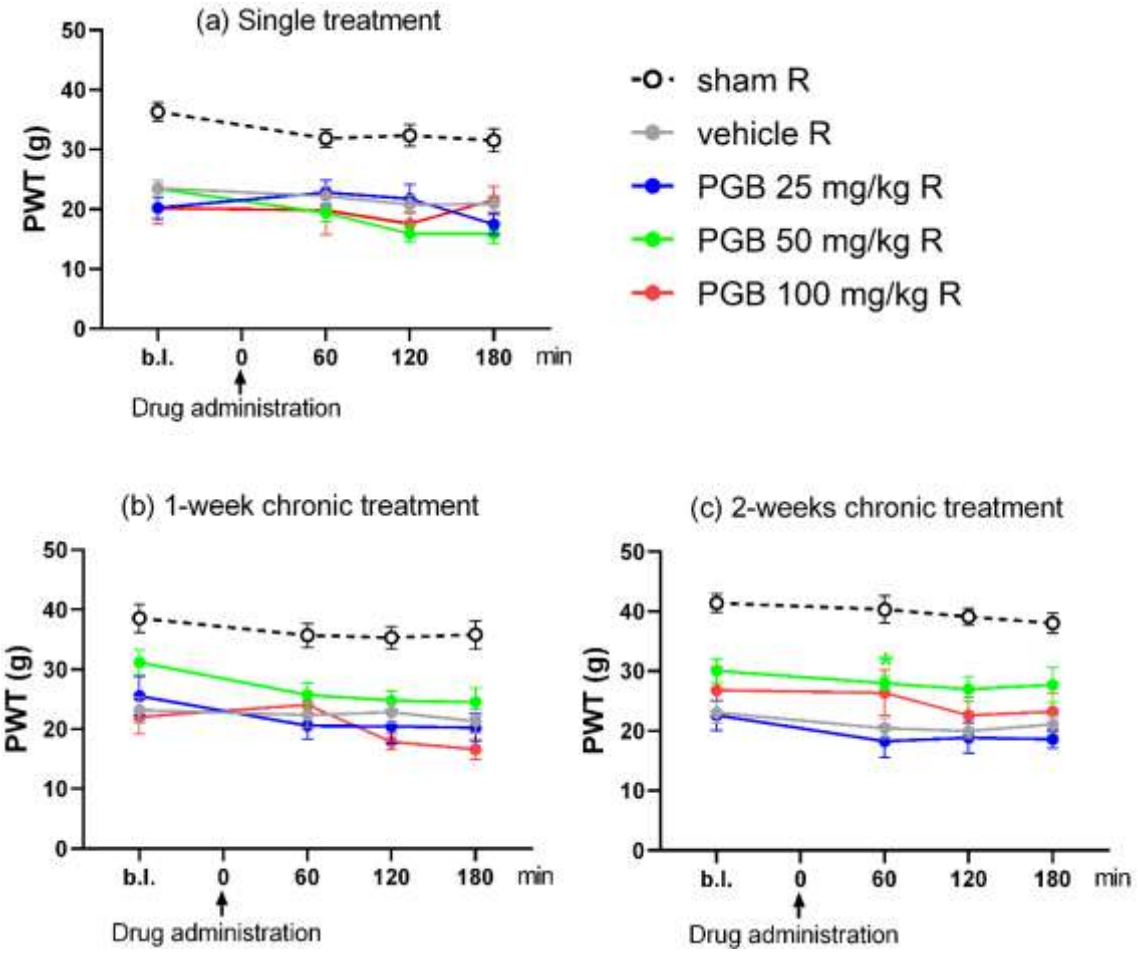

Figure 2. shows the antiallodynic effect of PGB on tactile allodynia induced by pSNL in rats. On day 7 post-operation, the PWTs were measured before and after a single administration (panel a). Also, on days 14 and 21 post-operation, PWTs were measured after 1 and 2 weeks of chronic administration, as shown in panels b and c, respectively. After oral treatment, tactile allodynia was assessed at 60, 120, and 180 min by DPA. Values are presented as the mean ± SEM of 6-13 animals/group. Data were analyzed by two-way ANOVA and Dunnett's post-hoc test. *P < 0.05 means statistical significance versus the vehicle's right (R) operated paw at the indicated time points after administration. PWTs measured before the first administration are called baseline (b.l.), whereas single treatment indicates the PWTs measured after a single oral administration on day 7 post-operation.

4.2. Oral DUL and CBZ Fail to Produce Anti-tactile Allodynic Effects After Acute or Chronic Treatment in Rats with Mono-neuropathic Pain Induced by pSNL

The acute effect was measured after a single oral treatment on day 7 post-operation, and the chronic effect was measured after 1 and 2 weeks of chronic oral treatment on days 14 and 21 post-operation, respectively. DUL was given at 2 different doses (10 and 20 mg/kg), and CBZ at 3 different doses (16.25, 32.5, and 65 mg/kg). Both drugs at all tested doses and treatment periods failed to attenuate the developed right hind-paw allodynia compared to vehicle-treated rats at all tested time points, as presented in Figures 3 and 4 (a–c).

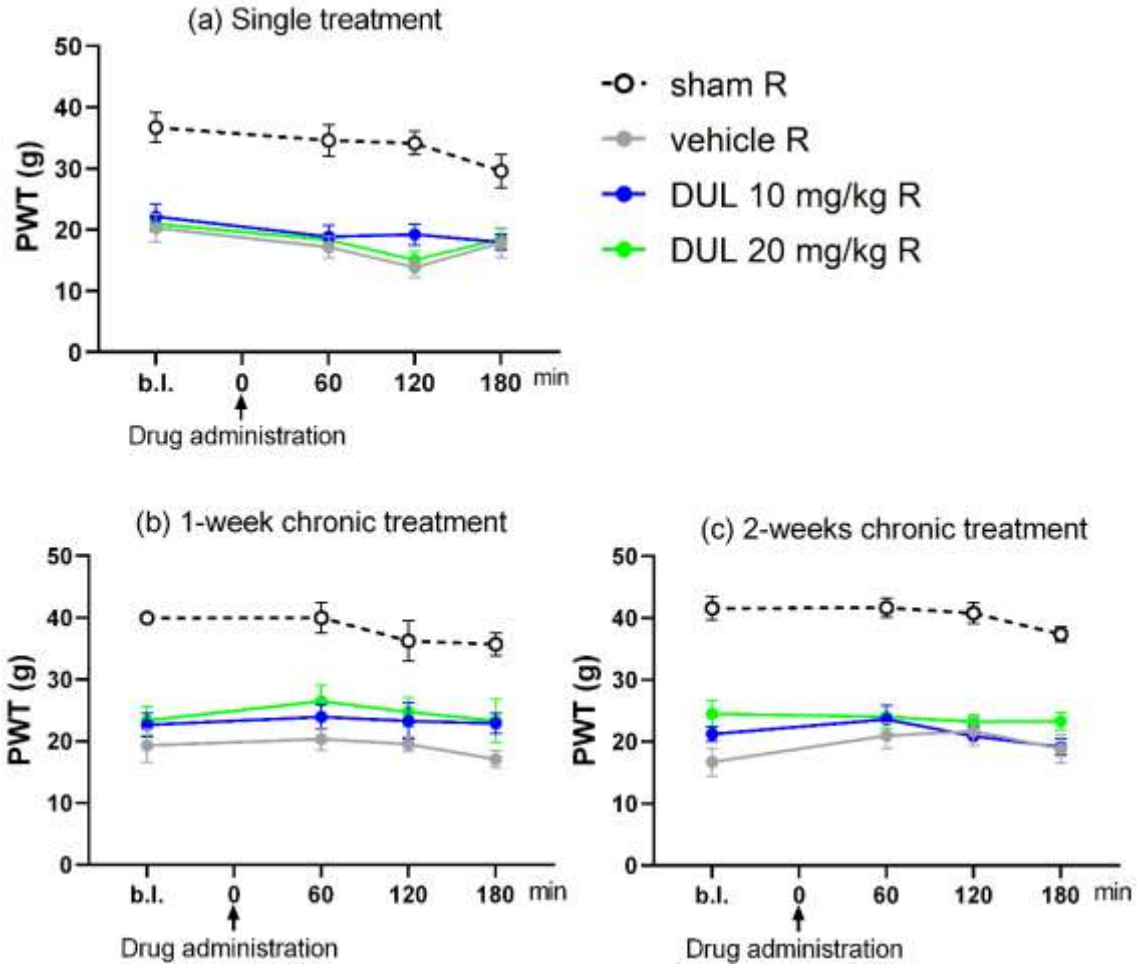

Figure 3. shows the antiallodynic effect of DUL on tactile allodynia induced by pSNL in rats. On day 7 post-operation, the PWTs were measured before and after a single administration (panel a). Also, on days 14 and 21 post-operation, PWTs were measured after 1 and 2 weeks of chronic administration, as shown in panels b and c, respectively.

After oral treatment, tactile allodynia was assessed at 60, 120, and 180 min by DPA. Values are presented as the mean ± SEM of 5–7 animals/group. Data were analyzed by two-way ANOVA and Dunnett's post-hoc test. P > 0.05, statistically non-significant: treated groups versus the vehicle's right (R) operated paw at the indicated time points after administration. PWTs measured before the first administration are called baseline (b.l.), whereas single treatment indicates the PWTs measured after a single oral administration on day 7 post-operation.

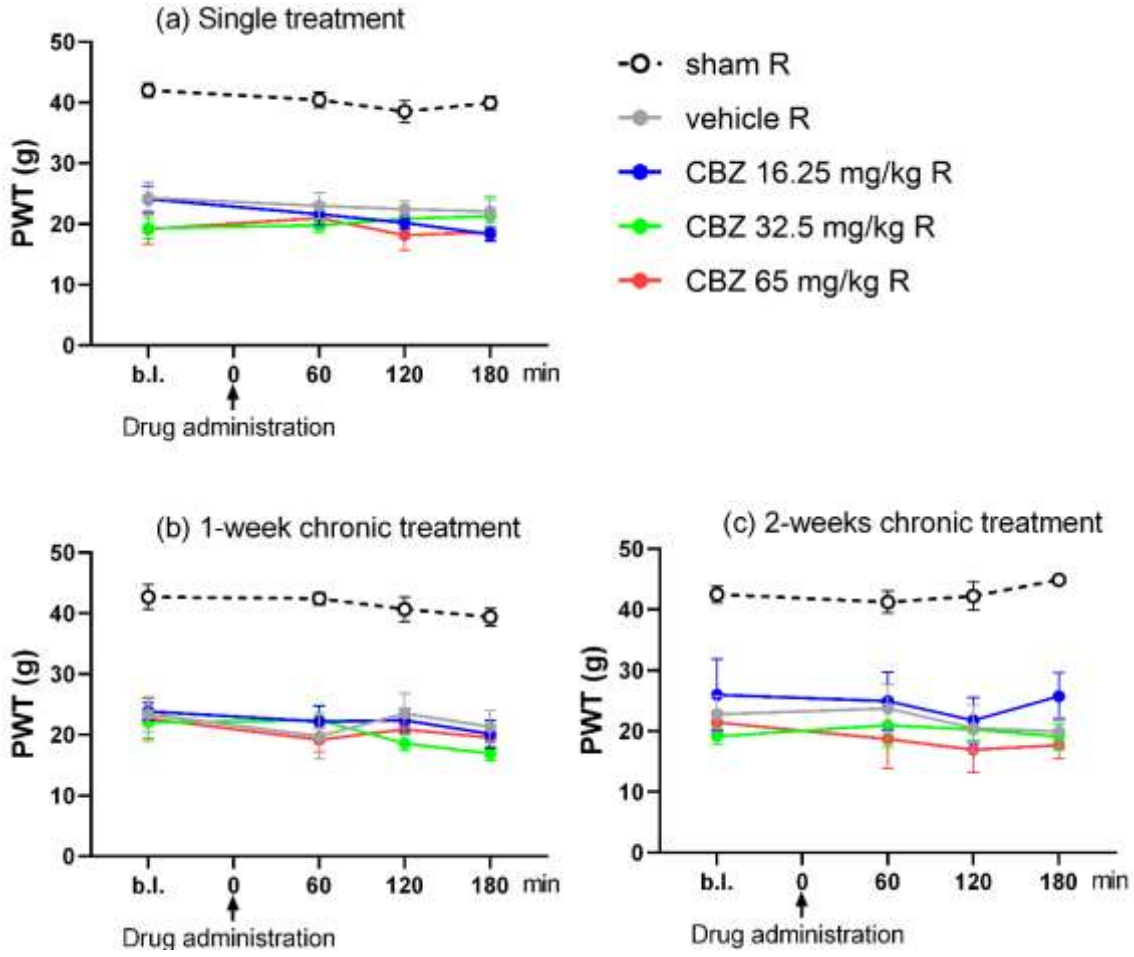

Figure 4. shows the antiallodynic effect of CBZ on tactile allodynia induced by pSNL in rats. On day 7 post-operation, the PWTs were measured before and after a single administration (panel a). Also, on days 14 and 21 post-operation, PWTs were measured after 1 and 2 weeks of chronic administration, as shown in panels b and c, respectively. After oral treatment, tactile allodynia was assessed at 60, 120, and 180 min by DPA. Values are presented as the mean ± SEM of 6–7 animals/group. Data were analyzed by two-way ANOVA and Dunnett's post-hoc test. P > 0.05, statistically non-significant:

treated groups versus the vehicle's right (R) operated paw at the indicated time points after administration. PWTs measured before the first administration are called baseline (b.l.), whereas single treatment indicates the PWTs measured after a single oral administration on day 7 post-operation.

4.3. Acute Oral Treatment of TOLP, PGB, DUL, and CBZ Fail to Restore the Tactile Allodynia Evoked by pSNL in Rats on Day 14 Post-operation

In this set of animals, the acute anti-tactile allodynic effects of TOLP (25, 50, and 100 mg/kg), PGB (25, 50, and 100 mg/kg), DUL (10 and 20 mg/kg), and CBZ (16.25, 32.5, and 65 mg/kg) at the same doses were tested on day 14 post-operation, as shown in Figure 5a, b, c, and d, respectively. All tested drugs failed to alleviate the developed allodynia measured at 60, 120, and 180 min after acute oral treatment, as presented in Figure 5 (a-d).

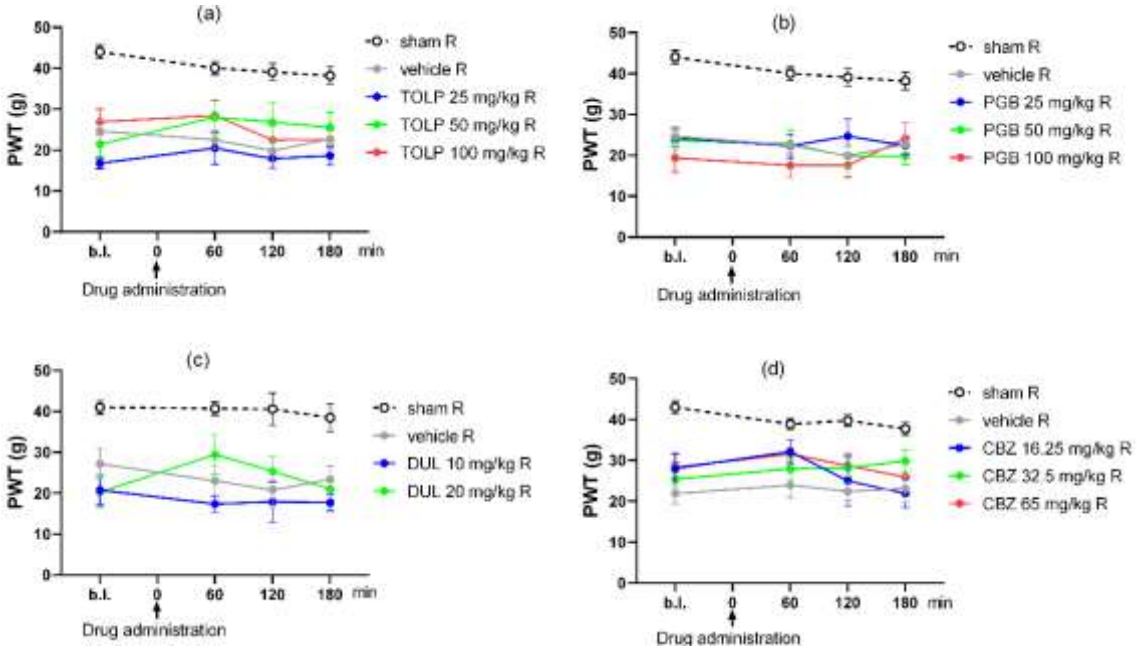

Figure 5. shows the acute antiallodynic effect of TOLP (panel a), PGB (panel b), DUL (panel c), and CBZ (panel d) on tactile allodynia induced by pSNL in rats measured by DPA at day 14 post-operation. After oral treatment, tactile allodynia was assessed at 60, 120, and 180 min. Values are presented as the mean ± SEM of 6–8 animals/group panel (a), 8 animals/group panel (b), 4–5 panel (c), and 4–13 animals/group panel (d). Data were analyzed by two-way ANOVA and Dunnett's post-hoc test. $P > 0.05$, statistically

non-significant: treated groups versus the vehicle's right (R) operated paw at the indicated time points after administration. Baseline (b.l.): was measured before the treatment.

4.4. Acute Oral Co-Administration of TOLP with PGB but not with DUL or Morph Alleviates Tactile Allodynia Evoked by pSNL in Rats on Day 14 Post-operation

In this set of animals, combinations of two different drugs with different modes of action, namely multimodal analgesia, were applied, aiming to increase the efficacy and decrease the side effects. So, we investigated a combination of TOLP/PGB at the smallest doses (25 mg/kg for both) in rats that underwent pSNL on day 14 post-operation (Figure 6a).

As previously mentioned, acute or chronic oral treatment with 25 mg/kg of either TOLP or PGB did not induce any significant antiallodynic effect (Figures 1 and 2). Moreover, the oral acute treatment with TOLP, PGB, or DUL failed to restore the developed allodynia in pSNL rats at day 14 post-operation, as presented in Figures 5a, b, and c, respectively. Surprisingly, the developed tactile allodynia was acutely alleviated by TOLP/PGB combination (both at 25 mg/kg) in pSNL rats 120 min post-acute oral treatment versus the vehicle's right (R) operated paw (two-way ANOVA: F (treatment group; 4, 28) = 17.81, $p < 0.0001$, Dunnett’s post-hoc test: $p = 0.0266$), PGB- or TOLP-treated rats (Figure 6a).

On the other hand, combinations of TOLP/DUL or s.c. Morph (3.22 mg/kg) failed to show an antiallodynic effect after acute oral treatment in pSNL rats at all tested doses and time points shown in Figures 6b and c. With respect to the antiallodynic effect of Morph per se, our previous results showed that acute Morph treatment in a small dose of 3.22 mg/kg failed to produce an antiallodynic effect, but a dose of 6.44 mg/kg produced an effect on operated and non-operated paws at day 14 post-operation, indicating an antinociceptive effect (79).

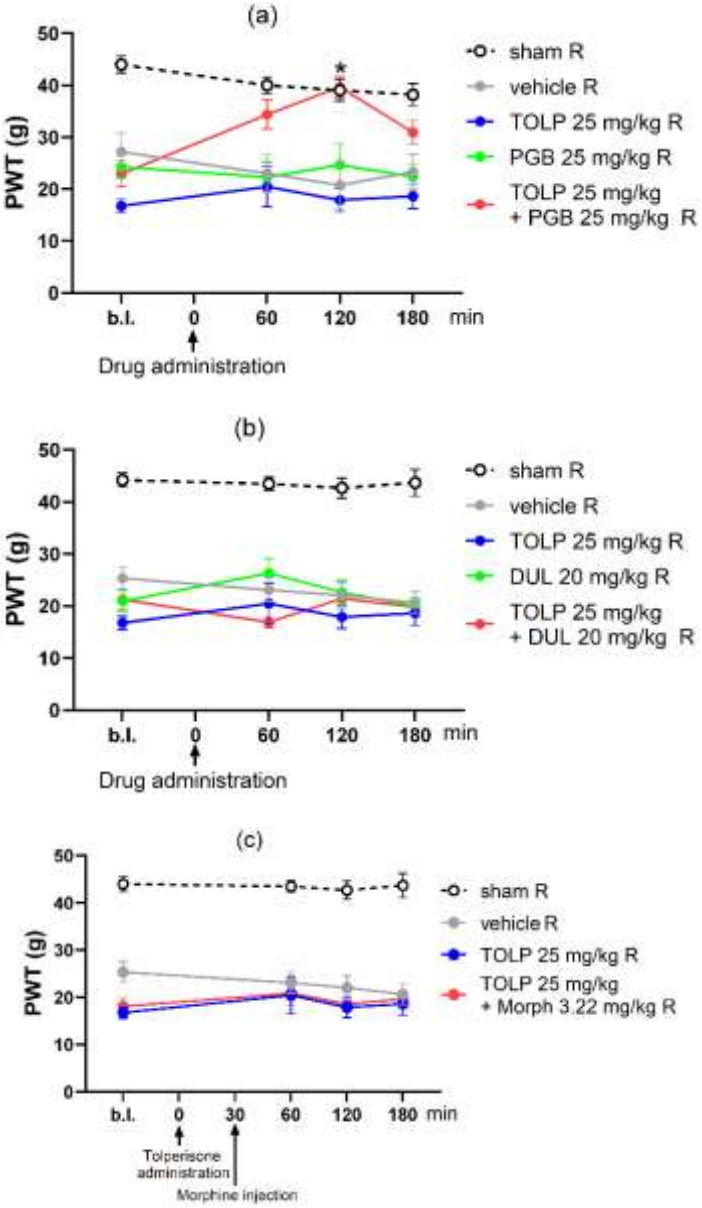

Figure 6. shows the acute antiallodynic effect of TOLP/PGB combination panel (a), TOLP/DUL combination panel (b), and TOLP/Morph combination panel (c) on tactile allodynia induced by pSNL in rats measured by DPA at day 14 post-operation. After oral treatment, tactile allodynia was assessed at 60, 120, and 180 min. Values are presented as the mean ± SEM of 5–8 animals panel (a), 5–8 animals panel (b), and 6–12 animals panel (c). Data were analyzed by two-way ANOVA and Dunnett's post-hoc test. *P < 0.05 means statistical significance versus the vehicle's right (R) operated paw at the indicated time points after administration. Baseline (b.l.): was measured before the treatment.

4.5. The Impact of Acute Oral Administration of TOLP, PGB, or their Combination on Cerebrospinal Fluid Glutamate Content in Rats with Mono-neuropathic Pain Evoked by pSNL

On day 14 post-operation, CSF samples were collected from rats with mono-neuropathic pain evoked by pSNL, and then, by capillary electrophoresis, the CSF glutamate content was measured. Figure 7 depicts that a significant elevation of the CSF glutamate content was detected in the oral vehicle-treated neuropathic rats compared to the sham group (one-way ANOVA: $F(4, 64) = 6.435$, $p = 0.0002$, Dunnett's post-hoc test: $p = 0.0032$). In addition, the elevation in the CSF glutamate content was significantly inhibited by the administration of per os TOLP, PGB, or their combination and reached the normal level of the sham group.

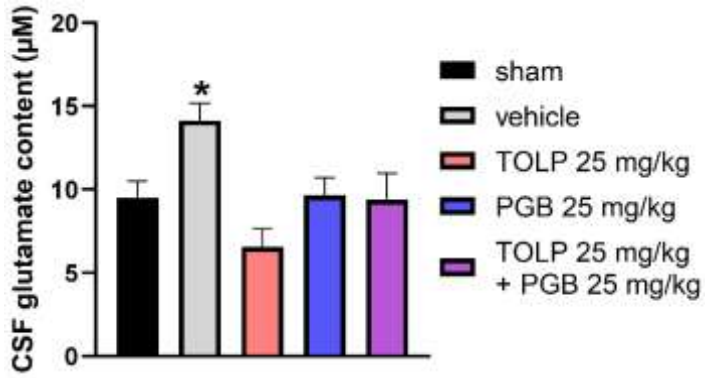

Figure 7. CSF glutamate content of rats with mono-neuropathic pain evoked by pSNL and sham-operated rats following acute oral treatment with 25 mg/kg of either TOLP, PGB, or their combination (both at 25 mg/kg) on day 14 post-operation. Values are presented as mean ± SEM of 4–21 animals/group. Data were analyzed by one-way ANOVA and Dunnett's post-hoc test, *$P < 0.05$ means statistical significance versus other groups.

4.6. Impact of Treatment with TOLP, PGB, or their Combination on 4-Aminopyridine-Induced Glutamate Release from Rat Brain Synaptosomes

The impact of the tested drugs or their combination on the glutamate release from naïve rat brain synaptosomes was made to elaborate on the possible mechanism behind their antiallodynic effects. Depolarization-induced glutamate release was induced by 4-aminopyridine, which is a K^+-channel inhibitor (137). TOLP, PGB, or their combination was applied at 100, 250, and 100 + 250 μM, respectively. 4-aminopyridine-induced

transmitter release through sodium and calcium channels activation (138) that was inhibited by TOLP but not by PGB, according to our previous study (74). In the current study, the TOLP/PGB combination significantly inhibited 4-aminopyridine-induced glutamate release (one-way ANOVA: F (3, 24) = 8.686, p = 0.0004, Dunnett's post-hoc test: 100 μM TOLP, p = 0.0012; 100 μM TOLP and 250 μM PGB, p = 0.0016) as shown in Figure 8.

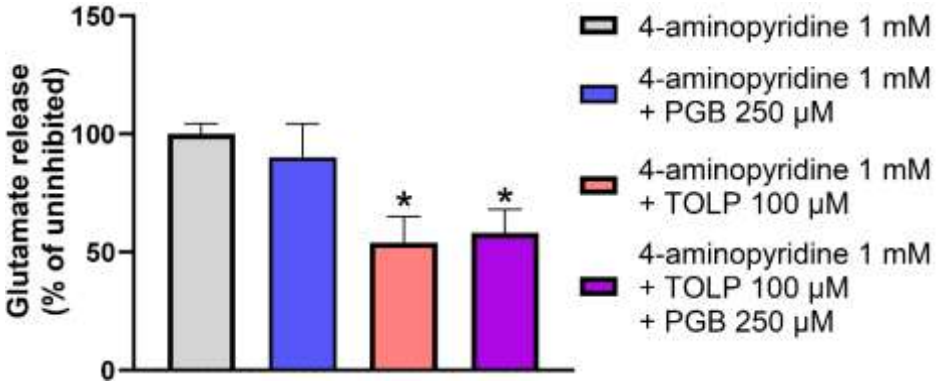

Figure 8. shows the impact of 100 μM of TOLP, 250 μM of PGB, or their combination on 1 mM 4-aminopyridine-evoked glutamate release from rat brain synaptosomes. Twenty min before stimulation, tested drugs were given as a pretreatment, and six min after stimulation, released glutamate concentration was detected. All data points were normalized using the unstimulated baseline release and expressed as % of the stimulated glutamate release in the absence of the tested drugs (gray bar). Values are presented as the mean of glutamate release ± SEM in % in the indicated groups. In each treatment group, 4–13 parallel experiments were used. Data were analyzed by one-way ANOVA and Dunnett's post-hoc test, *P < 0.05 means statistical significance versus stimulated glutamate release by 1 mM 4-aminopyridine alone and treatment groups.

4.7. The Effect of Acute Oral Administration of PGB, TOLP, or their Combination on Peripheral Diabetic Polyneuropathy in Rats

The promising combination, TOLP/PGB (25 mg/kg), was further investigated in peripheral diabetic polyneuropathy induced by STZ in rats. Diabetes mellitus was induced based on our previous investigation (79). Type 1 diabetes-induced allodynia was induced by intraperitoneal injection of a single large dose of STZ (60 mg/kg). After 72 hr, significant hyperglycemia was observed in diabetic rats compared to age-matched non-diabetic rats that were kept till the end of the study (9 weeks), as shown in Figure 9a.

There was a significant change in body weight of the diabetic and age-matched non-diabetic rats that was detected after the first week and thereafter (Figure 9b).

Three weeks after diabetes induction, tactile allodynia was detected by DPA and evidenced by the reduction in the PWTs of both paws that was maintained till week 9. Tactile allodynia was measured every third week till the end of the study period (Figure 9c). To investigate the effect of body weight on the PWT, weight-matched non-diabetic rats were also used (Figure 9d). We found similar PWTs between both weight-matched and age-matched non-diabetic rats after 9 weeks at all tested time points. Therefore, in this experiment, age-matched non-diabetic rats were selected for comparison (9e). Nine weeks after STZ injection, tested drugs (TOLP and PGB) at 25 mg/kg and their combination were given orally, and tactile allodynia was tested at 60 and 120 min after treatment. Of the given treatments, only PGB treatment significantly alleviated the tactile allodynia 120 min post-administration (one-way ANOVA: $F(11, 31) = 7.167$, $p < 0.0001$, Dunnett's post-hoc test: $p = 0.0139$) (Figure 9f).

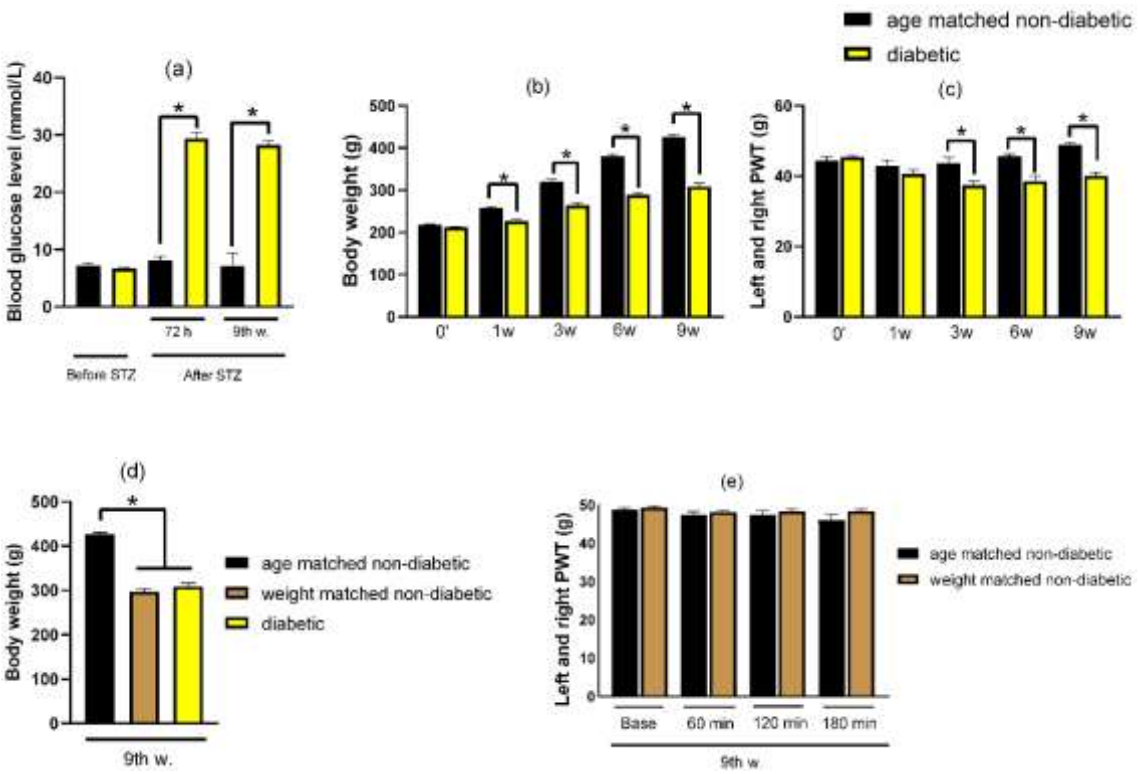

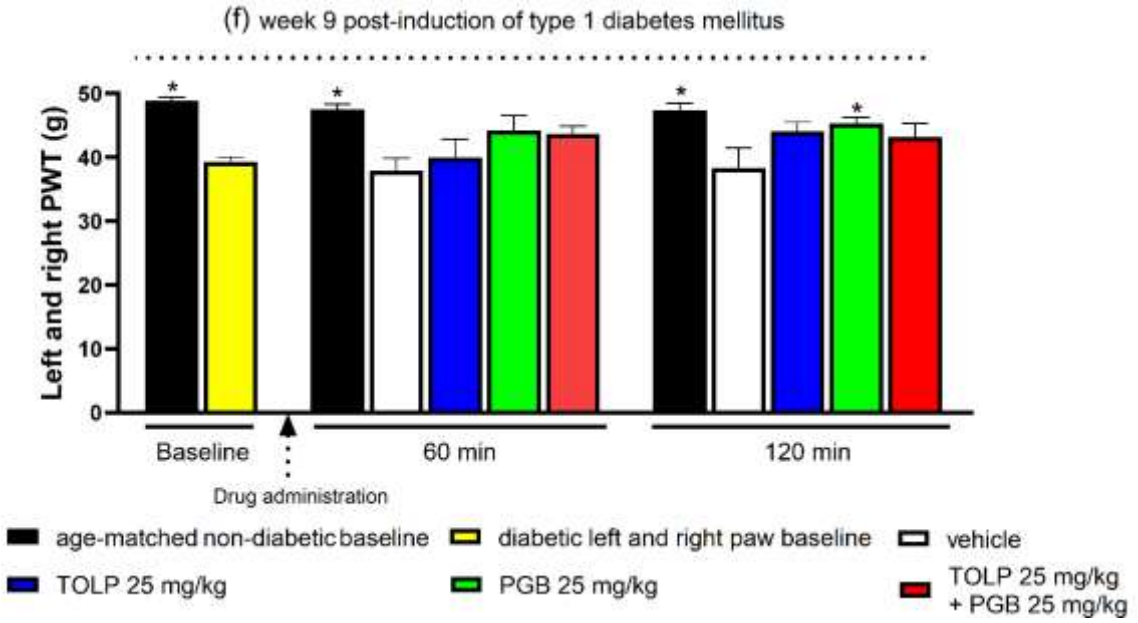

Figure 9. shows the level of blood glucose panel (a), age-matched non-diabetic and diabetic rats' body weight over the study period panel (b), PWTs of both paws in diabetic and age-matched non-diabetic rats over the study period panel (c), age-, weight-matched non-diabetic, and diabetic animals' body weight at the ninth-week panel (d), and age and weight-matched non-diabetic rats' PWTs of both paws at the ninth-week at 60, 120, and 180 min panel (e). Values are presented as mean ± S.E.M. of 6 weight-matched non-diabetic, 6 age-matched non-diabetic, and 20 diabetic rats. Data were analyzed by unpaired t-test for panels (a-c, e). For panel (d), one-way ANOVA and Dunnett's post-hoc test were used. *P < 0.05 means statistical significance versus the age-matched non-diabetic rats. Figure 9f shows the acute antiallodynic impact of TOLP (25 mg/kg), PGB (25 mg/kg), or their combination on type 1 diabetes-induced tactile allodynia. Nine weeks after diabetes induction, the left and right PWT was measured by DPA at 60 and 120 min after acute oral administration. Values are presented as the mean ± S.E.M. of 3–5 animals/group. Data were analyzed by one-way ANOVA and Dunnett's post-hoc test. *P < 0.05 means statistical significance versus the vehicle-treated rats. Baseline: PWTs measured before the treatment.

4.8. Acute PGB Treatment Induced a Significant Increase in the Spinal Cord MOR Protein Level in Rats with Peripheral Diabetic Polyneuropathy

To decipher the mechanism by which only PGB, among the tested drugs (see Figure 9f), produced a significant antiallodynic effect against allodynia developed as a consequence

of persistent high glucose levels in diabetic neuropathic rats, spinal cord tissues from diabetic neuropathic rats were subjected to measurement using Western blotting to quantify if there is an alteration in the protein level of MOR in response to treatments. For this purpose, tissues from rats acutely treated with TOLP (25 mg/kg), PGB (25 mg/kg), or their combination were used. The vehicle-treated diabetic rats showed a decrease in the MOR protein level compared to the age- or weight-matched non-diabetic rats. After acute treatment with the tested compounds, only PGB alone induced a significant elevation in MOR protein level compared to the vehicle-treated diabetic rats (Figure 10). This study suggests a connection between the opioid system and diabetic neuropathy, but more research is necessary to reach a firm conclusion.

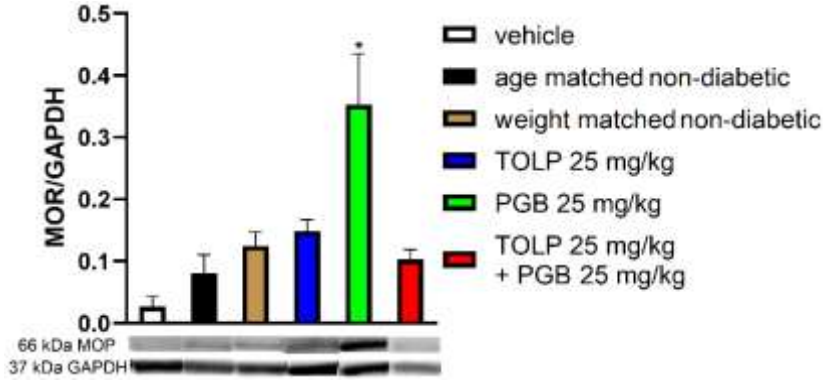

Figure 10. Spinal cord MOR protein levels relative to GAPDH after acute treatment in diabetic and non-diabetic rats. Representative bands are taken from the same membrane. Values are presented as mean ± S.E.M of 5-6 tissues/group. Data were analyzed by One-way ANOVA and Dunnett's post-hoc test, *P < 0.05 means statistical significance versus the vehicle group.

4.9. PGB but not TOLP Delays the Development of Morph Antinociceptive Tolerance in the Rat Tail-Flick Assay

The acute antinociceptive effect of 10 mg/kg Morph (s.c.) and per os 100 mg/kg TOLP or PGB was assessed by the rat tail-flick assay acutely on the first day and after 10 days of chronic treatment (Figure 11). Morph (10 mg/kg, s.c.) displayed a significant antinociceptive effect after acute administration (1st day) that peaked at 60 min (100 %) following treatment and was retained until 120 min (panel a). After 10 days of chronic treatment, this effect was significantly decreased, indicating the development of Morph antinociceptive tolerance (38.38 % at 30 min and 22.39 % at 60 min, Panel c). Acute or

chronic administration of TOLP per se did not show antinociception at all tested time points (Figure 11a, b, c). On the other hand, acute Morph administration alone or in combination with PGB or TOLP produced comparable effects and was statistically significant in comparison to the group that received vehicle. At day 10, the chronic treatment with the combination of Morph and TOLP did not exhibit an antinociceptive effect, yet it showed a comparable effect to that seen in vehicle or Morph groups (panels a, b, c). This indicates that TOLP has no impact on Morph antinociceptive tolerance. Finally, when compared to the effects of vehicle or Morph per se chronic treatment, Morph/PGB combination showed a significant antinociceptive effect (panel c), indicating that PGB delays the development of Morph antinociceptive tolerance.

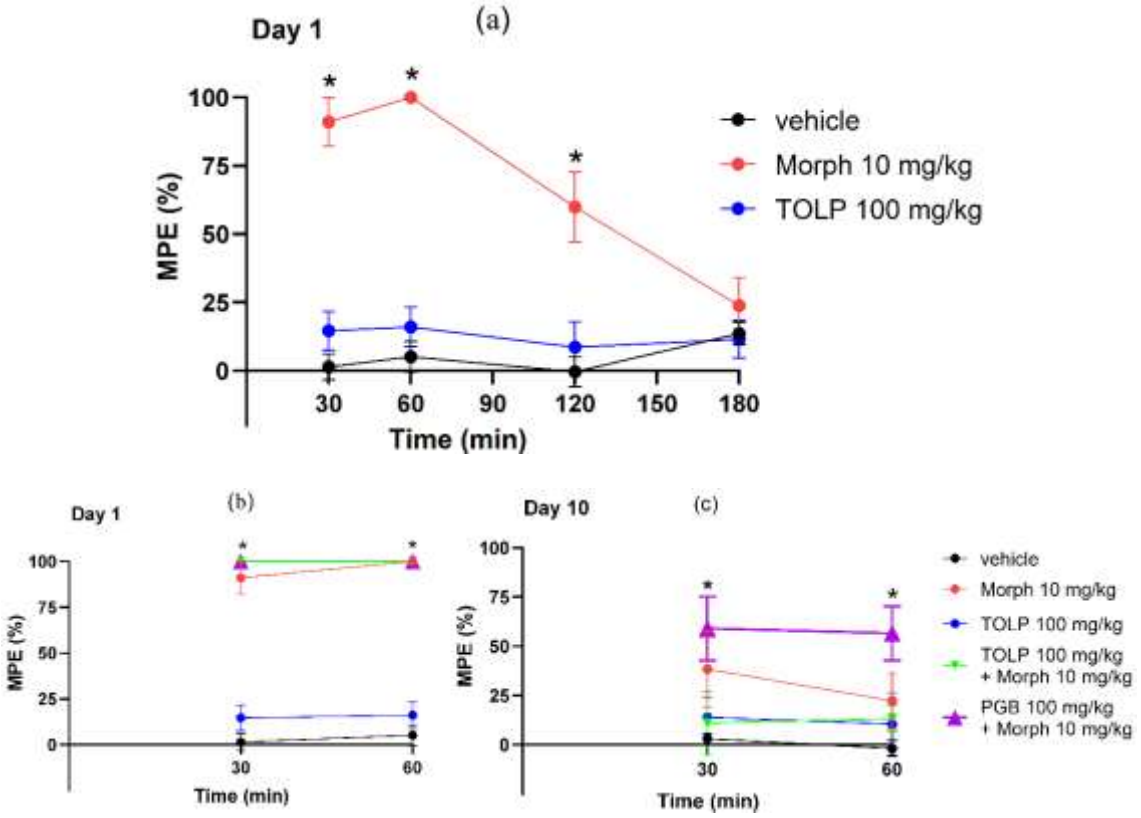

Figure 11. Panel (a) shows the effect of acute treatment with s.c. 10 mg/kg Morph, oral 100 mg/kg TOLP, or their vehicle on the tail-flick latency of naïve rats expressed as % MPE and measured at 30, 60, 120, and 180 min after administration (Day 1). Panels b and c show the acute and chronic effects, respectively, of TOLP (100 mg/kg, per os), Morph (10 mg/kg, s.c.), either alone or co-administered with oral 100 mg/kg of TOLP or PGB on the tail-flick latency of rats (% MPE) measured at 30 and 60 min after administration. Acute treatment (Day 1, panel b) and following 10 days of chronic

treatment (Day 10, panel c). Data were analyzed by two-way ANOVA followed by Dunnett's post hoc test. Values are presented as mean ± S.E.M of 5-6 animals/group. *P < 0.05 indicates statistical significance versus the vehicle group.

4.10. D-serine but not Glycine Levels are Decreased in Rat Cerebrospinal Fluid After Chronic Concurrent Treatment with Morph and PGB

To have insight into the possible mechanisms underlying the development of Morph antinociceptive tolerance, we have measured D-serine and glycine levels in CSF obtained from rats treated for 10 days with Morph, TOLP, or a Morph combination with either TOLP or PGB (Figure 12). Co-administering PGB with Morph resulted in a decrease in D-serine level compared to the vehicle group. It is worth noting that the TOLP/Morph combination was able to reduce the D-serine level, however, this decrease was not significant (panel a). On the other hand, none of the treatment groups affected the glycine levels compared to the vehicle group (panel b).

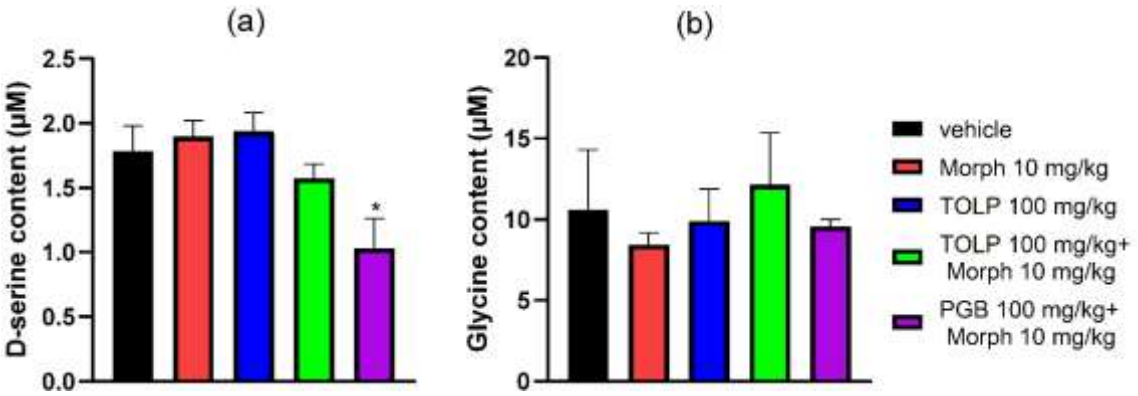

Figure 12. CSF D-serine (panel a) or glycine (panel b) content of rats chronically treated with Morph, TOLP, or Morph combination with either TOLP or PGB. Values are presented as mean ± SEM of 3–5 animals/group. Data were analyzed by one-way ANOVA and Dunnett's post-hoc test; *P < 0.05 indicates statistical significance versus the vehicle group.

4.11. TOLP and PGB Combination Produces a More Potent inhibitory Effect than TOLP or PGB Per se in Isolated Mouse Vas Deferens

In order to examine how the combination of TOLP and PGB affected MVD contraction induced by electrical field stimulation, the effect of each test compound was first assessed independently. As controls, Morph and DAMGO were used. The E_{max} of test compounds

was calculated from the concentration-response curves and served as a parameter to indicate the magnitude of the efficacy of the tested compounds. Before the drugs were administered, a calibration time of 50–60 minutes was used, as explained in section 3.14. As depicted in Figure 13a, TOLP, PGB, Morph, or DAMGO, in a concentration-dependent manner, inhibited the electrically evoked MVD smooth muscle contractions. The measured E_{max} for TOLP, PGB, Morph, or DAMGO was 84.85, 36.57, 74.01, or 91.06%, respectively. Next, TOLP, PGB, and Morph at concentrations that produced an equipotent inhibitory effect (20% inhibition) were tested separately or in drug combinations. In these series of experiments, the submaximal concentrations chosen were 1000 nM, 10000 nM, and 25 nM for TOLP, PGB, and Morph, respectively (Figure 13b). As a result, only the TOLP/PGB-based combination produced 26% inhibition versus 16% evoked by either TOLP or PGB per se (Figure 13b). This character was not seen when TOLP or PGB was combined with Morph.

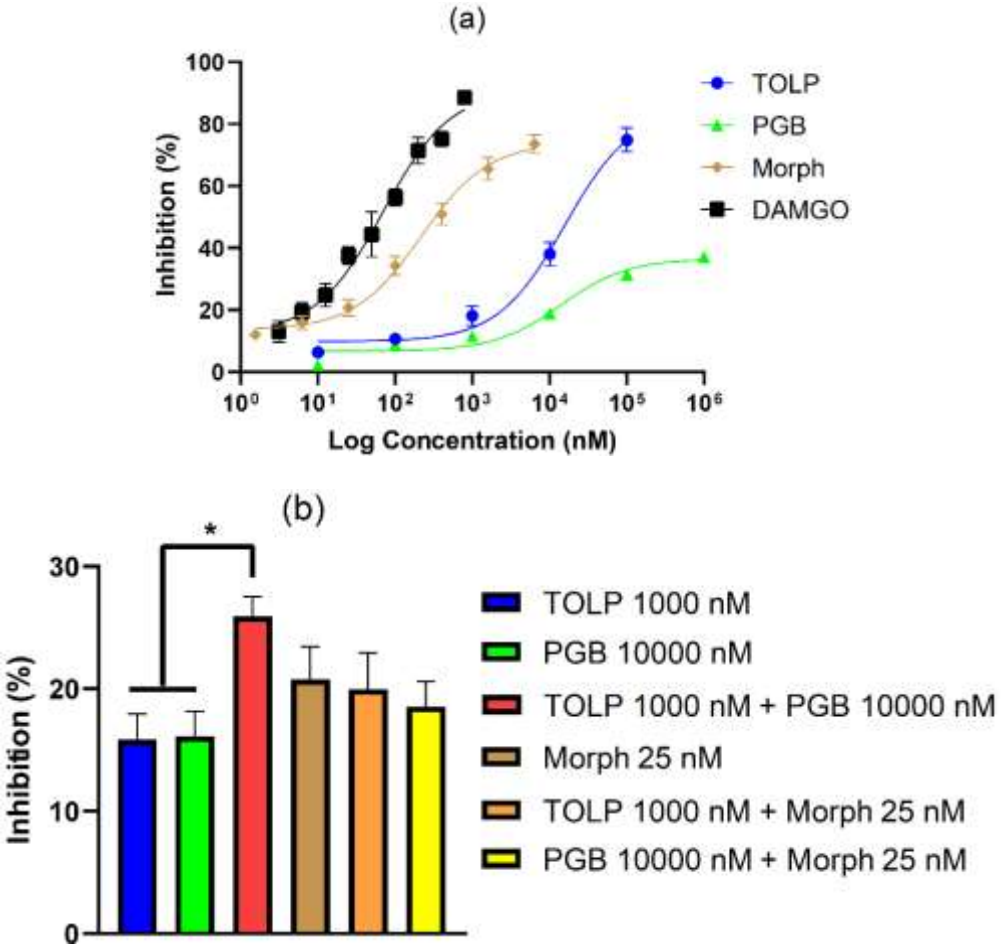

Figure 13. Shows the effect of tested compounds on isolated MVD assay. (a) shows the concentration-response curves for TOLP, PGB, Morph, and DAMGO. TOLP (10-100000 nM), PGB (10-1000000 nM), Morph (1.56-6400 nM), and DAMGO (3.125-800 nM) induced inhibition in the smooth muscle contractions in a concentration-dependent manner. E_{max} was calculated from individual concentration-response curves by nonlinear regression (Hill slope, three parameters) of logarithmic concentration-response curves. Values are presented as the mean ± SEM of n = 5-9. (b) shows the effect (%) of the submaximal concentrations of TOLP (1000 nM), PGB (10000 nM), and Morph (25 nM) alone and in combination on the contractions of the MVD in response to electrical stimulation. Values are presented as the mean ± SEM of n = 4-12. Data were analyzed by one-way ANOVA and Tukey's multiple comparisons post-hoc test, *P < 0.05 indicates statistical significance versus TOLP/PGB combination.

4.12. PGB and TOLP Restore the Developed Morph Tolerance in Isolated Mouse Vas Deferens

A 60.95% inhibitory effect of Morph (500 nM) was measured in MVD that received vehicle treatments. On the other hand, Morph produced a 27.22% inhibitory effect on muscle contractions of organs that underwent three consecutive treatments with 1000 nM Morph. These data indicate the development of Morph tolerance in MVD. Next, pretreatments with Morph (1000 nM) in the presence of 1000 nM PGB or 100 nM TOLP and Morph (500 nM) caused 59.35% and 46.28% inhibitory effects, respectively. These data indicate that both PGB and TOLP when co-administered with Morph, restore the developed Morph tolerance in MVD. It is worth noting that 1000 nM PGB and 100 nM TOLP per se produce an equipotent inhibitory effect, namely, 13.82% and 10.73%, respectively (Figure 14), and this effect was statistically significant compared to their combinations with Morph (Figure 14).

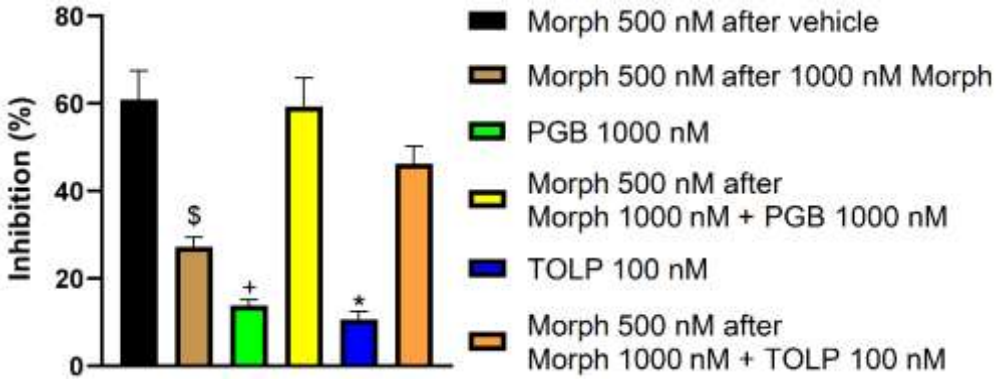

Figure 14. shows the effect of 100 nM TOLP or 1000 nM PGB co-administered with 1000 nM Morph on the developed Morph tolerance in isolated mouse vas deferens. Values are presented as the mean ± SEM of n = 5-11. Data were analyzed by one-way ANOVA and Tukey's multiple comparisons post-hoc test. *P < 0.05 indicates statistical significance versus (Morph 500 nM after Morph 1000 nM + TOLP 100 nM), $^{+}$P < 0.05 indicates statistical significance versus (Morph 500 nM after Morph 1000 nM + PGB 1000 nM), and $^{\$}$P < 0.05 indicates statistical significance versus (TOLP 100 nM).

4.13. The Effect of PGB, TOLP, and PGB/TOLP Combination on Motor Coordination and Balance in Naïve Rats

Acute oral treatment with PGB at doses of 50 and 100 mg/kg induced motor dysfunction and coordination imbalance in naïve rats, as confirmed by a significant reduction in the latency time, a time when the animal can stay on the rotating rod (one-way ANOVA: F (13, 84) = 11.12, p < 0.0001, Dunnett's post-hoc test: 50 mg/kg, 60 min, p = 0.0326; 100 mg/kg, 60 min, p = 0.0010, 50 mg/kg; 120 min, p < 0.0001, 100 mg/kg; 120 min, p < 0.0001). However, oral administration of 100 and 150 mg/kg of TOLP and 25 mg/kg of PGB didn't affect the motor function and coordination of naïve rats. After oral administration, the TOLP/PGB combination (both at 25 mg/kg) didn't alter rats' motor coordination and balance versus the vehicle-treated rats, either 60 or 120 min post-treatment (Figure 15).

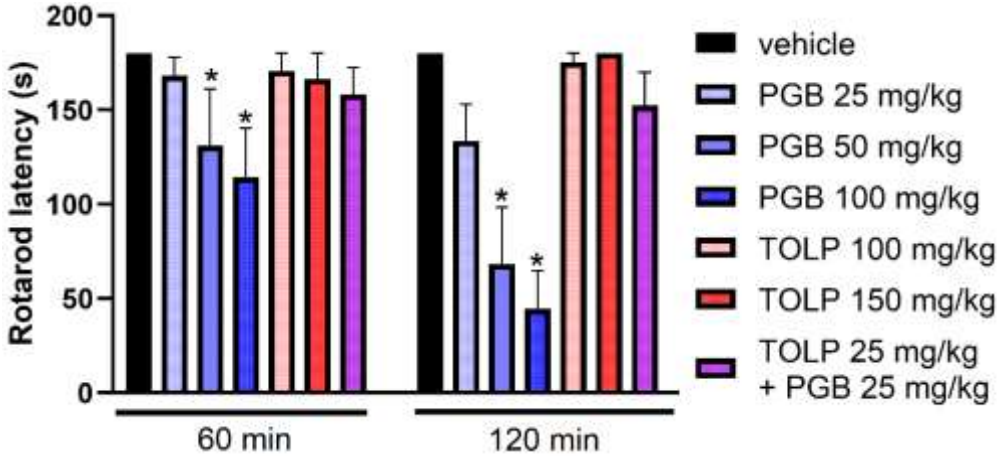

Figure 15. Impact of acute oral treatment of TOLP (100 and 150 mg/kg), PGB (25, 50, and 100 mg/kg), and TOLP/PGB combination (both at 25 mg/kg) or vehicle on motor coordination and balance of naïve rats at 60 and 120 min post-treatment. Columns show the time latency in the rotarod test. Values are presented as the mean ± SEM of 5–19 animals/group, measured at the peak effect of test drugs. Data were analyzed by one-way ANOVA and Dunnett's post-hoc test, *P < 0.05 means statistical significance versus the vehicle group.

4.14. The Impact of PGB, TOLP, and PGB/TOLP Combination on Gastrointestinal Transit in Naïve Rats

Treatment with 25 and 50 mg/kg of TOLP, 25 mg/kg of PGB, and TOLP/PGB combination both at 25 mg/kg, didn't elicit any delay in GI transit after oral charcoal suspension in naïve rats. On the other hand, acute treatment with 50 mg/kg of PGB induced a moderate delay in the GI transit in rats compared to the vehicle group, albeit such delay was statistically significant (one-way ANOVA: $F(5, 29) = 3.297$, $p = 0.0177$, Dunnett's post-hoc test: $p = 0.0110$), as shown in Figure 16.

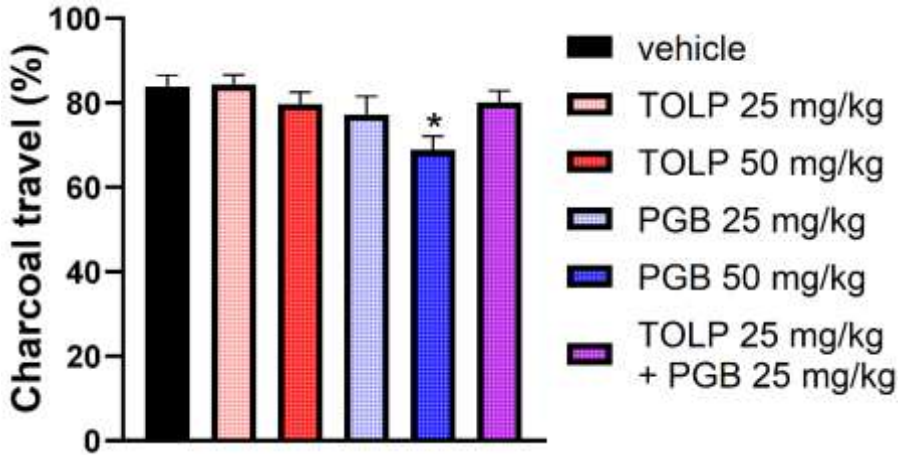

Figure 16. Impact of acute oral treatment of 25 and 50 mg/kg of TOLP, 25 and 50 mg/kg of PGB, and the TOLP/PGB combination both at 25 mg/kg on the GI transit of naïve rats 30 min post oral administration of a charcoal suspension. Columns show the % of charcoal travel in the charcoal meal test. Values are presented as the mean ± SEM of 5–6 animals/group, measured at the peak effect of test drugs. Data were analyzed by one-way ANOVA and Dunnett's post-hoc test, *P < 0.05 means statistical significance versus the vehicle group.

5. Discussion

Chronic pain, especially NP, is a debilitating condition that impacts the patient's everyday life and the income of the entire society. NP results from a disease or damage affecting the somatosensory neurons as defined by IASP (139). The various etiologies and the intricacy of the underlying mechanisms make treating painful neuropathy difficult. Although there are several monotherapy-based treatments available in the clinical setting, a high and variable number needed to treat (NNT) indicates that adequate NP control is still necessary (8). Therefore, the development of mono- or combination-based novel treatment approaches to treat NP remains a major unmet need. The potential for repurposing medications used to treat other diseases in clinical settings to manage NP is thus the focus of the current thesis. In addition, we sought for novel combination-based approaches to treat NP. In this regard, drugs with various modes of action are being applied in clinical settings in the hope of achieving analgesia of rapid onset, significant efficacy, and tolerable side effects (106). To this aim, we have focused on the mechanisms of the majority of first-line medications that are prescribed for various forms of NP as well as drugs that share pharmacological targets with them but are indicated for other diseases (8,140). In light of this, we have chosen TOLP because it has a pharmacodynamic effect hosted by drugs that are considered first or third-line medication to treat NP, namely the blockage of VGSCs and VGCCs, which are explained in more depth below (140). In this stage of the study, we examined the short-term and long-term antiallodynic effects of oral TOLP in an animal model of mono-neuropathic pain brought on by pSNL, comparing it to PGB, DUL, or CBZ administered per se. Then, applying the same pain model, we have further investigated the antiallodynic effect of TOLP combined with either PGB, DUL, or Morph. After that, we extended our study to investigate the antiallodynic effect of the effective combination of TOLP/PGB on type 1 diabetes-induced polyneuropathic pain in rats. Further investigations were being done to determine how glutamate, as an excitatory neurotransmitter, has been changed in the CSF of mono-neuropathic rats treated with either PGB, TOLP, or both. An imbalance between these two systems has been documented in numerous previous studies on animals with NP. Glutamate release from rat brain synaptosomes was further investigated in relation to treatments with either PGB, TOLP, or both. To further understand how TOLP and PGB affect transmitter release and their positive effects on NP and opioid antinociceptive

tolerance, the interaction between these two drugs was also examined in MVD. To look into the side effects, the impact of TOLP/PGB on motor coordination and balance, and GI transit was evaluated.

In line with our previous results, the potential mechanism implicated in the antiallodynic effect was also explored (74). In this regard, we have previously found that acute administration of TOLP or PGB alleviated mechanical allodynia in pSNL rats (74). However, herein, we used another technique, called DPA, which is applied to measure more localized tactile allodynia in a narrow dynamic range.

In order to assess the antiallodynic effect of the substances under test, the first step was to create a mono-neuropathic pain model in rats using the Seltzer technique that based on pSNL (120). Allodynia, the cardinal symptom of NP, was identified as the onset of NP. In our investigation, allodynia was confirmed by a decrease in the pain threshold of the operated paws on days 7, 14, and 21 following the operation, which is consistent with earlier works (120,141,142). In these trials, we have investigated the acute and chronic antiallodynic effects of the tested drugs, namely, TOLP, PGB, DUL, or CBZ. Days 7 and 14 following the operation were chosen as the two time points to assess the effects of the tested drugs following acute administration. Neuropathic rats were selected on day 7, following the baseline PWT measurement, and the tested drugs were administered orally. Then, the effect of these compounds was evaluated at 60, 120, and 180 min post-administration and considered as acute effects of the tested drugs. In terms of evaluating the long-term impact, the treatment was extended for 14 days, and the chronic antiallodynic effect was evaluated 1 week and 2 weeks after treatment on days 14 and 21 post-operation, respectively. In the current study, pSNL rat model was applied to test the effect of the single drugs or combination therapies against tactile allodynia within the indicated test period. We started the measurements on day 7 post-operation, and it was planned to end it before day 28, after which regeneration of the neurons occurs, which may conflict with our results (141,143).

The results obtained in these trials indicate that acute TOLP treatment failed to alleviate tactile allodynia of rats with mono-neuropathic pain. This ineffectiveness was also observed after acute treatment with PGB or DUL, first-line treatments for NP, and CBZ, a third-line therapy for NP (144,145). On the other hand, two weeks of chronic treatment with TOLP and PGB at doses of 100 mg/kg and 50 mg/kg, respectively, produced

significant antiallodynic effects that peaked at 60 minutes post-treatment. These rat doses are equivalent to 1000 mg and 500 mg in human doses, as calculated previously by other research teams (92,146). Our and other previous studies confirmed the development of tactile allodynia on day 7 after the ligation and continued till day 28 post-operation; based on that, study design, including the start of the treatment and the days for the PWT measurements, was established (120,147). The results of the acute treatment contrasted with our previous finding, where PGB or TOLP acutely alleviated mechanical allodynia evoked by pSNL. However, a different experimental tool was applied for the measurement of mechanical allodynia (74). To shed light on this, our previous study detected the mechanical allodynia using the Randall–Selitto assay. This assay evaluates how the tested compounds affect pain thresholds triggered by mechanical pressure, and although it is effective, it is generally considered a complement to cutaneous mechanical hyperalgesic assays (148). In contrast, the DPA was used in this work to detect static tactile allodynia, also known as cutaneous mechanical hyperalgesia, by applying a tiny metal filament to the rat's hind paw's plantar surface (141). This suggests that DPA detects tactile allodynia, which needs long-term medication therapy to relieve. Furthermore, in this assay, even first-line drugs like amitriptyline did not exhibit an anti-tactile allodynic effect following long-term therapy (141). Our lab has previously shown (121) that when DPA is employed, substantially higher analgesic doses are needed, which is considered a difference between DPA and Randall-Selitto. Apart from our previous results, herein, we have shown that TOLP is comparable to PGB in its ability to relieve tactile allodynia during long-term treatment.

In fact, several studies have reported conflicting results regarding the onset of the antiallodynic effect of either PGB or DUL (149–152). For example, an earlier study carried out by Kuo et al., 2021 reported the acute anti-allodynic and anti-hyperalgesic effects of 3-100 mg/kg per os bolus doses of PGB, whereas DUL acutely reversed the developed mechanical hyperalgesia in a dose-dependent manner (10 to 100 mg/kg) in cisplatin-induced peripheral neuropathy in rats (73). Additionally, three days of oral PGB administration alleviated the allodynia induced by cuffing the main branch of the sciatic nerve in mice, where allodynia was assessed by Von Frey filaments similar to our applied assay, DPA (153), though the phenotype of animal is different. Indeed, several factors could affect the analgesic effect of the tested compounds, PGB and DUL, including the

analgesic test, the administration route, and especially the type of NP being applied (108,154–158). Regarding the chronic effect of the tested drugs, both TOLP and PGB were able to induce an antiallodynic effect 2 weeks after treatment. Similar lag durations have been documented by a number of preclinical and clinical investigations for PGB, but not for TOLP because it has never been examined (159–161). This validates our new discovery about TOLP's antiallodynic activity in rats with preexisting tactile allodynia, and the findings support its potential use in NP management.

In the present work, in relation to DUL, no significant antiallodynic effect could be measured either after acute or 1 or 2 weeks of chronic oral administration in pSNL model, which conflicts with the previous results (162). DUL is an SNRI that was primarily used as an antidepressant. It facilitates the descending inhibitory pathway by inhibiting serotonin and norepinephrine reuptake to relieve pain (84). In 2004, the US Food and Drug Administration approved it as a first-line therapy for people suffering from painful diabetic peripheral neuropathy (163). DUL induces pain relief that starts sooner and at a lower dosage than that used for the treatment of depression, and its pain-relieving action is the same either in patients with or without depression (164). The descending serotonergic pathways for NP have been demonstrated to have either facilitative or inhibitory effects by several pharmacological studies, including SNRIs. The applied stimuli, the inconsistent techniques, and the time of pain measurement were all attributed to this controversial or inadequate effect of serotonin (165,166).

CBZ is a VGSC blocker that is used for the treatment of epilepsy and is used as an analgesic medication for the management of chronic pain, specifically trigeminal neuralgia (167–170). Several studies have discussed the effect of CBZ, either alone or in combination with other drugs, to treat NP. A previous preclinical study carried out by Fox et al. have explored that a single treatment with CBZ failed to reverse the developed mechanical hyperalgesia or tactile allodynia in pSNL rat model, whereas it reversed mechanical hyperalgesia in guinea-pig NP induced by pSNL (151,171). In the present study, CBZ failed to reverse the developed tactile allodynia either after acute or chronic administration in rats, which is consistent with the previously reported data. Furthermore, Hahm et al., 2012 reported that higher doses of the PGB/CBZ combination produced a synergistic antiallodynic effect in the spinal nerve ligation model in rats. This combination alleviated the developed allodynia when both drugs were administered at

dosages higher than the ED_{75} values. However, the side effects were not evaluated (172). Although trigeminal neuralgia is not the subject of the present work, it is important to note that several preclinical and clinical studies have examined the effectiveness of CBZ, gabapentin, and PGB in the management of trigeminal neuralgia (96,173–176).

In line with our and other previous studies, the acute antiallodynic effect of the TOLP, PGB, DUL, or CBZ was also tested on day 14 post-operation. None of the tested compounds induced significant antiallodynic effects in the mono-neuropathic rats. Regardless of the evaluation period, these data once again demonstrate that the tested compounds do not show an effect against tactile allodynia after acute administration, either 7 or 14 days post-operation. These outcomes compelled us to use a combination approach in the hopes of identifying a combination that has a fast onset antiallodynic effect. In this regard, we have kept in mind the pharmacodynamic profile of each in the combination to increase the chance of finding one that has an acute effect on tactile allodynia. Furthermore, it is widely acknowledged that combining drugs with distinct modes of action is unlikely to result in a more severe side effect. Therefore, in the present study, drugs that have different modes of action, such as PGB, DUL, or Morph, were combined with TOLP. CBZ works by blocking VGSCs, so its mechanism is similar to TOLP, in addition to its liver microsomal enzyme stimulatory effect (177,178); thereby, the TOLP/CBZ combination wasn’t evaluated. It is worth noting that it's too early to predict whether combining drugs will result in a lower or higher risk of side effects without having insight into the pharmacokinetic profile of both the combination and the individual drug. Future research is necessary to explore this issue further, since while these studies are essential, they are not part of the current work's scope and serve as a limitation. Herein, our results have demonstrated that TOLP/PGB, but not TOLP/DUL or TOLP/Morph, produced a significant antiallodynic effect after acute oral treatment on day 14 post-operation. To the best of our knowledge, this is the first study to investigate the acute antiallodynic effect of oral TOLP/PGB combination at low doses (25 mg/kg) in rats with mono-neuropathic pain. Also, a combination of TOLP/PGB is devoid of adverse effects related to motor incoordination and imbalance or delay in the GI transit of naïve rats. In fact, numerous clinical and preclinical studies have already examined the analgesic efficacy and safety of PGB per se or in combination with several medications, but not with TOLP, for NP management (179–183). The antiallodynic impact of the PGB

and TOLP combination is attributed to their ability to block the α_2-δ subunit of the VGCC in addition to different VGSCs, respectively (74,108,109,184). As a consequence, calcium influx is reduced, which in turn decreases excitatory neurotransmitter release from the primary afferent neuron's central terminal, particularly at the spinal cord level. It is important to note that these channels are targets for first-line drugs currently applied for treating different types of NP of mono- and polyneuropathic pain character (108,185–187). In recent decades, the uncovered mechanism of action of PGB in relation to NP relief has been extensively studied (109,188,189). Although PGB is a GABA analog, it does not interact with GABA receptors. The generally accepted mechanism of the effect of PGB on NP is attributed to its ability to block VGCCs on neurons that host the α_2-δ subunit, though new studies have revealed that it also has a facilitating effect on the descending pain pathway (108,190,191).

With respect to the mechanism of action of TOLP, the first proposed mechanism was the VGSC blocking effect (184,192) due to its chemical similarities with lidocaine, an approved local anesthetic that blocks the VGSCs and is used topically as first-line therapy for NP treatment (106). Also, a study by Kastrup and co-workers has shown that intravenous infusion of lidocaine can produce measurable analgesia in humans with chronic painful diabetic neuropathy (193). Since lidocaine has poor bioavailability after oral administration, it is thus inconvenient for long-term treatment by the intravenous route. Several medications, including mexiletine and phenytoin, that block VGSCs have been shown to have analgesic effects in humans with NP; however, controversial data were also reported (86,194–196). Thus, none of these medications are included in the most modern approaches of controlling NP. Recently, our group has also reported on the effectiveness of TOLP to decrease glutamate release from rat brain synaptosomes (74). This opens the door for its possible application in the treatment of NP by blocking the excitatory pain pathway, which uses glutamate as a neurotransmitter (30).

TOLP was originally used as a skeletal muscle relaxant and acts within the CNS. Several clinical trials have approved its efficacy in relieving post-stroke spasticity, painful reflex muscle spasms, and muscle-related pain (104). TOLP has also been reported to inhibit muscle spasms with an advantageous side effect profile compared to other centrally acting skeletal muscle relaxants (197). These properties encouraged us to test its effect in combination with PGB. The current study was carried out to find a new combination-

based therapy that has higher efficacy and fewer side effects. Regarding the side effects, PGB induces unwanted effects where more than 50% of patients are seen with excessive sedation (198). Considering previous findings along with our current data, the TOLP/PGB combination might be of clinical value, paving the way for drug repurposing. Peripheral nerve injury-induced NP triggers both peripheral and central sensitization, which further induce disturbance in the spinal excitatory and inhibitory systems (21). Elevations in spinal glutamate have been identified as a primary factor in the process behind NP development. Indeed, NMDAR blockers are among the effective management approaches for chronic pain (21,199). The inhibition of glutamate activity is being considered among the proposed mechanisms of mono- and polyneuropathic pain relief (59–62,66,74). In the current study, the CSF glutamate content was also measured, which was found to be increased in neuropathic rats. On the other hand, the increased level was restored by TOLP or PGB alone as well as by TOLP/PGB combination. Based on these data, we can assume that one of the mechanisms underlying the antiallodynic action of PGB, TOLP, or their combination is the suppression of the CNS's glutamate-based excitatory effect. It thereby corrects the imbalance between the pain-related excitatory and inhibitory circuits that arises in NP (21). In fact, the pathophysiology of NP in mammals involves the glutamatergic system in a more intricate way than just stimulating or inhibiting it.

To decipher the mechanism of action of TOLP, PGB, or their combination, we also assessed their impact on glutamate release from rat synaptosomes. Our findings support the in vivo results for TOLP but not for PGB in terms of glutamate release inhibition. This inhibitory trend was also observed with the combination. In the synaptosomes experiment, the neurotransmitter release induced by 4-aminopyridine mechanistically involves the contributions of both VGCCs and VGSCs. 4-Aminopyridine selectively blocks A-type potassium channels, initiating synaptic depolarization, yet evokes glutamate release in a tetrodotoxin-sensitive and calcium channel-dependent manner. It also generates repeated action potentials that resemble natural neuronal signaling (200). A preclinical study investigated how VGSCs affect the levels of intracellular sodium, potassium, and calcium, as well as the release of neurotransmitters such as dopamine, glutamate, and GABA in response to applying different concentrations of 4-aminopyridine to striatal synaptosomes. When a low concentration of 4-aminopyridine

was used, tetrodotoxin was able to block the increase in intracellular sodium. However, when a high concentration (1 mM) of 4-aminopyridine was applied, tetrodotoxin only reduced the rise in intracellular sodium by about 30 percent. Therefore, these data show that the impact of 4-aminopyridine on sodium levels and neurotransmitter release is concentration-dependent and implies a complex interaction between sodium channels and other cellular mechanisms (201). In another study, 1 mM of 4-aminopyridine induced glutamate release and an increase in cytosolic free calcium concentration were almost inhibited by tetrodotoxin. This indicates that glutamate release associated with 4-aminopyridine is largely dependent on VGSCs. These data support the distinct role of sodium channels in mediating transmitter release in this scenario (202).

Therefore, the inhibitory effect of TOLP can be attributed to its ability to block these channels, as mentioned above and as previously described by other research groups (137,200). This effect was also observed when TOLP was combined with PGB. The α_2-δ containing VGCCs have been reported to be upregulated under NP conditions, which may explain PGB's ability to inhibit glutamate content in vivo. In contrast, the synaptosomes used in this study were obtained from naïve animals, which are free from pathophysiological changes. To gain insight into the differences between the effect of PGB in synaptosomes and the in vivo conditions, synaptosomes should be prepared from neuropathic animals. Furthermore, these results explain the outcome of the present study under the given circumstances and the concentrations used. Finally, additional experiments are necessary to elucidate the extent of participation of each specific channel type within synaptosomes derived from animals with NP.

The current pharmacological treatment options for the treatment of NP include TCAs, SNRI antidepressants (DUL, venlafaxine), anticonvulsants (PGB, gabapentin), opioid analgesics, and topical medications (lidocaine, capsaicin) (203–205). The treatment options for PDPN type include PGB, gabapentin, DUL, opioid analgesics (tapentadol, tramadol), and 8% capsaicin; nonetheless, 35% of diabetic patients continue to experience pain (205–207). Despite the fact that VGSC blockers, specifically CBZ, are not included among the first-line medications to manage PDPN, they have historically been and continue to be used in certain cases for the management of diabetic neuropathy, indicating that VGSCs have an effect in this type of pain (208–210). In addition, the non-selective inhibitors of VGSCs with current clinical use, such as CBZ, lidocaine, and mexiletine,

have demonstrated effectiveness against certain pain conditions related to mutations in the NaV 1.7 channel. These mutations can cause pain by increasing their response to stimuli. NaV 1.7 variants have been reported to contribute to the development of NP in subjects with diabetic neuropathy (211,212).

Given these facts, the impact of the promising combination of TOLP/PGB was further investigated in type 1 diabetic polyneuropathy. In this test, we used a PDPN pain model of advanced diabetes, namely six weeks after allodynia onset and nine weeks following elevated blood glucose levels (Figure 9). The experiment showed that only acute PGB administration induced a more effective antiallodynic effect compared to the combination of TOLP and PGB, which was superior to the individual drugs in the pSNL rat model of mono-neuropathic pain. The antiallodynic effect of PGB in diabetic neuropathic rats was expected, as numerous preclinical and clinical studies have confirmed its efficacy in diabetic NP (213–216). On the other hand, TOLP alone or in combination with PGB failed to produce a significant effect. However, to the best of our knowledge, no studies have been reported on such treatment strategies in advanced rat diabetes at 9 weeks. Preclinical studies on allodynia in diabetic peripheral neuropathy have demonstrated a response to topical and systemic medications that block VGSCs, such as CBZ and lidocaine; however, there is currently no clinical evidence to support the use of oral lidocaine (217,218). However, drugs that block VGSCs, such as CBZ, have been shown to improve NP in diabetic patients following 12 weeks of treatment (219). It is worth mentioning that the mono-pharmacotherapy treatment algorithm recently published by Preston and coworkers shows that CBZ is considered a first-line medication in PDPN only in one guideline, which was issued by the American Academy of Neurology (220). As mentioned above, in contrast to PGB, several guidelines do not include CBZ as a first-line for PDPN (220,221). This indicates that inhibiting the VGCCs hosting the α_2-δ subunit is a more relevant target in NP evoked by diabetes. Indeed, the discovery of more selective blockers for individual VGSCs may be of future value in managing NP associated with diabetes (222). Even yet, the TOLP, which was administered orally and inhibits VGSC channels, was unable to have an impact that was significant in terms of inhibition of allodynia under the present experiment conditions. The concurrent administration of PGB did not improve this effect. Rigorous testing using a multiple-dose

strategy to assess the impact of acute versus chronic treatments with TOLP, alone or in combination with PGB, may develop an effective algorithm for managing PDPN.

Western blot analysis and immunohistological assays of spinal tissues from diabetic neuropathic rats revealed a decrease in MOR protein levels and numbers, as previously reported (79,223,224). Acute treatment with TOLP, PGB, and their combination tends to increase the MOR level, with a significant effect observed only following PGB treatment. These findings lend more credence to the earlier that the opioid system plays a role in the analgesic effects of both gabapentin and PGB (225–227). In this regard, previous studies have shown that acute PGB injection (100 mg/kg) induced an antinociceptive effect in the tail flick test in naive mice, and this effect was naloxone reversible (225). Furthermore, acute administration of gabapentin has been reported to elicit a naltrexone-sensitive antinociceptive effect in a model of acute inflammatory pain, namely the orofacial formalin test in mice (226). These data indicate the involvement of the endogenous opioid system since naloxone and naltrexone, the classical opioid antagonists, could reverse the analgesic effect of gabapentinoids. Nevertheless, future in-depth research is necessary to fully understand the effects of TOLP on PDPN type, taking into account both the drug's long-term effects alone and in combination with PGB. The current findings support its effectiveness in peripheral nerve injury-induced NP, especially in combination with PGB. A key limitation of this work was that, in the diabetic induced polyneuropathic pain model, only TOLP, PGB, and their combination were evaluated at a fixed dose of 25 mg/kg. Notably, the TOLP/PGB combination showed effectiveness solely in mono-neuropathic pain resulting from peripheral nerve injury. To gain a more comprehensive understanding, future research should investigate the antiallodynic impact of these drugs at different doses and explore potential alternative mechanisms of action. Additionally, assessing the effects of chronic administration of the combination in this and other NP models would help further validate its therapeutic potential.

Since TOLP's impact on the development of Morph antinociceptive tolerance has not yet been studied, we have also evaluated the impact of TOLP alone versus PGB or their combination in this scenario. It is known that if opioid analgesics are used for a long time, the development of opioid analgesic tolerance occurs. Rats treated with 10 mg/kg Morph developed significant antinociceptive tolerance in thermal pain models within 10 days

(132,228,229). Our results have corroborated those previously reported on Morph antinociceptive tolerance by our and other research teams using the rat tail-flick assay (132,230–232). The current findings highlight the fact that Morph antinociceptive tolerance development has been delayed by co-administered PGB, but not by TOLP. The role of NMDARs in Morph antinociceptive tolerance has been our primary focus to elucidate the mechanism of action, as NMDAR antagonists have been recognized to delay morphine analgesic tolerance in both preclinical and clinical settings (233–236). Among other mechanisms, NMDARs have been implicated in the development of NP and opioid tolerance, which are accompanied by central sensitization (237–241). NMDAR activation requires co-agonists such as glycine or D-serine in addition to glutamate; any change in the level of these co-agonists may affect the NMDARs function (242–244).

PGB and gabapentin inhibit Ca^{2+} influx into glutamatergic terminals by acting presynaptically on the α_2-δ subunit of VGCCs, subsequently attenuating the release of the excitatory amino acids, glutamate, and aspartate. A previous study demonstrated that intrathecal gabapentin not only enhances the antinociceptive effects of Morph but also reduces morphine tolerance by lowering excitatory amino acids (glutamate and aspartate) in CSF (245). In the present work, co-administering PGB with Morph resulted in a decrease in D-serine levels. This can be explained by the reduction in calcium influx by PGB leads to decreased activity of serine racemase, the enzyme responsible for converting L-serine to D-serine. This results in a lowering of the concentration of D-serine, which is an NMDA receptor co-agonist, so it decreases NMDA overactivity that has been reported in animals with opioid tolerance and may thus delay Morph tolerance (246). In addition, differences in the pharmacokinetics of both drugs could be the reason why the PGB/Morph combination but not the TOLP/Morph combination delays Morph antinociceptive tolerance. After oral administration, TOLP is quickly absorbed but has a low bioavailability of 16.7% (247). It is metabolized into hydroxymethyl-TOLP primarily by cytochrome P450 (CYP) enzymes, mainly CYP2D6, with minor contributions from CYP2C19 and CYP1A (248). In contrast, PGB shows about 90% oral bioavailability, which is consistent regardless of dose or dosing frequency, and undergoes minimal metabolism (249). It is extremely challenging to forecast the results of the interaction at the level of metabolism since we lack information on the interactions between the drugs

composing the tested combinations. Therefore, more research is needed to examine this matter.

In order to circumvent the in vivo drug metabolism, we have further examined the pharmacological characteristics of TOLP, PGB, Morph, and their combination in the MVD assay. This assay also enabled us to further decipher the mechanism underlying the effect and fast onset of the TOLP/PGB or Morph combination. This organ, besides hosting ion channels that mediate the effects of both PGB and TOLP, contains opioid, adrenergic, and purinergic receptors, among other receptors. The results obtained for TOLP, PGB, or Morph showed that all drugs induced an inhibitory effect on the MVD in a concentration-dependent manner, potentially through modulating calcium (250) and sodium channels (251) as well as MOR (252). The combined effect of PGB and TOLP was stronger than the effects of either medication per se. This feature was not present when TOLP and Morph were combined, though, which is consistent with the findings of studies intended to evaluate the effect of TOLP on Morph antinociceptive tolerance (see below). Our results suggest that the combination's acute antiallodynic impact in the current study may be explained by the simultaneous blocking of calcium and sodium channels, which is not limited to a single relay point on the pain transmission pathway.

As mentioned above, only the combination of TOLP and PGB showed a significant inhibitory effect on MVD contractions compared to the effect of TOLP or PGB per se. Additionally, the effects of PGB and TOLP on Morph-induced tolerance in this preparation have been assessed. The MVD test has been used for decades to evaluate the effects of various drugs. Studies have explored the potential for MVD to develop tolerance to morphine after multiple treatments. Regarding whether Morph tolerance develops in isolated MVD in conjunction with treating the organ or the entire animal, there is no agreement (253–255). In the current study, however, we discovered that Morph tolerance developed as a result of three consecutive treatments of MVD with 1000 nM Morph (see result section). These outcomes corroborate the findings from the PGB in vivo study, which was intended to look at how PGB affected Morph tolerance (see above). TOLP, on the other hand, inhibited the development of Morph tolerance in MVD but had no effect on Morph tolerance in rats. We may now speculate that factors related to pharmacokinetic and pharmacodynamic profiles, such as inhibitory effects on VGSCs and VGCCs, may play a major role in the current situation when it comes to Morph

antinociceptive tolerance. The impact of TOLP on the development of Morph tolerance in in vitro assays is very difficult to characterize and transfer to in vivo experiments appropriately; therefore, a more comprehensive study is required to fully define the mechanism of action beyond that.

In the MVD, both combinations were able to restore the developed Morph tolerance. This may be explained by TOLP's ability to act pre- and post-synaptically. Kocsis et al. (2005) showed that in an isolated hemisected spinal cord model, stimulation of the dorsal root evoked ventral root potentials (DR-VRP), which were recorded from the L5 ventral root. TOLP (50 to 400 μM) and its related compounds (eperisone, lanperisone, inaperisone, and silperisone) and lidocaine (200–800 μM) induced a concentration-dependent reduction in all measured DR-VRP components, suppressed monosynaptic reflexes, afferent fiber responses, and excitatory postsynaptic potentials (140).

Generally, when a combination therapy is developed, both the therapeutic and side effect profiles are considered. TOLP exerts a CNS-mediated skeletal muscle relaxant effect, lacking sedative effects, unlike other centrally acting muscle relaxants. Thus, we have anticipated that a combination of sub-analgesic doses of TOLP and PGB or Morph should have fewer side effects compared to mono-therapeutic dose of PGB per se. Our results are corroborated with previous data showing a significant motor dysfunction following oral PGB treatment, even in lower doses (187,256). With respect to TOLP, even higher oral doses (150 mg/kg) failed to alter the rats' motor function, supporting previous data that stated the absence of central side effects of TOLP (257). Since voltage-sensitive ion channels have indispensable pharmacological effects on GI function, we have extended our study to investigate the impact of TOLP and PGB or their combination in the GI tract. In this study, TOLP was devoid of GI side effects related to the GI transit. On the other hand, PGB induced a delay in GI transit, which is in line with previous data published by other research groups (258,259). In vitro, PGB strongly binds to the α_2-δ subunit of VGCSs, reducing calcium entry into presynaptic nerve terminals, thus decreasing the release of neurotransmitters participating in GI motility (260). Lastly, the PGB/TOLP combination, which showed promise in the NP model, was examined for GI transit. Regarding the side effects related to GI motility, our research has produced encouraging findings. As a result, the TOLP/PGB combination has opened up a new treatment option for NP that has a quick onset and fewer GI and motor adverse effects.

6. Conclusions

1. Like PGB, the onset of the antiallodynic effect of TOLP requires chronic treatment to be measured.
2. The present results for the first time suggest that the cooperation between TOLP and PGB, but not Morph, results in an acute anti-tactile allodynic effect of fast onset when combined. This suggests that it is worthwhile to use a combination of medications that target both VGSC and VGCC channels to treat NP acutely.
3. The fast onset of the TOLP/PGB combination may be attributed to the ability of the combination to inhibit glutamate release, the key transmitter in the neurochemical changes that occur in NP.
4. The fast onset of action of the TOLP/PGB combination may also be attributed to the ability of the single drugs to influence the glutamatergic system, a key player in NP development, through different mechanisms.
5. In the therapy of diabetic polyneuropathic pain, inhibition of VGCCs is more relevant than inhibition of VGSCs.
6. PGB's capacity to restore and even promote spinal opioid system function is one of its main advantageous effects in diabetic polyneuropathic pain.
7. The effect of PGB on delaying the development of Morph antinociceptive tolerance can be mediated by lowering the spinal level of D-serine, a co-agonist of NMDARs, a key transmitter in the development of opioid tolerance.
8. The augmented effect between drugs targeting VGSCs and VGCCs on MVD muscle contractions further supports the cooperation between the two channels in the context of transmitters' release.
9. The in vitro data related to Morph antinociceptive tolerance suggest that both VGSC and VGCC inhibitors can inhibit the development of opioid tolerance and point to the possibility of interference of pharmacokinetic factors when TOLP is investigated in the whole animal.

7. Summary

Two different pain models for NP, rat mono-neuropathic and polyneuropathic pains evoked by pSNL and STZ, respectively, were used. Tactile allodynia, which is the cardinal sign of NP, was assessed by DPA. TOLP and PGB produced an antiallodynic effect after 2 weeks of chronic treatment in rats with mono-neuropathic pain at 100 mg/kg and 50 mg/kg, respectively. As a novel finding, a combination of TOLP/PGB at the sub-antiallodynic doses (both at 25 mg/kg) has shown an acute anti-tactile allodynic effect of fast onset in the rat mono-neuropathic pain. Enhanced glutamate content in the CSF of neuropathic rats was measured. This elevation in glutamate contents was restored by the administration of either TOLP, PGB, or their combination. Likewise, except for PGB, this treatment strategy was able to decrease the glutamate release in vitro in the rat brain synaptosomes. The TOLP/PGB combination, which was proven to be effective against mono-neuropathic pain, was unable to reverse the established allodynia in rats with diabetic polyneuropathic pain under the current experimental conditions. However, only PGB per se caused a significant anti-tactile allodynic effect associated with an increase in the MOR level in the spinal tissue of treated rats. Morph antinociceptive tolerance was induced by chronic Morph treatments. Rats subjected to simultaneous treatment with Morph and PGB but not with TOLP have shown a delay in the development of Morph antinociceptive tolerance. D-serine level was low in the CSF samples of rats receiving chronic Morph/PGB but not TOLP/Morph combination. To avoid the systemic metabolism and interaction between the combined drugs, the possible mechanism of the interaction between TOLP and PGB or Morph was further investigated in the MVD assay. Combining TOLP with PGB, but not Morph, resulted in an augmented inhibitory effect in MVD muscle contraction evoked by field electrical stimulation. MVD treated with three subsequent Morph administrations has shown tolerance to Morph inhibitory effect. In this study, the development of Morph tolerance was inhibited by co-treatment with either PGB or TOLP. When comparing the in vitro and in vivo data, pharmacokinetic parameters may have an impact on the reported effects of TOLP with regard to Morph tolerance, which further urges more research. Finally, considering the side effects, the combination of TOLP/PGB has demonstrated significant promise in rat motor performance and GI transit.

8. References

1. Cao B, Xu Q, Shi Y, Zhao R, Li H, Zheng J, Liu F, Wan Y, Wei B. Pathology of pain and its implications for therapeutic interventions. *Signal Transduct Target Ther*. 2024 Jun 8;9(1):155.
2. Bouhassira D. Neuropathic pain: Definition, assessment and epidemiology. *Rev Neurol* (Paris). 2019;175(1–2):16–25.
3. Finnerup NB, Kuner R, Jensen TS. Neuropathic Pain: From Mechanisms to Treatment. *Physiol Rev*. 2021 Jan;101(1):259–301.
4. Jensen TS, Finnerup NB. Allodynia and hyperalgesia in neuropathic pain: clinical manifestations and mechanisms. *Lancet Neurol*. 2014 Sep;13(9):924–35.
5. Baskozos G, Hébert HL, Pascal MM, Themistocleous AC, Macfarlane GJ, Wynick D, Bennett DL, Smith BH. Epidemiology of neuropathic pain: an analysis of prevalence and associated factors in UK Biobank. *Pain rep*. 2023 Feb 8;8(2):e1066.
6. Breivik H, Collett B, Ventafridda V, Cohen R, Gallacher D. Survey of chronic pain in Europe: prevalence, impact on daily life, and treatment. *Eur J Pain*. 2006 May;10(4):287–333.
7. Debono DJ, Hoeksema LJ, Hobbs RD. Caring for patients with chronic pain: pearls and pitfalls. *J Am Osteopath Assoc*. 2013 Aug;113(8):620–7.
8. Finnerup NB, Attal N, Haroutounian S, McNicol E, Baron R, Dworkin RH, Gilron I, Haanpää M, Hansson P, Jensen TS, Kamerman PR. Pharmacotherapy for neuropathic pain in adults: a systematic review and meta-analysis. *The Lancet Neurol*. 2015 Feb 1;14(2):162-73.
9. Torrance N, Smith BH, Bennett MI, Lee AJ. The epidemiology of chronic pain of predominantly neuropathic origin. Results from a general population survey. *J Pain*. 2006 Apr;7(4):281–9.
10. Moulin DE, Boulanger A, Clark AJ, Clarke H, Dao T, Finley GA, Furlan A, Gilron I, Gordon A, Morley-Forster PK, Sessle BJ. Pharmacological

management of chronic neuropathic pain: revised consensus statement from the Canadian Pain Society. *Pain Res Manag*. 2014;19(6):328-35.

11. Van Hecke O, Austin SK, Khan RA, Smith BH, Torrance N. Neuropathic pain in the general population: a systematic review of epidemiological studies. *Pain*. 2014;155(4):654–62.

12. Zeng L, Alongkronrusmee D, van Rijn RM. An integrated perspective on diabetic, alcoholic, and drug-induced neuropathy, etiology, and treatment in the US. *J Pain Res*. 2017;219–28.

13. Scholz J, Finnerup NB, Attal N, Aziz Q, Baron R, Bennett MI, Benoliel R, Cohen M, Cruccu G, Davis KD, Evers S. The IASP classification of chronic pain for ICD-11: chronic neuropathic pain. *Pain*. 2019 Jan 1;160(1):53-9.

14. Attal N, Bouhassira D, Colvin L. Advances and challenges in neuropathic pain: a narrative review and future directions. *Br J Anaesth*. 2023 Jul 1;131(1):79-92.

15. Barrell K, Smith AG. Peripheral Neuropathy. *Med Clin North Am*. 2019 Mar;103(2):383-397.

16. Feldman EL, Nave KA, Jensen TS, Bennett DLH. New Horizons in Diabetic Neuropathy: Mechanisms, Bioenergetics, and Pain. *Neuron*. 2017 Mar 22;93(6):1296-1313.

17. Sun H, Saeedi P, Karuranga S, Pinkepank M, Ogurtsova K, Duncan BB, Stein C, Basit A, Chan JC, Mbanya JC, Pavkov ME. IDF Diabetes Atlas: Global, regional and country-level diabetes prevalence estimates for 2021 and projections for 2045. *Diabetes Res Clin Pract*. 2022 Jan 1;183:109119.

18. Phillips CJ. The Cost and Burden of Chronic Pain. *Rev Pain*. 2009 Jun;3(1):2–5.

19. Bannister K, Dickenson AH. Central Nervous System Targets: Supraspinal Mechanisms of Analgesia. *Neurotherapeutics*. 2020 Jul;17(3):839-845.

20. Sawynok J, Liu J. Contributions of peripheral, spinal, and supraspinal actions to analgesia. *Eur J Pharmacol*. 2014 Jul 5;734:114-21.

21. Al-Khrasani M, Mohammadzadeh A, Balogh M, Király K, Barsi S, Hajnal B, Köles L, Zádori ZS, Harsing Jr LG. Glycine transporter inhibitors: A new avenue for managing neuropathic pain. *Brain Res Bull*. 2019 Oct 1;152:143-58.

22. Baron R, Binder A, Wasner G. Neuropathic pain: diagnosis, pathophysiological mechanisms, and treatment. *Lancet Neurol*. 2010 Aug 1;9(8):807–19.

23. Meacham K, Shepherd A, Mohapatra DP, Haroutounian S. Neuropathic Pain: Central vs. Peripheral Mechanisms. *Curr Pain Headache Rep*. 2017 Jun 1;21(6):1–11.

24. Colloca L, Ludman T, Bouhassira D, Baron R, Dickenson AH, Yarnitsky D, Freeman R, Truini A, Attal N, Finnerup NB, Eccleston C. Neuropathic pain. *Nat Rev Dis Primers*. 2017 Feb 16;3.

25. Raja SN, Ringkamp M, Guan Y, Campbell JN. John J. Bonica Award Lecture: Peripheral neuronal hyperexcitability: the "low-hanging" target for safe therapeutic strategies in neuropathic pain. *Pain*. 2020 Sep 1;161(9):S14–26.

26. Ochoa JL, Campero M, Serra J, Bostock H. Hyperexcitable polymodal and insensitive nociceptors in painful human neuropathy. *Muscle Nerve*. 2005 Oct 1;32(4):459–72.

27. Wei SQ, Tao ZY, Xue Y, Cao DY. Peripheral Sensitization. *Trans St Johns Hosp Dermatol Soc*. 2019 Dec 4;56(2):178–9.

28. Gangadharan V, Kuner R. Pain hypersensitivity mechanisms at a glance. *Dis Models Mech.* 2013 Jul 1;6(4):889-95.

29. Devor M, Keller CH, Deerinck TJ, Levinson SR, Ellisman MH. Na^+ channel accumulation on axolemma of afferent endings in nerve end neuromas in Apteronotus. *Neurosci Lett*. 1989 Jul 31;102(2–3):149–54.

30. Lai J, Porreca F, Hunter JC, Gold MS. Voltage-gated sodium channels and hyperalgesia. *Annu Rev Pharmacol Toxicol*. 2004;44:371–97.

31. Dib-Hajj SD, Waxman SG. Sodium Channels in Human Pain Disorders: Genetics and Pharmacogenomics. *Annu Rev Neurosci*. 2019 Jul;42:87–106.

32. Bennett DL, Clark AJ, Huang J, Waxman SG, Dib-Hajj SD. The Role of Voltage-Gated Sodium Channels in Pain Signaling. *Physiol Rev.* 2019 Apr;99(2):1079–151.

33. Blesneac I, Themistocleous AC, Fratter C, Conrad LJ, Ramirez JD, Cox JJ, Tesfaye S, Shillo PR, Rice AS, Tucker SJ, Bennett DL. Rare NaV1.7 variants associated with painful diabetic peripheral neuropathy. *Pain*. 2018 Mar 1;159(3):469–80.

34. Chen L, Huang J, Zhao P, Persson AK, Dib-Hajj FB, Cheng X, Tan A, Waxman SG, Dib-Hajj SD. Conditional knockout of NaV1.6 in adult mice ameliorates neuropathic pain. *Sci Rep*. 2018 Mar 1;8(1):3845.

35. Eijkelkamp N, Linley JE, Baker MD, Minett MS, Cregg R, Werdehausen R, Rugiero F, Wood JN. Neurological perspectives on voltage-gated sodium channels. *Brain*. 2012 Sep 1;135(9):2585-612.

36. Goodwin G, McMahon SB. The physiological function of different voltage-gated sodium channels in pain. *Nat Rev Neurosci*. 2021 May;22(5):263-74.

37. Osteen JD, Immani S, Tapley TL, Indersmitten T, Hurst NW, Healey T, Aertgeerts K, Negulescu PA, Lechner SM. Pharmacology and Mechanism of Action of Suzetrigine, a Potent and Selective NaV1.8 Pain Signal Inhibitor for the Treatment of Moderate to Severe Pain. *Pain Ther*. 2025 Jan 8:1-20.

38. McCoun J, Winkle P, Solanki D, Urban J, Bertoch T, Oswald J, Swisher MW, Taber LA, Healey T, Jazic I, Correll DJ. Suzetrigine, a Non-Opioid NaV1.8 Inhibitor With Broad Applicability for Moderate-to-Severe Acute Pain: A Phase 3 Single-Arm Study for Surgical or Non-Surgical Acute Pain. *J Pain Res*. 2025;18:1569–76.

39. Jones J, Correll DJ, Lechner SM, Jazic I, Miao X, Shaw D, Simard C, Osteen JD, Hare B, Beaton A, Bertoch T. Selective inhibition of NaV1. 8 with VX-548 for acute pain. *N Engl J Med*. 2023 Aug 3;389(5):393-405.

40. Beninger P. Journavx (suzetrigine). Clinical Therapeutics. Elsevier Inc.; 2025.

41. NCT05660538. Evaluation of Efficacy and Safety of VX-548 for Painful Diabetic Peripheral Neuropathy (DPN). VX21-548-103.

42. Loeser JD, Treede RD. The Kyoto protocol of IASP Basic Pain Terminology. *Pain*. 2008 Jul;137(3):473–7.

43. Gracely RH, Lynch SA, Bennett GJ. Painful neuropathy: altered central processing maintained dynamically by peripheral input. *Pain*. 1992;51(2):175–94.

44. Woolf CJ. Evidence for a central component of post-injury pain hypersensitivity. *Nature*. 1983 Dec;306(5944):686–8.

45. Mayer ML, Westbrook GL, Guthrie PB. Voltage-dependent block by Mg^{2+} of NMDA responses in spinal cord neurones. *Nature*. 1984 May 17;309(5965):261-3.

46. Latremoliere A, Woolf CJ. Central sensitization: a generator of pain hypersensitivity by central neural plasticity. *J Pain*. 2009 Sep 1;10(9):895-926.

47. Temmermand R, Barrett JE, Fontana AC. Glutamatergic systems in neuropathic pain and emerging non-opioid therapies. *Pharmacol Res*. 2022 Nov 1;185:106492.

48. Sung B, Lim G, Mao J. Altered expression and uptake activity of spinal glutamate transporters after nerve injury contribute to the pathogenesis of neuropathic pain in rats. *J Neurosci*. 2003;23(7).

49. Al-Ghoul WM, Volsi GL, Weinberg RJ, Rustioni A. Glutamate immunocytochemistry in the dorsal horn after injury or stimulation of the sciatic nerve of rats. *Brain Res Bull*. 1993;30(3–4):453–9.

50. Mohammadzadeh A, Lakatos PP, Balogh M, Zádor F, Karádi DÁ, Zádori ZS, Király K, Galambos AR, Barsi S, Riba P, Benyhe S. Pharmacological evidence on augmented antiallodynia following systemic co-treatment with

glyt-1 and glyt-2 inhibitors in rat neuropathic pain model. *Int J Mol Sci*. 2021 Mar 2;22(5):1–15.

51. Wang H, Kohno T, Amaya F, Brenner GJ, Ito N, Allchorne A, Ji RR, Woolf CJ. Bradykinin produces pain hypersensitivity by potentiating spinal cord glutamatergic synaptic transmission. *J Neurosci*. 2005 Aug 31;25(35):7986-92.

52. Carvalho AL, Duarte CB, Carvalho AP. Regulation of AMPA receptors by phosphorylation. *Neurochem* Res. 2000 Oct;25:1245-55.

53. Lau CG, Zukin RS. NMDA receptor trafficking in synaptic plasticity and neuropsychiatric disorders. *Nat Rev Neurosci*. 2007 Jun;8(6):413-26.

54. Fagni L, Chavis P, Ango F, Bockaert J. Complex interactions between mGluRs, intracellular Ca^{2+} stores and ion channels in neurons. *Trends Neurosci*. 2000 Feb 1;23(2):80-8.

55. Yashpal K, Fisher K, Chabot JG, Coderre TJ. Differential effects of NMDA and group I mGluR antagonists on both nociception and spinal cord protein kinase C translocation in the formalin test and a model of neuropathic pain in rats. *Pain*. 2001 Oct 1;94(1):17-29.

56. Magnaghi V, Castelnovo LF, Faroni A, Cavalli E, Caffino L, Colciago A, Procacci P, Pajardi G. Nerve regenerative effects of GABA-B ligands in a model of neuropathic pain. *Biomed Res Int*. 2014;2014.

57. Davar G, Hama A, Deykin A, Vos B, Maciewicz R. MK-801 blocks the development of thermal hyperalgesia in a rat model of experimental painful neuropathy. *Brain Res*. 1991 Jul 12;553(2):327–30.

58. Mao J, Price DD, Mayer DJ, Lu J, Hayes RL. Intrathecal MK-801 and local nerve anesthesia synergistically reduce nociceptive behaviors in rats with experimental peripheral mononeuropathy. *Brain Res*. 1992 Apr 3;576(2):254-62.

59. Mao J, Price DD, Hayes RL, Lu J, Mayer DJ, Frenk H. Intrathecal treatment with dextrorphan or ketamine potently reduces pain-related behaviors in a

rat model of peripheral mononeuropathy. *Brain Res*. 1993 Mar 5;605(1):164-8.

60. Eisenberg E, LaCross S, Strassman AM. The clinically tested N-methyl-D-aspartate receptor antagonist memantine blocks and reverses thermal hyperalgesia in a rat model of painful mononeuropathy. *Neurosci Lett*. 1995 Feb 24;187(1):17-20.

61. Chaplan SR, Malmberg AB, Yaksh TL. Efficacy of spinal NMDA receptor antagonism in formalin hyperalgesia and nerve injury evoked allodynia in the rat. *J Pharmacol Exp Ther*. 1997 Feb 1;280(2):829-38.

62. Suzuki R, Matthews EA, Dickenson AH. Comparison of the effects of MK-801, ketamine and memantine on responses of spinal dorsal horn neurones in a rat model of mononeuropathy. *Pain*. 2001 Mar 1;91(1–2):101–9.

63. Qian J, Brown SD, Carlton SM. Systemic ketamine attenuates nociceptive behaviors in a rat model of peripheral neuropathy. *Brain Res*. 1996 Apr 9;715(1–2):51–62.

64. Bennett AD, Everhart AW, Hulsebosch CE. Intrathecal administration of an NMDA or a non-NMDA receptor antagonist reduces mechanical but not thermal allodynia in a rodent model of chronic central pain after spinal cord injury. *Brain Res*. 2000 Mar 17;859(1):72-82.

65. Holtman Jr JR, Crooks PA, Johnson-Hardy JK, Hojomat M, Kleven M, Wala EP. Effects of norketamine enantiomers in rodent models of persistent pain. *Pharmacol Biochem Behav*. 2008 Oct 1;90(4):676-85.

66. Chen SR, Samoriski G, Pan HL. Antinociceptive effects of chronic administration of uncompetitive NMDA receptor antagonists in a rat model of diabetic neuropathic pain. *Neuropharmacology*. 2009 Aug 1;57(2):121-6.

67. Saegusa H, Kurihara T, Zong S, Minowa O, Kazuno AA, Han W, Matsuda Y, Yamanaka H, Osanai M, Noda T, Tanabe T. Altered pain responses in mice lacking α1E subunit of the voltage-dependent Ca^{2+} channel. *Proc Natl Acad Sci U S A.* 2000 May 23;97(11):6132-7.

68. Staats PS, Hekmat H, Staats AW. The psychological behaviorism theory of pain and the placebo: its principles and results of research application. *Adv Psychosom Med*. 2004:25:28-40.

69. Ohashi N, Uta D, Ohashi M, Hoshino R, Baba H. Omega-conotoxin MVIIA reduces neuropathic pain after spinal cord injury by inhibiting N-type voltage-dependent calcium channels on spinal dorsal horn. *Front Neurosci*. 2024 Feb 26;18:1366829.

70. Vedder H, Otten U. Biosynthesis and release of tachykinins from rat sensory neurons in culture. *J Neurosci Res*. 1991 Oct;30(2):288-99.

71. Attal N. Pharmacological treatments of neuropathic pain: The latest recommendations. *Rev Neurol (Paris)*. 2019 Jan 1;175(1-2):46-50.

72. Chincholkar M. Gabapentinoids: pharmacokinetics, pharmacodynamics and considerations for clinical practice. *Br J Pain*. 2020 May;14(2):104-14.

73. Kuo A, Corradini L, Nicholson JR, Smith MT. Assessment of the anti-allodynic and anti-hyperalgesic efficacy of a glycine transporter 2 inhibitor relative to pregabalin, duloxetine and indomethacin in a rat model of cisplatin-induced peripheral neuropathy. *Biomolecules*. 2021 Jun 24;11(7):940.

74. Lakatos PP, Karádi DÁ, Galambos AR, Essmat N, Király K, Laufer R, Geda O, Zádori ZS, Tábi T, Al-Khrasani M, Szökő É. The Acute Antiallodynic Effect of Tolperisone in Rat Neuropathic Pain and Evaluation of Its Mechanism of Action. *Int J Mol Sci*. 2022;23(17).

75. Guyton ACMD. Textbook of medical physiology. China; 2006.

76. Bourne S, Machado AG, Nagel SJ. Basic anatomy and physiology of pain pathways. *Neurosurg Clin*. 2014;25(4):629–38.

77. Moon HC, Park YS. Reduced GABAergic neuronal activity in zona incerta causes neuropathic pain in a rat sciatic nerve chronic constriction injury model. *J Pain Res*. 2017 May 11:1125-34.

78. Lee MC, Nam TS, Jung SJ, Gwak YS, Leem JW. Modulation of Spinal GABAergic Inhibition and Mechanical Hypersensitivity following Chronic Compression of Dorsal Root Ganglion in the Rat. *Neural Plast*. 2015;2015(1):924728.

79. Balogh M, Zádor F, Zádori ZS, Shaqura M, Király K, Mohammadzadeh A, Varga B, Lázár B, Mousa SA, Hosztafi S, Riba P. Efficacy-based perspective to overcome reduced opioid analgesia of advanced painful diabetic neuropathy in rats. *Front Pharmacol*. 2019 Apr 9;10:347.

80. Reeves KC, Shah N, Muñoz B, Atwood BK. Opioid receptor-mediated regulation of neurotransmission in the brain. *Front Mol Neurosci*. 2022 Jun 15;15:919773.

81. Cherny NI. Opioid analgesics: comparative features and prescribing guidelines. *Drugs*. 1996 May;51(5):713-37.

82. Dick IE, Brochu RM, Purohit Y, Kaczorowski GJ, Martin WJ, Priest BT. Sodium Channel Blockade May Contribute to the Analgesic Efficacy of Antidepressants. *J Pain.* 2007;8(4).

83. Obata H. Analgesic mechanisms of antidepressants for neuropathic pain. *Int J Mol Sci*. 2017 Nov 21;18(11):2483.

84. Woolf CJ. Pain: moving from symptom control toward mechanism-specific pharmacologic management. *Ann Intern Med*. 2004 Mar;140(6):441–51.

85. Finnerup NB, Sindrup SH, Jensen TS. The evidence for pharmacological treatment of neuropathic pain. *Pain*. 2010 Sep;150(3):573–81.

86. Kalso E. Sodium Channel Blockers in Neuropathic Pain. *Curr Pharm Des*. 2005;11(23).

87. Hine LK, Laird N, Hewitt P, Chalmers TC. Meta-analytic evidence against prophylactic use of lidocaine in acute myocardial infarction. *Arch Intern Med.* 1989;149(12).

88. Beaussier M, Delbos A, Maurice-Szamburski A, Ecoffey C, Mercadal L. Perioperative Use of Intravenous Lidocaine. *Drugs*. 2018 Aug;78(12):1229-1246.

89. Lee IWS, Schraag S. The Use of Intravenous Lidocaine in Perioperative Medicine: Anaesthetic, Analgesic and Immune-Modulatory Aspects. *J Clin Med.* 2022 Jun 20;11(12):3543.

90. Smith ER, Duce BR, Boyes RN. Antiarrhythmic effects in dogs of lidocaine administered orally and intravenously. *Am Heart J*. 1972;83(3).

91. Chaplan SR, Bach FW, Shafer SL, Yaksh TL. Prolonged alleviation of tactile allodynia by intravenous lidocaine in neuropathic rats. *Anesthesiology*. 1995;83(4).

92. Nair A, Jacob S. A simple practice guide for dose conversion between animals and human. *J Basic Clin Pharm*. 2016;7(2).

93. Khaliq W, Alam S, Puri NK. Topical lidocaine for the treatment of postherpetic neuralgia. *Cochrane Database of Syst Rev*. 2007 Apr 18:(2):CD004846.

94. Voute M, Morel V, Pickering G. Topical Lidocaine for Chronic Pain Treatment. *Drug Des Devel Ther*. 2021;15:4091–103.

95. Mert T, Gunes Y. Antinociceptive activities of lidocaine and the nav1.8 blocker a803467 in diabetic rats. *J Ame Assoc Lab Anim Sci*. 2012;51(5).

96. Taylor JC, Brauer S, Espir MLE. Long-term treatment of trigeminal neuralgia with carbamazepine. *Postgrad Med J*. 1981 Jan 1;57(663):16–8.

97. Freo U, Romualdi P, Kress HG. Tapentadol for neuropathic pain: a review of clinical studies. *J Pain Res*. 2019 May 16:12:1537-1551.

98. Lee YC, Chen PP. A review of SSRIs and SNRIs in neuropathic pain. *Expert Opin Pharmacother*. 2010 Dec;11(17):2813-25.

99. McAnally H, Bonnet U, Kaye AD. Gabapentinoid Benefit and Risk Stratification: *Mechanisms Over Myth*. Vol. 9, Pain and Therapy. 2020.

100. Maloney J, Pew S, Wie C, Gupta R, Freeman J, Strand N. Comprehensive Review of Topical Analgesics for Chronic Pain. *Curr Pain Headache Rep*. 2021 Feb 3;25(2):7.

101. Faria J, Barbosa J, Moreira R, Queirós O, Carvalho F, Dinis-Oliveira RJ. Comparative pharmacology and toxicology of tramadol and tapentadol. *Eur J Pain*. 2018 May;22(5):827-44.

102. Meng Z, Yu J, Acuff M, Luo C, Wang S, Yu L, Huang R. Tolerability of Opioid Analgesia for Chronic Pain: A Network Meta-Analysis. *Sci Rep*. 2017;7(1).

103. Raffa RB, Clark-Vetri R, Tallarida RJ, Wertheimer AI. Combination strategies for pain management. *Expert Opin Pharmacother*. 2003 Oct;4(10):1697–708.

104. Pratzel HG, Alken RG, Ramm S. Efficacy and tolerance of repeated oral doses of tolperisone hydrochloride in the treatment of painful reflex muscle spasm: results of a prospective placebo-controlled double-blind trial. *Pain*. 1996;67(2–3):417–25.

105. Navratilova E, Nation K, Remeniuk B, Neugebauer V, Bannister K, Dickenson AH, Porreca F. Selective modulation of tonic aversive qualities of neuropathic pain by morphine in the central nucleus of the amygdala requires endogenous opioid signaling in the anterior cingulate cortex. *Pain*. 2020;161(3).

106. Bannister K, Sachau J, Baron R, Dickenson AH. Neuropathic Pain: Mechanism-Based Therapeutics. *Annu Rev Pharmacol Toxicol*. 2020 Jan 6;60:257–74.

107. Gilron I, Bailey JM, Tu D, Holden RR, Jackson AC, Houlden RL. Nortriptyline and gabapentin, alone and in combination for neuropathic pain: a double-blind, randomised controlled crossover trial. *Lancet*. 2009;374(9697):1252–61.

108. Field, M. J., Cox, P. J., Stott, E., Melrose, H., Offord, J., Su, T. Z., Bramwell, S., Corradini, L., England, S., Winks, J., Kinloch, R. A., Hendrich, J.,

Dolphin, A. C., Webb, T., & Williams, D. Identification of the alpha2-delta-1 subunit of voltage-dependent calcium channels as a molecular target for pain mediating the analgesic actions of pregabalin. *Proc Natl Acad Sci U S A*. 2006 Nov 14;103(46):17537-42.

109. Verma V, Singh N, Jaggi A. Pregabalin in Neuropathic Pain: Evidences and Possible Mechanisms. *Curr Neuropharmacol*. 2014;12(1).

110. Gilron I, Bailey JM, Tu D, Holden RR, Weaver DF, Houlden RL. Morphine, gabapentin, or their combination for neuropathic pain. *N Engl J Med*. 2005;352(13):1324–34.

111. Hanna M, O'Brien C, Wilson MC. Prolonged-release oxycodone enhances the effects of existing gabapentin therapy in painful diabetic neuropathy patients. *Eur J Pain*. 2008;12(6):804–13.

112. Zin CS, Nissen LM, O'Callaghan JP, Duffull SB, Smith MT, Moore BJ. A Randomized, Controlled Trial of Oxycodone Versus Placebo in Patients With Post-Herpetic Neuralgia and Painful Diabetic Neuropathy Treated With Pregabalin. *J Pain*. 2010;11(5):462–71.

113. Matthews EA, Dickenson AH. A combination of gabapentin and morphine mediates enhanced inhibitory effects on dorsal horn neuronal responses in a rat model of neuropathy. *Anesthesiology*. 2002;96(3):633–40.

114. Naseri K, Sabetkasaei M, Moini Zanjani T, Saghaei E. Carbamazepine potentiates morphine analgesia on postoperative pain in morphine-dependent rats. *Eur J Pharmacol*. 2012;674(2–3).

115. Jun IG, Park JY, Choi YS, Im SH. Effect of intrathecal oxcarbazepine on rat tail flick test-determined morphine tolerance. *Korean J Anesthesiol*. 2009;57(3).

116. Jun IG, Park JY, Choi YS, Kim T hee. Intrathecal lamotrigine blocks and reverses antinociceptive morphine tolerance in rats. *Korean J Anesthesiol*. 2009;56(6).

117. Zhang Y, Tao GJ, Hu L, Qu J, Han Y, Zhang G, Qian Y, Jiang CY, Liu WT. Lidocaine alleviates morphine tolerance via AMPK-SOCS3-dependent

neuroinflammation suppression in the spinal cord. *J Neuroinflammation*. 2017;14(1).

118. Saito Y, Kaneko M, Kirihara Y, Sakura S, Kosaka Y. Interaction of intrathecally infused morphine and lidocaine in rats (part II): effects on the development of tolerance to morphine. *Anesthesiology*. 1998 Dec 1;89(6):1464-70.

119. Balogh M, Varga BK, Karádi DÁ, Riba P, Puskár Z, Kozsurek M, Al-Khrasani M, Király K. Similarity and dissimilarity in antinociceptive effects of dipeptidyl-peptidase 4 inhibitors, Diprotin A and vildagliptin in rat inflammatory pain models following spinal administration. *Brain Res Bull*. 2019 Apr 1;147:78-85.

120. Seltzer Z, Dubner R, Shir Y. A novel behavioral model of neuropathic pain disorders produced in rats by partial sciatic nerve injury. *Pain*. 1990;43(2).

121. Király K, Kozsurek M, Lukácsi E, Barta B, Alpár A, Balázsa T, Fekete C, Szabon J, Helyes Z, Bölcskei K, Tékus V. Glial cell type-specific changes in spinal dipeptidyl peptidase 4 expression and effects of its inhibitors in inflammatory and neuropatic pain. *Sci Rep*. 2018 Feb;8(1):3490.

122. Jakó T, Szabó E, Tábi T, Zachar G, Csillag A, Szöko É. Chiral analysis of amino acid neurotransmitters and neuromodulators in mouse brain by CE-LIF. *Electrophoresis*. 2014 Oct 1;35(19):2870–6.

123. Modi J, Prentice H, Wu JY. Preparation, Stimulation and Other Uses of Adult Rat Brain Synaptosomes. *Bio Protoc*. 2017;7(24).

124. Shimamoto K. Glutamate transporter blockers for elucidation of the function of excitatory neurotransmission systems. *Chem Rec*. 2008 Jan 1;8(3):182–99.

125. Courteix C, Bardin M, Chantelauze C, Lavarenne J, Eschalier A. Study of the sensitivity of the diabetes-induced pain model in rats to a range of analgesics. *Pain*. 1994;57(2):153–60.

126. Rajaei Z, Hadjzadeh MAR, Nemati H, Hosseini M, Ahmadi M, Shafiee S. Antihyperglycemic and antioxidant activity of crocin in streptozotocin-induced diabetic rats. *J Med Food*. 2013 Mar 1;16(3):206–10.

127. Courteix C, Eschalier A, Lavarenne J. Streptozocin-induced diabetic rats: behavioural evidence for a model of chronic pain. *Pain*. 1993;53(1):81–8.

128. Hutka B, Várallyay A, László SB, Tóth AS, Scheich B, Paku S, Vörös I, Pós Z, Varga ZV, Norman DD, Balogh A. A dual role of lysophosphatidic acid type 2 receptor (LPAR2) in nonsteroidal anti-inflammatory drug-induced mouse enteropathy. *Acta Pharmacol Sin*. 2024 Feb 1;45(2):339–53.

129. Kiraly K, Caputi FF, Hanuska A, Kató E, Balogh M, Köles L, Palmisano M, Riba P, Hosztafi S, Romualdi P, Candeletti S. A new potent analgesic agent with reduced liability to produce morphine tolerance. *Brain Res Bull*. 2015;117:32–8.

130. Tulunay FC, Takemori AE. The increased efficacy of narcotic antagonists induced by various narcotic analgesics. *J Pharmacol Exp Ther*. 1974 Sep;190(3):395–400.

131. Gupta H, Verma D, Ahuja RK, Srivastava DN, Wadhwa S, Ray SB. Intrathecal co-administration of morphine and nimodipine produces higher antinociceptive effect by synergistic interaction as evident by injecting different doses of each drug in rats. *Eur J Pharmacol*. 2007;561(1–3).

132. Karádi DÁ, Galambos AR, Lakatos PP, Apenberg J, Abbood SK, Balogh M, Király K, Riba P, Essmat N, Szűcs E, Benyhe S. Telmisartan Is a Promising Agent for Managing Neuropathic Pain and Delaying Opioid Analgesic Tolerance in Rats. *Int J Mol Sci*. 2023;24(9).

133. Lacko E, Varadi A, Rapavi R, Zador F, Riba P, Benyhe S, Borsodi A, Hosztafi S, Timar J, Noszal B, Furst S. A novel μ-opioid receptor ligand with high in vitro and in vivo agonist efficacy. *Curr Med Chem*. 2012;19(27):4699–707.

134. Contreras EN, Martí MC. Sensitivity of mouse vas deferens to neurotransmitters: changes after morphine treatment. Br J Pharmacol. 1979 Apr;65(4):623.

135. Hanlon KE, Vanderah TW. Constitutive activity at the cannabinoid CB (1) receptor and behavioral responses. *Methods Enzymol*. 2010;484:3–30.

136. Zádor F, Balogh M, Váradi A, Zádori ZS, Király K, Szűcs E, Varga B, Lázár B, Hosztafi S, Riba P, Benyhe S. 14-O-Methylmorphine: A Novel Selective Mu-Opioid Receptor Agonist with High Efficacy and Affinity. *Eur J Pharmacol*. 2017 Nov;814:264–73.

137. Thesleff S. Aminopyridines and synaptic transmission. *Neuroscience*. 1980 Aug 1;5(8):1413-9.

138. Sanchez-Prieto J, Budd DC, Herrero I, Vázquez E, Nicholls DG. Presynaptic receptors and the control of glutamate exocytosis. *Trends Neurosci*. 1996;19(6):235–9.

139. Jensen TS, Baron R, Haanpää M, Kalso E, Loeser JD, Rice AS, Treede RD. A new definition of neuropathic pain. *Pain*. 2011;152(10):2204–5.

140. Kocsis P, Farkas S, Fodor L, Bielik N, Than M, Kolok S, Gere A, Csejtei M, Tarnawa I. Tolperisone-type drugs inhibit spinal reflexes via blockade of voltage-gated sodium and calcium channels. *J Pharmacol Exp Ther*. 2005 Dec 1;315(3):1237-46.

141. Esser MJ, Chase T, Allen G V., Sawynok J. Chronic administration of amitriptyline and caffeine in a rat model of neuropathic pain: multiple interactions. *Eur J Pharmacol*. 2001 Nov 2;430(2–3):211–8.

142. Attal N, Jazat F, Kayser V, Guilbaud G. Further evidence for “pain-related” behaviours in a model of unilateral peripheral mononeuropathy. *Pain*. 1990;41(2).

143. Jergova S, Cizkova D. Long-term changes of c-Fos expression in the rat spinal cord following chronic constriction injury. *Eur J Pain*. 2005 Jun 1;9(3):345–54.

144. Sharma U, Griesing T, Emir B, Young JPJ. Time to onset of neuropathic pain reduction: A retrospective analysis of data from nine controlled trials of pregabalin for painful diabetic peripheral neuropathy and postherpetic neuralgia. *Am J Ther*. 2010;17(6):577–85.

145. Rodrigues RF, Kawano T, Placido RV, Costa LH, Podesta M, Santos RS, Galdino G, Barros CM, Boralli VB. Investigation of the combination of pregabalin with duloxetine or amitriptyline on the pharmacokinetics and antiallodynic effect during neuropathic pain in rats. *Pain Physician*. 2021;24(4):E511.

146. Shin J woo, Seol I chan, Son C gue. Interpretation of Animal Dose and Human Equivalent Dose for Drug Development. *The Journal of Korean Oriental Medicine*. 2010;31(3).

147. Pan HL, Eisenach JC, Chen SR. Gabapentin suppresses ectopic nerve discharges and reverses allodynia in neuropathic rats. *J Pharmacol Exp Ther*. 1999 Mar;288(3):1026–30.

148. Santos-Nogueira E, Redondo Castro E, Mancuso R, Navarro X. Randall-selitto test: A new approach for the detection of neuropathic pain after spinal cord injury. *J Neurotrauma*. 2012;29(5):898–904.

149. Baron R, Mayoral V, Leijon G, Binder A, Steigerwald I, Serpell M. Efficacy and safety of combination therapy with 5% lidocaine medicated plaster and pregabalin in post-herpetic neuralgia and diabetic polyneuropathy. *Curr Med Res Opin*. 2009 Jul;25(7):1677–87.

150. Tesfaye S, Wilhelm S, Lledo A, Schacht A, Tölle T, Bouhassira D, Cruccu G, Skljarevski V, Freynhagen R. Duloxetine and pregabalin: High-dose monotherapy or their combination? the “COMBO-DN study” - A multinational, randomized, double-blind, parallel-group study in patients with diabetic peripheral neuropathic pain. *Pain*. 2013;154(12):2616–25.

151. Fox A, Gentry C, Patel S, Kesingland A, Bevan S. Comparative activity of the anti-convulsants oxcarbazepine, carbamazepine, lamotrigine and

gabapentin in a model of neuropathic pain in the rat and guinea-pig. *Pain*. 2003;105(1):355–62.

152. Chincholkar M. Analgesic mechanisms of gabapentinoids and effects in experimental pain models: a narrative review. *Br J Anaesth*. 2018;120(6):1315–34.

153. Kremer M, Yalcin I, Nexon L, Wurtz X, Ceredig RA, Daniel D, Hawkes RA, Salvat E, Barrot M. The antiallodynic action of pregabalin in neuropathic pain is independent from the opioid system. *Mol Pain*. 2016;12:1744806916633477.

154. Bender G, Florian Jr JA, Bramwell S, Field MJ, Tan KK, Marshall S, DeJongh J, Bies RR, Danhof M. Pharmacokinetic–pharmacodynamic analysis of the static allodynia response to pregabalin and sildenafil in a rat model of neuropathic pain. *J Pharmacol Exp Ther*. 2010 Aug 1;334(2):599-608.

155. Ito S, Suto T, Saito S, Obata H. Repeated Administration of Duloxetine Suppresses Neuropathic Pain by Accumulating Effects of Noradrenaline in the Spinal Cord. *Anesth Analg*. 2018 Jan 1;126(1):298–307.

156. Tanenberg RJ, Irving GA, Risser RC, Ahl J, Robinson MJ, Skljarevski V, Malcolm SK. Duloxetine, pregabalin, and duloxetine plus gabapentin for diabetic peripheral neuropathic pain management in patients with inadequate pain response to gabapentin: An open-label, randomized, noninferiority comparison. *Mayo Clin Proc*. 2011;86(7):615–26.

157. Lee BS, Jun IG, Kim SH, Park JY. Intrathecal gabapentin increases interleukin-10 expression and inhibits pro-inflammatory cytokine in a rat model of neuropathic pain. *J Korean Med Sci*. 2013;28(2):308–14.

158. Park HJ, Joo HS, Chang HW, Lee JY, Hong SH, Lee Y, Moon DE. Attenuation of neuropathy-induced allodynia following intraplantar injection of pregabalin. *Can J Anaesth*. 2010 Jul 1;57(7):664.

159. Freynhagen R, Strojek K, Griesing T, Whalen E, Balkenohl M. Efficacy of pregabalin in neuropathic pain evaluated in a 12-week, randomised, double-

blind, multicentre, placebo-controlled trial of flexible-and fixed-dose regimens. *Pain*. 2005;115(3):254–63.

160. Sabatowski R, Gálvez R, Cherry DA, Jacquot F, Vincent E, Maisonobe P, Versavel M, 1008-045 Study Group. Pregabalin reduces pain and improves sleep and mood disturbances in patients with post-herpetic neuralgia: results of a randomised, placebo-controlled clinical trial. *Pain*. 2004;109(1–2):26–35.

161. Mangaiarkkarasi A, Rameshkannan S, Ali RM. Effect of gabapentin and pregabalin in rat model of taxol induced neuropathic pain. *J Clin Diagn Res*. 2015;9(5):FF11.

162. Kremer M, Yalcin I, Goumon Y, Wurtz X, Nexon L, Daniel D, Megat S, Ceredig RA, Ernst C, Turecki G, Chavant V. A Dual Noradrenergic Mechanism for the Relief of Neuropathic Allodynia by the Antidepressant Drugs Duloxetine and Amitriptyline. *J Neurosci*. 2018 Nov 14;38(46):9934–54.

163. Wright A, Luedtke KE, Vandenberg C. Duloxetine in the treatment of chronic pain due to fibromyalgia and diabetic neuropathy. *J Pain Res*. 2010 Dec;4:1–10.

164. Gahimer J, Wernicke J, Yalcin I, Ossanna MJ, Wulster-Radcliffe M, Viktrup L. A retrospective pooled analysis of duloxetine safety in 23,983 subjects. *Curr Med Res Opin*. 2007 Jan;23(1):175–84.

165. Rahman W, Suzuki R, Webber M, Hunt SP, Dickenson AH. Depletion of endogenous spinal 5-HT attenuates the behavioural hypersensitivity to mechanical and cooling stimuli induced by spinal nerve ligation. *Pain*. 2006;123(3):264–74.

166. Suzuki R, Rahman W, Hunt SP, Dickenson AH. Descending facilitatory control of mechanically evoked responses is enhanced in deep dorsal horn neurones following peripheral nerve injury. *Brain Res*. 2004;1019(1–2):68–76.

167. Guo M, Shen W, Zhou M, Song Y, Liu J, Xiong W, Gao Y. Safety and efficacy of carbamazepine in the treatment of trigeminal neuralgia: A metanalysis in biomedicine. *Math. Biosci. Eng*. 2024 Mar 7;21(4):5335-59.

168. Jo S, Bean BP. Sidedness of carbamazepine accessibility to voltage-gated sodium channels. *Mol Pharmacol*. 2014;85(2).

169. Killian JM, Fromm GH. Carbamazepine in the Treatment of Neuralgia: Use and Side Effects. *Arch Neurol*. 1968;19(2).

170. Agbo J, Ibrahim ZG, Magaji SY, Mutalub YB, Mshelia PP, Mhyha DH. Therapeutic efficacy of voltage-gated sodium channel inhibitors in epilepsy. *Acta Epileptologica*. 2023 Jun 28;5(1):16.

171. Chogtu B, Bairy KL, Himabindu P, Dhar S. Comparing the efficacy of carbamazepine, gabapentin and lamotrigine in chronic constriction injury model of neuropathic pain in rats. *Int J Nutr Pharmacol Neurol Dis*. 2013;3(1):34–8.

172. Hahm TS, Ahn HJ, Ryu S, Gwak MS, Choi SJ, Kim JK, Yu JM. Combined carbamazepine and pregabalin therapy in a rat model of neuropathic pain. *Br J Anaesth*. 2012;109(6):968–74.

173. Magnus L. Nonepileptic uses of gabapentin. *Epilepsia*. 1999;40:s66–72.

174. Obermann M, Yoon MS, Sensen K, Maschke M, Diener HC, Katsarava Z. Efficacy of pregabalin in the treatment of trigeminal neuralgia. *Cephalalgia*. 2008;28(2):174–81.

175. Taheri A, Firouzi-Marani S, Khoshbin M, Beygi M. A retrospective review of efficacy of combination therapy with pregabalin and carbamazepine versus pregabalin and amitriptyline in treatment of trigeminal neuralgia. *Anaesthesia, Pain & Intensive Care*. 2019;8–12.

176. Prisco L, Ganau M, Bigotto F, Zornada F. Trigeminal neuralgia: successful antiepileptic drug combination therapy in three refractory cases. *Drug Healthc Patient Saf*. 2011;43–5.

177. Brodie MJ. Sodium channel blockers in the treatment of epilepsy. *CNS Drugs.* 2017;31(7):527–34.

178. Spina E, Pisani F, Perucca E. Clinically significant pharmacokinetic drug interactions with carbamazepine. An update. *Clin Pharmacokinet*. 1996 Sep;31(3):198–214.

179. Lim HS, Kim JM, Choi JG, Ko YK, Shin YS, Jeon BH, Park JB, Lee JH, Kim HW. Intrathecal ketamine and pregabalin at sub-effective doses synergistically reduces neuropathic pain without motor dysfunction in mice. *Biol Pharm Bull*. 2013;36(1).

180. Mittal M, Pasnoor M, Mummaneni RB, Khan S, McVey A, Saperstein D, Herbelin L, Ridings L, Wang Y, Dimachkie MM, Barohn RJ. Retrospective chart review of duloxetine and pregabalin in the treatment of painful neuropathy. *Int J Neurosci*. 2011 Aug 18;121(9):521-7.

181. Christoph T, De Vry J, Schiene K, Tallarida RJ, Tzschentke TM. Synergistic antihypersensitive effects of pregabalin and tapentadol in a rat model of neuropathic pain. *Eur J Pharmacol*. 2011 Sep 1;666(1–3):72–9.

182. Nozawa K, Karasawa Y, Shidahara Y, Ushida T. Efficacy of Combination Therapy with Pregabalin in Neuropathic Pain: A Preclinical Study in the Rat L5 Spinal Nerve Ligation Model. *J Pain Res*. 2022;15.

183. Dou Z, Jiang Z, Zhong J. Efficacy and safety of pregabalin in patients with neuropathic cancer pain undergoing morphine therapy. *Asia Pac J Clin Oncol.* 2017;13(2).

184. Hofer D, Lohberger B, Steinecker B, Schmidt K, Quasthoff S, Schreibmayer W. A comparative study of the action of tolperisone on seven different voltage dependent sodium channel isoforms. *Eur J Pharmacol*. 2006;538(1–3).

185. Dib-Hajj SD, Fjell J, Cummins TR, Zheng Z, Fried K, LaMotte R, Black JA, Waxman SG. Plasticity of sodium channel expression in DRG neurons in the chronic constriction injury model of neuropathic pain. *Pain*. 1999;83(3):591–600.

186. Pancrazio JJ, Kamatchi GL, Roscoe AK, Lynch III C. Inhibition of neuronal Na^+ channels by antidepressant drugs. *J Pharmacol Exp Ther*. 1998 Jan 1;284(1):208-14.

187. Murai N, Sekizawa T, Gotoh T, Watabiki T, Takahashi M, Kakimoto S, Takahashi Y, Iino M, Nagakura Y. Spontaneous and evoked pain-associated behaviors in a rat model of neuropathic pain respond differently to drugs with different mechanisms of action. *Pharmacol Biochem Behav*. 2016;141.

188. Bauer CS, Nieto-Rostro M, Rahman W, Tran-Van-Minh A, Ferron L, Douglas L, Kadurin I, Ranjan YS, Fernandez-Alacid L, Millar NS, Dickenson AH. The increased trafficking of the calcium channel subunit α2δ-1 to presynaptic terminals in neuropathic pain is inhibited by the α2δ ligand pregabalin. *J Neurosci*. 2009 Apr 1;29(13):4076-88.

189. Song S, Wang Q, Qu Y, Gao W, Li D, Xu X, Yue S. Pregabalin inhibits purinergic P2Y2 receptor and TRPV4 to suppress astrocyte activation and to relieve neuropathic pain. *Eur J Pharmacol*. 2023 Dec 5;960:176140.

190. Bee LA, Dickenson AH. Descending facilitation from the brainstem determines behavioural and neuronal hypersensitivity following nerve injury and efficacy of pregabalin. *Pain*. 2008;140(1).

191. Takeuchi Y, Takasu K, Ono H, Tanabe M. Pregabalin, S-(+)-3-isobutylgaba, activates the descending noradrenergic system to alleviate neuropathic pain in the mouse partial sciatic nerve ligation model. *Neuropharmacology*. 2007;53(7).

192. Tekes K. Basic Aspects of the Pharmacodynamics of Tolperisone, A Widely Applicable Centrally Acting Muscle Relaxant. *Open Med Chem J*. 2014;8(1).

193. Kastrup J, Petersen P, Dejgård A, Angelo HR, Hilsted J. Intravenous lidocaine infusion - a new treatment of chronic painful diabetic neuropathy? *Pain*. 1987;28(1).

194. Saudek CD, Warns S, Reidenberg MM. Phenytoin in the treatment of diabetic symmetrical polyneuropathy. *Clin Pharmacol Ther*. 1977;22(2).

195. Oskarsson P, Ljunggren JG, Lins PE. Efficacy and safety of mexiletine in the treatment of painful diabetic neuropathy. *Diabetes Care*. 1997;20(10).

196. Bhattacharya A, Wickenden AD, Chaplan SR. Sodium Channel Blockers for the Treatment of Neuropathic Pain. *Neurotherapeutics*. 2009 Oct 1;6(4):663–78.

197. Dulin J, Kovacs L, Ramm S, Horvath F, Ebeling L, Kohnen R. Evaluation of sedative effects of single and repeated doses of 50 mg and 150 mg tolperisone hydrochloride. Results of a prospective, randomized, double-blind, placebo-controlled trial. *Pharmacopsychiatry*. 1998;31(04):137–42.

198. Gooch C, Podwall D. The diabetic neuropathies. *Neurologist*. 2004;10(6):311–22.

199. D'Mello R, Dickenson AH. Spinal cord mechanisms of pain. *Br J Anaesth*. 2008;101(1):8–16.

200. Sânchez-Prieto J, Budd DC, Herrero I, Vázquez E, Nicholls DG. Presynaptic receptors and the control of glutamate exocytosis. *Trends Neurosci*. 1996 Jun 1;19(6):235–9.

201. Galván E, Sitges M. Characterization of the Participation of Sodium Channels on the Rise in Na^+ Induced by 4-Aminopyridine (4-AP) in Synaptosomes. *Neurochem Res*. 2004;29(2).

202. Tibbs GR, Barrie AP, Van Mieghem FJE, McMahon HT, Nicholls DG. Repetitive Action Potentials in Isolated Nerve Terminals in the Presence of 4-Aminopyridine: Effects on Cytosolic Free Ca^{2+} and Glutamate Release. *J Neurochem*. 1989;53(6).

203. Qureshi Z, Ali MN, Khalid M. An Insight into Potential Pharmacotherapeutic Agents for Painful Diabetic Neuropathy. *J Diabetes Res*. 2022;2022(1):9989272.

204. Iyer S, Tanenberg RJ. Pharmacologic management of diabetic peripheral neuropathic pain. *Expert Opin Pharmacother*. 2013 Sep;14(13):1765–75.

205. Bates D, Schultheis BC, Hanes MC, Jolly SM, Chakravarthy KV, Deer TR, Levy RM, Hunter CW. A Comprehensive Algorithm for Management of Neuropathic Pain. Vol. 20, *Pain Medicine (United States)*. Oxford University Press; 2019. p. S2–12.

206. Pop-Busui R, Boulton AJ, Feldman EL, Bril V, Freeman R, Malik RA, Sosenko JM, Ziegler D. Diabetic neuropathy: A position statement by the American diabetes association. *Diabetes Care*. 2017;40(1).

207. Attal N, Cruccu G, Baron RA, Haanpää M, Hansson P, Jensen TS, Nurmikko T. EFNS guidelines on the pharmacological treatment of neuropathic pain: 2010 revision. *Eur J Neurol*. 2010 Sep;17(9):1113-e88.

208. Blom S. Trigeminal neuralgia: its treatment with a new anticonvulsant drug (G-32883). *Lancet*. 1962 Apr 21;279(7234):839-40.

209. Gonz H, Castaneda L. Symptomatic Treatment of Peripheral Diabetic Neuropathy with Carbamazepine (Tegretol) Double Blind Crossover Trial. Vol. 5, *Diabetologia*. 1969.

210. B. Kharatmal S, N. Singh J, S. Sharma S. Voltage-gated sodium channels as therapeutic targets for treatment of painful diabetic neuropathy. *Mini Rev Med Chem.* 2015 Dec 1;15(14):1134-47.

211. Waxman SG, Merkies IS, Gerrits MM, Dib-Hajj SD, Lauria G, Cox JJ, Wood JN, Woods CG, Drenth JP, Faber CG. Sodium channel genes in pain-related disorders: phenotype–genotype associations and recommendations for clinical use. *Lancet Neurol.* 2014 Nov 1;13(11):1152-60.

212. Bennett DLH, Woods CG. Painful and painless channelopathies. *Lancet Neurol*. 2014 Jun 1;13(6):587-99.

213. Richter RW, Portenoy R, Sharma U, Lamoreaux L, Bockbrader H, Knapp LE. Relief of painful diabetic peripheral neuropathy with pregabalin: A randomized, placebo-controlled trial. *J Pain*. 2005 Apr 1;6(4):253–60.

214. Li J, Chen X, Lu X, Zhang C, Shi Q, Feng L. Pregabalin treatment of peripheral nerve damage in a murine diabetic peripheral neuropathy model. *Acta Endocrinol (Buchar)*. 2018 Jul;14(3):294.

215. Lesser H, Sharma U, LaMoreaux L, Poole RM. Pregabalin relieves symptoms of painful diabetic neuropathy. *Neurology*. 2004;63(11):2104–10.

216. Satoh J, Yagihashi S, Baba M, Suzuki M, Arakawa A, Yoshiyama T, Shoji S. Efficacy and safety of pregabalin for treating neuropathic pain associated with diabetic peripheral neuropathy: a 14 week, randomized, double-blind, placebo-controlled trial. *Diabet Med*. 2011 Jan;28(1):109-16.

217. Schreiber AK. Diabetic neuropathic pain: Physiopathology and treatment. *World J Diabetes*. 2015;6(3).

218. Yang XD, Fang PF, Xiang DX, Yang YY. Topical treatments for diabetic neuropathic pain. *Exp Ther Med*. 2019 Mar 1;17(3):1963-76.

219. Saeed T, Nasrullah M, Ghafoor A, Shahid R, Islam N, Khattak MU, Maheshwary N, Siddiqi A, Khan MA. Efficacy and tolerability of carbamazepine for the treatment of painful diabetic neuropathy in adults: a 12-week, open-label, multicenter study. *Int J Gen Med*. 2014 Jul 2:339-43.

220. Preston FG, Riley DR, Azmi S, Alam U. Painful Diabetic Peripheral Neuropathy: Practical Guidance and Challenges for Clinical Management. Vol. 16, Diabetes. *Metab Syndr Obes*. 2023.

221. Price R, Smith D, Franklin G, Gronseth G, Pignone M, David WS, Armon C, Perkins BA, Bril V, Rae-Grant A, Halperin J. Oral and topical treatment of painful diabetic polyneuropathy: practice guideline update summary: report of the AAN guideline subcommittee. *Neurology*. 2022 Jan 4;98(1):31-43.

222. Bigsby S, Neapetung J, Campanucci VA. Voltage-gated sodium channels in diabetic sensory neuropathy: Function, modulation, and therapeutic potential. *Front Cell Neurosci*. 2022 Nov 17;16:994585.

223. Shaqura M, Khalefa BI, Shakibaei M, Winkler J, Al-Khrasani M, Fürst S, Mousa SA, Schäfer M. Reduced number, G protein coupling, and antinociceptive efficacy of spinal mu-opioid receptors in diabetic rats are reversed by nerve growth factor. *J Pain*. 2013 Jul 1;14(7):720-30.

224. Kou ZZ, Wan FP, Bai Y, Li CY, Hu JC, Zhang GT, Zhang T, Chen T, Wang YY, Li H, Li YQ. Decreased endomorphin-2 and μ-opioid receptor in the spinal cord are associated with painful diabetic neuropathy. *Front Mol Neurosci*. 2016 Sep 7;9:80.

225. Kaygisiz B, Kilic FS, Senguleroglu N, Baydemir C, Erol K. The antinociceptive effect and mechanisms of action of pregabalin in mice. *Pharmacol Rep*. 2015 Feb 1;67(1):129–33.

226. Miranda HF, Sierralta F, Lux S, Troncoso R, Ciudad N, Zepeda R, Zanetta P, Noriega V, Prieto JC. Involvement of nitridergic and opioidergic pathways in the antinociception of gabapentin in the orofacial formalin test in mice. *Pharmacol Rep*. 2015 Mar;67:399-403.

227. Garza-Carbajal A, Bavencoffe A, Herrera JJ, Johnson KN, Walters ET, Dessauer CW. Mechanism of gabapentinoid potentiation of opioid effects on cyclic AMP signaling in neuropathic pain. *Proc Natl Acad Sci U S A*. 2024 Aug 20;121(34).

228. Song L, Wu C, Zuo Y. Melatonin prevents morphine-induced hyperalgesia and tolerance in rats: role of protein kinase C and N-methyl-D-aspartate receptors. *BMC Anesthesiol*. 2015 Dec;15:1-8.

229. Cheppudira BP, Trevino A V., Petz LN, Christy RJ, Clifford JL. Anti-nerve growth factor antibody attenuates chronic morphine treatment-induced tolerance in the rat. *BMC Anesthesiol*. 2016 Sep 5;16(1).

230. Wang L, Yin C, Xu X, Liu T, Wang B, Abdul M, Zhou Y, Cao J, Lu C. Pellino1 Contributes to Morphine Tolerance by Microglia Activation via MAPK Signaling in the Spinal Cord of Mice. *Cell Mol Neurobiol*. 2020 Oct 1;40(7):1117–31.

231. Chu CC, Shieh JP, Shui HA, Chen JY, Hsing CH, Tzeng JI, Wang JJ, Ho ST. Tianeptine reduces morphine antinociceptive tolerance and physical dependence. *Behav Pharmacol*. 2010 Sep 1;21(5-6):523-9.

232. Joshi D, Singh A, Naidu PS, Kulkarni SK. Protective effect of bupropion on morphine tolerance and dependence in mice. *Methods Find Exp Clin Pharmacol*. 2004 Oct;26(8):623–6.

233. Fürst S, Zádori ZS, Zádor F, Király K, Balogh M, László SB, Hutka B, Mohammadzadeh A, Calabrese C, Galambos AR, Riba P. On the role of peripheral sensory and gut mu opioid receptors: Peripheral analgesia and tolerance. *Molecules*. 2020 May 26;25(11):2473.

234. Trujillo KA, Akil H. Inhibition of morphine tolerance and dependence by the NMDA receptor antagonist MK-801. *Science*. 1991 Jan 4;251(4989):85-7.

235. Mao J, Sung B, Ji RR, Lim G. Chronic morphine induces downregulation of spinal glutamate transporters: implications in morphine tolerance and abnormal pain sensitivity. *J Neurosci*. 2002 Sep 15;22(18):8312-23.

236. Gong K, Bhargava A, Jasmin L. GluN2B n-methyl-d-aspartate receptor and excitatory amino acid transporter 3 are upregulated in primary sensory neurons after 7 days of morphine administration in rats: Implication for opiate-induced hyperalgesia. *Pain*. 2016 Jan 1;157(1):147–58.

237. Zhao YL, Chen SR, Chen H, Pan HL. Chronic opioid potentiates presynaptic but impairs postsynaptic N-methyl-D-aspartic acid receptor activity in spinal cords: Implications for opioid hyperalgesia and tolerance. *J Biol Chem*. 2012 Jul 20;287(30):25073–85.

238. Grande LA, O'Donnell BR, Fitzgibbon DR, Terman GW. Ultra-low dose ketamine and memantine treatment for pain in an opioid-tolerant oncology patient. *Anesth Analg*. 2008;107(4):1380–3.

239. Deng M, Chen SR, Chen H, Pan HL. α2δ-1-Bound N-Methyl-d-aspartate Receptors Mediate Morphine-induced Hyperalgesia and Analgesic Tolerance by Potentiating Glutamatergic Input in Rodents. *Anesthesiology*. 2019 May 1;130(5):804–19.

240. Zhou HY, Chen SR, Pan HL. Targeting N-methyl-D-aspartate receptors for treatment of neuropathic pain. *Expert Rev Clin Pharmacol*. 2011 May;4(3):379-88.

241. Zhang YY, Liu F, Fang ZH, Li YL, Liao HL, Song QX, Zhou C, Shen JF. Differential roles of NMDAR subunits 2A and 2B in mediating peripheral and central sensitization contributing to orofacial neuropathic pain. *Brain Behav Immun.* 2022 Nov 1;106:129–46.

242. Long KD, Mastropaolo J, Rosse RB, Manaye KF, Deutsch SI. Modulatory effects of d-serine and sarcosine on NMDA receptor-mediated neurotransmission are apparent after stress in the genetically inbred BALB/c mouse strain. *Brain Res Bull*. 2006 May 31;69(6):626–30.

243. Piniella D, Zafra F. Functional crosstalk of the glycine transporter GlyT1 and NMDA receptors. *Neuropharmacology*. 2023 Jul 1;232:109514.

244. Mothet JP, Parent AT, Wolosker H, Brady Jr RO, Linden DJ, Ferris CD, Rogawski MA, Snyder SH. D-serine is an endogenous ligand for the glycine site of the N-methyl-D-aspartate receptor. *Proc Natl Acad Sci U S A*. 2000 Apr 25;97(9):4926-31.

245. Lin JA, Lee MS, Wu CT, Yeh CC, Lin SL, Wen ZH, Wong CS. Attenuation of morphine tolerance by intrathecal gabapentin is associated with suppression of morphine-evoked excitatory amino acid release in the rat spinal cord. *Brain Res*. 2005 Aug 30;1054(2):167-7.

246. Singh NS, Paul RK, Torjman MC, Wainer IW. Gabapentin and (S)-pregabalin decrease intracellular d-serine concentrations in PC-12 cells. *Neurosci Lett*. 2013 Feb 22;535(1):90–4.

247. Miskolczi P, Vereczkey L, Frenkl R. Gas—liquid chromatographic method for the determination of tolperisone in human plasma: pharmacokinetic and comparative bioavailability studies. *J Pharm Biomed Anal*. 1987 Jan 1;5(7):695–700.

248. Dalmadi B, Leibinger J, Szeberényi S, Borbás T, Farkas S, Szombathelyi Z, Tihanyi K. Identification of metabolic pathways involved in the

biotransformation of tolperisone by human microsomal enzymes. *Drug Metab Dispos*. 2003 May 1;31(5):631-6.

249. Bockbrader HN, Radulovic LL, Posvar EL, Strand JC, Alvey CW, Busch JA, Randinitis EJ, Corrigan BW, Haig GM, Boyd RA, Wesche DL. Clinical pharmacokinetics of pregabalin in healthy volunteers. *J Clin Pharmacol*. 2010;50(8).

250. Waterman SA. Role of N-, P-and Q-type voltage-gated calcium channels in transmitter release from sympathetic neurones in the mouse isolated vas deferens. *Br J Pharmacol*. 1997 Feb;120(3):393-8.

251. Zhu HL, Aishima M, Morinaga H, Wassall RD, Shibata A, Iwasa K, Nomura M, Nagao M, Sueishi K, Cunnane TC, Teramoto N. Molecular and biophysical properties of voltage-gated Na+ channels in murine vas deferens. *Biophys J.* 2008 Apr 15;94(8):3340-51.

252. Leslie FM. Methods used for the study of opioid receptors. *Pharmacol Rev.* 1987;39(3).

253. Takemori AE, Portoghese PS. The use of μ opioid receptors in the mouse vas deferens for the study of opiate tolerance. *Eur J Pharmacol*. 1989 Dec 19;174(2-3):267-71.

254. Marshall I, Phillips DG, Nasmyth PA. Calcium ions, morphine tolerance and noradrenergic transmission in the mouse vas deferens. *Eur J Pharmacol*. 1981 Nov 5;75(4):205-13.

255. Rubini P, Schulz R, Wüster M, Herz A. Opiate receptor binding studies in the mouse vas deferens exhibiting tolerance without dependence. *Naunyn-Schmiedeberg's Arch Pharmacol.* 1982 May;319:142-6.

256. Li N, Li C, Han R, Wang Y, Yang M, Wang H, Tian J. LPM580098, a novel triple reuptake inhibitor of serotonin, noradrenaline, and dopamine, attenuates neuropathic pain. *Front Pharmacol*. 2019 Feb 14;10:53.

257. Quasthoff S, Möckel C, Zieglgänsberger W, Schreibmayer W. Tolperisone: a typical representative of a class of centrally acting muscle relaxants with less sedative side effects. *CNS Neurosci Ther*. 2008 Jun;14(2):107-19.

258. Freynhagen R, Serpell M, Emir B, Whalen E, Parsons B, Clair A, Latymer M. A comprehensive drug safety evaluation of pregabalin in peripheral neuropathic pain. *Pain Pract*. 2015 Jan;15(1):47-57.

259. Kamel JT, D'Souza WJ, Cook MJ. Severe and disabling constipation: an adverse effect of pregabalin. *Epilepsia*. 2010 Jun;51(6):1094-6.

260. Houghton LA, Fell C, Whorwell PJ, Jones I, Sudworth DP, Gale JD. Effect of a second-generation α2δ ligand (pregabalin) on visceral sensation in hypersensitive patients with irritable bowel syndrome. *Gut*. 2007 Sep 1;56(9):1218-25.

9. Bibliography of the Candidate's Publications

9.1. The Publications of the Candidate Involved in the Current Thesis

1. **Essmat, N**., Galambos, A. R., Lakatos, P. P., Karádi, D. Á., Mohammadzadeh, A., Abbood, S. K., Geda, O., Laufer, R., Király, K., Riba, P., Zádori, Z. S., Szökő, É., Tábi, T., & Al-Khrasani, M. (2023). Pregabalin–TOLP Combination to Treat Neuropathic Pain: Improved Analgesia and Reduced Side Effects in Rats. *Pharmaceuticals, 16*(8), 1115. https://doi.org/10.3390/ph16081115.

2. Zádor, F., Király, K., **Essmat, N**., & Al-Khrasani, M. (2022). Recent Molecular Insights into Agonist-specific Binding to the Mu-Opioid Receptor. *Frontiers in molecular biosciences, 9*, 900547. https://doi.org/10.3389/fmolb.2022.900547.

9.2. The Publications of the Candidate not Involved in the Current Thesis

1. Lakatos, P. P., Karádi, D. Á., Galambos, A. R., **Essmat, N**., Király, K., Laufer, R., Geda, O., Zádori, Z. S., Tábi, T., Al-Khrasani, M., & Szökő, É. (2022). The Acute Antiallodynic Effect of TOLP in Rat Neuropathic Pain and Evaluation of Its Mechanism of Action. *International Journal of Molecular Sciences*, *23*(17), 9564. https://doi.org/10.3390/ijms23179564.

2. Karádi, D. Á., Galambos, A. R., Lakatos, P. P., Apenberg, J., Abbood, S. K., Balogh, M., Király, K., Riba, P., **Essmat, N**., Szűcs, E., Benyhe, S., Varga, Z. V., Szökő, É., Tábi, T., & Al-Khrasani, M. (2023). Telmisartan Is a Promising Agent for Managing Neuropathic Pain and Delaying Opioid Analgesic Tolerance in Rats. *International Journal of Molecular Sciences*, *24*(9), 7970. https://doi.org/10.3390/ijms24097970.

3. Costanzo, G., Turnaturi, R., Parenti, C., Spoto, S., Piana, S., Dichiara, M., Zagni, C., Galambos, A. R., **Essmat, N**., Marrazzo, A., Amata, E., Al-Khrasani, M., & Pasquinucci, L. (2023). New Insights into the Opioid Analgesic Profile of *cis*-(−)-*N*-Normetazocine-derived Ligands. *Molecules*, *28*(12), 4827. https://doi.org/10.3390/molecules28124827.

4. Angyal, P., Hegedüs, K., Mészáros, B. B., Daru, J., Dudás, Á., Galambos, A. R., **Essmat, N**., Al-Khrasani, M., Varga, S., & Soós, T. (2023). Total Synthesis and Structural Plasticity of Kratom Pseudoindoxyl Metabolites. *Angewandte Chemie (International ed. in English)*, *62*(35), e202303700. https://doi.org/10.1002/anie.202303700.

5. **Essmat, N**., Karádi, D. Á., Zádor, F., Király, K., Fürst, S., & Al-Khrasani, M. (2023). Insights into the Current and Possible Future Use of Opioid Antagonists in Relation to Opioid-Induced Constipation and Dysbiosis. *Molecules, 28*(23), 7766. https://doi.org/10.3390/molecules28237766.

6. Galambos, A. R., **Essmat, N**., Lakatos, P. P., Szücs, E., Boldizsár, I., Jr., Abbood, S. K., Karádi, D. Á., Kirchlechner-Farkas, J. M., Király, K., Benyhe, S., Riba, P., Tábi, T., Harsing, L. G., Jr., Zádor, F., & Al-Khrasani, M. (2024). Glycine Transporter 1 Inhibitors Minimize the Analgesic Tolerance to Morph. *International Journal of Molecular Sciences, 25*(20), 11136. https://doi.org/10.3390/ijms252011136.

10. Acknowledgements

First and foremost, I would like to thank my supervisor, **Prof. Mahmoud Al-Khrasani**. His dedicated helpfulness, thoughtfulness, and inspiring ideas have taught me an incredible amount over the years.

I thank **Prof. Péter Ferdinandy**, head of the Department of Pharmacology and Pharmacotherapy, for the opportunity to work in the Department.

I would like to thank **Prof. Kornél Király** and **Prof. Zoltán S. Zádori** for their help and support during my research studies.

For their devoted experimental work, I thank my colleagues **Dr. Ferenc Zádor, Dr. David Arpad Karadi, Anna Galambos, Sarah Abbood,** and **Dr. Imre Boldizsár.**

For their outstanding scientific, experimental work and partnership, I would like to thank **Prof. Tamás Tábi, Prof. Éva Szökő, Dr. Péter Lakatos,** and all co-workers at the Department of Pharmacodynamics.

I would like to thank our TDK student, **Kirchlechner-Farkas Judit Mária,** for her exceptional work.

I would like to thank all **my colleagues** at the Semmelweis University Department of Pharmacology and Pharmacotherapy.

I would like to express my deepest gratitude to my family members, **my parents**, **my parents-in-law**, my husband (**Dr. Ahmed Aioub**), and my son (**Omar**) for their unwavering support throughout my academic journey. Your constant encouragement, love, and sacrifices have been my guiding light.

I would like to thank the financial support of Semmelweis University as **SE 250^{+} excellence PhD scholarship** and **EKÖP Grant** (Egyetemi Kutatói Ösztöndíj Program) for the support of the present research study.

This work has been supported by the "Competitiveness and Excellence Cooperations" **2018-1.3.1-VKE-2018-00030 project** and the **TKP 2021 EGA-25 project** provided by the National Research, Development, and Innovation Fund of Hungary.

frontiers | Frontiers in Molecular Biosciences

MINI REVIEW
published: 13 June 2022
doi: 10.3389/fmolb.2022.900547

Recent Molecular Insights into Agonist-specific Binding to the Mu-Opioid Receptor

Ferenc Zádor[1*†], *Kornél Király*[1], *Nariman Essmat*[1] *and Mahmoud Al-Khrasani*[1]

[1]*Department of Pharmacology and Pharmacotherapy, Faculty of Medicine, Semmelweis University, Budapest, Hungary*

Opioid agonists produce their analgesic effects primarily by acting at the μ-opioid receptor (μOR). μOR agonists with different efficacies exert diverse molecular changes in the μOR which dictate the faith of the receptor's signaling pathway and possibly it's the degree of desensitization. Since the development of the active conformations of the μOR, growing data have been published in relation to ligand-specific changes in μOR activation. In this regard, this review summarizes recent data regarding the most studied opioid agonists in *in silico* μOR activation, including how these ligands are recognized by the μOR, how their binding signal is transmitted toward the intracellular parts of the μOR, and finally, what type of large-scale movements do these changes trigger in the μOR's domains.

Keywords: μ-opioid receptor, agonist-specific receptor activation, prototypic μ-opioid receptor agonist, TRV-130, PZM21

OPEN ACCESS

Edited by:
Fabio Arturo Iannotti, Consiglio Nazionale delle Ricerche (CNR), Italy

Reviewed by:
Haiguang Liu, Beijing Computational Science Research Center (CSRC), China

****Correspondence:***
Ferenc Zádor
zador.ferenc@gmail.com

†Present address:
Pharmacological and Drug Safety Research, Gedeon Richter Plc, Budapest, Hungary

Specialty section:
This article was submitted to Structural Biology, a section of the journal Frontiers in Molecular Biosciences

Received: *20 March 2022*
Accepted: *21 April 2022*
Published: *13 June 2022*

Citation:
Zádor F, Király K, Essmat N and Al-Khrasani M (2022) Recent Molecular Insights into Agonist-specific Binding to the Mu-Opioid Receptor. Front. Mol. Biosci. 9:900547. doi: 10.3389/fmolb.2022.900547

INTRODUCTION

Growing data support that the rate of opioid side-effects including analgesic tolerance development strongly correlates with the pharmacodynamic properties of opioid ligands. Opioids with different efficacies distinctly induce molecular mechanisms related to tolerance, namely receptor phosphorylation and endocytosis, as the basis of G-protein coupled μ-opioid receptor (μOR) desensitization (Williams et al., 2013; Allouche et al., 2014; Lemel et al., 2020). It has been proposed that the selective and sequential phosphorylation of the C-terminus is due to the possible different conformational states of the receptor-triggered agonist specifically (Lemel et al., 2020). In recent years, we have gained more information regarding the nature of opioid agonists binding to the active conformation of the μOR (Huang et al., 2015; Koehl et al., 2018). This review will focus on the current knowledge of agonist specific residue contacts (**Figure 1B**), how the different agonists transmit the ligand-binding signal toward the intracellular receptor parts (**Figure 1C**), and finally, how these affect the orientation of certain receptor domains (e.g., transmembrane regions (TM) or intracellular loops (IL)) (**Table 1**), which eventually decide the faith of the receptor's downstream signaling and the rate of desensitization. In addition, only data with the active conformation of the μOR will be reviewed here, namely the BU72 co-crystallized form and μOR-G_i complex co-crystallized with D-Ala^2, N-$MePhe^4$, and Gly-ol-enkephalin (DAMGO; PDB: 5C1M and PDB: 6DDF, respectively). Data on prototypic μOR-specific agonist ligands (**Figure 1A**), namely morphine, DAMGO, and fentanyl, will be reviewed alongside BU72, the first compound to be crystallized with the active conformational state of the μOR (Huang et al., 2015). TRV-130 and PZM21, newly developed G-protein-biased agonists, will be also reviewed (**Figure 1A**). In general, in the highlighted studies CHARMM (Brooks et al., 2009) and/or AMBER (Maier et al., 2015) force field was used, with 0.1–3.5 μs simulation time (in some cases, 24 μs; see Vo et al. (2020) in POPC (palmitoyl-oleoyl-phosphatidylcholine) lipid membrane model at ~1 bar

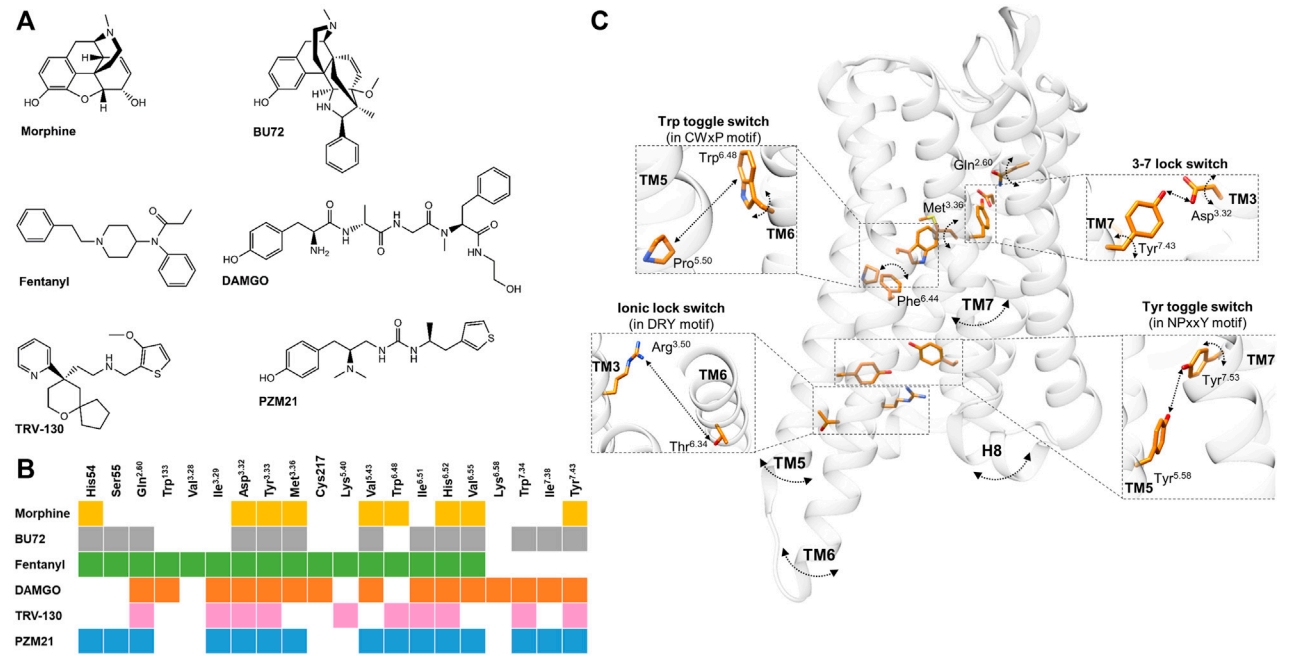

FIGURE 1 | (A) Chemical structures of μOR-selective agonists discussed in the review. **(B)** The known μOR residual contacts of the indicated agonists. The original concept of the figure was based on Figure 4 of Podlewska and co-workers' study (Podlewska et al., 2020) and extended by other data (Huang et al., 2015; Cheng et al., 2018; Koehl et al., 2018; Mafi et al., 2020; Ricarte et al., 2021). **(C)** Individual movements of the highlighted residues, molecular switches, and TM domains based on the data reviewed in the 3rd and 4th sections.. Participating residues are indicated in orange, arched arrows indicate the presence of spatial movements (but not the direction itself), while straight arrows depict the presence of altered distance between two residues. The corresponding agonists inducing these movements and alterations are not indicated for clarity; for details see in the 3rd and 4th sections. μOR is transparent for better visibility. The figure was constructed with UCSF Chimera 1.13.1 (Pettersen et al., 2004) based on Huang and co-workers using the BU72 co-crystallized active μOR structure (PDB: 5C1M) (Huang et al., 2015).

pressure and 310 K temperature in a ~75–85 x 75–85 x 90–140 Å size simulation box. Some studies also used NMR spectroscopy to obtain dynamic structural information (Okude et al., 2015; Sounier et al., 2015). Such a pool of data will help us to better understand the basic molecular factors of ligand-specific receptor activation and tolerance, and allow us to purposefully develop opioids with delayed analgesic tolerance profiles and ameliorated side effects.

LIGAND RECOGNITION: RESIDUE CONTACTS, BINDING MODES, AND BINDING POSES

Based on site-directed mutagenesis and *in silico* studies, multiple conserved residues have been identified in the μOR binding pocket, which have significant roles in ligand orientation and receptor activation (Mansour et al., 1997; Manglik et al., 2012, 2015, 2016; Katritch et al., 2013; Kaserer et al., 2016; Koehl et al., 2018; Marino et al., 2018; Manglik, 2020; Ricarte et al., 2021). Hitherto, data on the agonist-specific residue contacts and binding modes will be reviewed in this section.

Despite morphine and fentanyl interacting with the same contact residues (**Figure 1B**), their binding poses were less overlapped (Lipiński et al., 2019). Accordingly, fentanyl is in close proximity to seven TM3 residues and three TM6 residues, while in the case of morphine these numbers are four and five with respect to the same transmembrane domains. They also interact with TM7 to a similar extent but with different positions. Fentanyl is also able to reach the ECL1, ECL2, and the N-terminus. These findings were later confirmed by another group (Ricarte et al., 2021).

Analyzing the dissociation of morphine from the μOR, it showed that morphine directly dissociated from the orthosteric site region and also transitioned to the vestibule region after the $Asp^{3.32}$ salt bridge was disrupted (Ribeiro et al., 2020) (superscript numbering refers to the Ballesteros and Weinstein's generic numbering scheme (Ballesteros and Weinstein, 1995)).

Fentanyl binds deeper compared to morphinan structures (for fentanyl it is indicated by a lower ΔZ value, the distance between the centers of mass (COM) of fentanyl and μOR z direction) and it can form a salt-bridge interaction between the piperidine amine and the conserved $Asp^{3.32}$ (Vo et al., 2020) similar to DAMGO or BU72 (Huang et al., 2015; Weis and Kobilka, 2018). Vo and co-workers described a $His^{6.52}$ binding mode unique to fentanyl, which was also dependent on the protonation state of this residue (Vo et al., 2020). Another study found that the dissociation pathways, time, the depth of insertion, and the strength of TM6 interaction of fentanyl are dependent on the protonation state of $His^{6.52}$ (Mahinthichaichan et al., 2021).

TABLE 1 | Main differences and similarities within the highlighted ligands once bound to the μOR in terms of ligand recognition, binding signal transmission, and global movements.

Aspects	Differences	Similarities	References
Residue contacts, binding modes, and poses	Fentanyl has a deeper binding pose compared to morphine and has a unique $His^{6.52}$ binding mode, which is dependent on the residue's protonation state	All compounds interact with $Asp^{3.32}$, $Tyr^{3.33}$, and $His^{6.52}$	Huang et al. (2015); Koehl et al. (2018); Lipiński et al. (2019); Dumitrascuta et al. (2020); Mafi et al. (2020); Podlewska et al. (2020); Vo et al. (2020); Lee et al. (2021); Mahinthichaichan et al. (2021)
	DAMGO binding pose extends further toward the ECLs	Fentanyl and morphine interact with TM7 to a similar extent	
	TRV-130 has stronger contacts with TM2 and TM3 compared to morphine and DAMGO	DAMGO and BU72 have similar binding poses	
	PZM21 has the strongest contact with $Asp^{3.32}$ compared to fentanyl and morphine	Morphine, BU72, fentanyl, and DAMGO interact with $Val^{6.55}$	
Ligand binding signal transmission	TM1 is necessary for morphine-induced μOR activation	Similar changes in microswitches with bound DAMGO and BU72	Huang et al. (2015); Schneider et al. (2016); Kapoor et al. (2017); Sader et al. (2018); Lipiński et al.(2019); Zhao et al. (2020); Liao et al. (2021); Ricarte et al. (2021)
	The H-bond within the 3–7 lock switch was stronger with fentanyl	Morphine and PZM21 have similar activated network paths toward the intracellular end of TM6	
	Different torsion angles of $Phe^{6.44}$ and $Trp^{6.48}$ with morphine and fentanyl		
	Overall, more information is transferred across the receptor when TRV-130 is bound compared to morphine		
	With PZM21 certain molecular switches behaved differently and the activated network paths were different at the end of TM7 compared to morphine		
	With PZM21, $Trp^{6.48}$ and $Tyr^{7.43}$ behaved differently compared to morphine or TRV-130		
Higher-order structural changes	With morphine, μOR exists in equilibrium between the closed and open conformations, with DAMGO the receptor mainly adopts the open conformation toward the intracellular space, while with TRV-130 μOR exists in equilibrium between the closed and open conformations, but with larger intracellular cavity	Morphine and fentanyl stabilize TM6 in active-like conformation from the activated state	Huang et al. (2015); Okude et al. (2015); Sounier et al. (2015); Kapoor et al. (2017); Mafi et al. (2020); Zhao et al. (2020); Liao et al. (2021); Ricarte et al. (2021)
	Fentanyl induces TM3 for a more upward conformation compared to morphine	Both BU72 and DAMGO induced ICL1 and H8 for a larger conformational change compared to TM5 and TM6	
	With BU72, TM6 makes a large outward movement and a smaller inward movement of TM5 and TM7		
	TM6 repositions when TRV-130 is bound, which hinders β-arrestin2 binding to phosphorylated μOR		
	With PZM21, intracellular ends of TM5–7 bent further outward compared to morphine, which is more favorable for G-protein binding		
	With PZM21, smaller ECL1–3 and ICL3 fluctuations compared to TRV-130		

In the case of BU72, most of its interactions with the active μOR are hydrophobic or aromatic. The phenolic hydroxyl group of BU72 interacts with $His^{6.52}$ in a water-mediated fashion (Huang et al., 2015). There is also an ionic interaction between $Asp^{3.32}$ and the morphinan tertiary amine structure of BU72. BU72 stabilizes the rearrangement of a triad of conserved residues upon receptor activation (Huang et al., 2015). BU72 also forms a hydrophobic surface with $Ile^{6.51}$ and $Val^{6.55}$ in TM6 and $Ile^{7.39}$ in TM7, similarly to other morphinan structures (**Figure 1B**) (Huang et al., 2015). Another study demonstrated that BU72 binding poses distinct from the active μOR crystal structures and presumed that the high affinity and agonist character of BU72 is in part presented by its configurational entropy (Feinberg et al., 2017).

Koehl et al. found that the conformation of the active-state binding pocket and the orientation of the residues that interact

with the agonist are highly similar between BU72 and DAMGO, despite the structural differences (**Figure 1B**) (Koehl et al., 2018). On the other hand, compared to BU72, the C-terminus of DAMGO extends further toward the ECLs. Another study with DAMGO has shown that the tyrosine of the peptide forms lipophilic contacts with $Met^{3.36}$, $Ile^{6.51}$, and $Val^{6.55}$ residues and forms a charge interaction with $Asp^{3.32}$ (**Figure 1B**) (Dumitrascuta et al., 2020).

It has been proved that TRV-130 has stronger interactions (a greater number of hydrophobic contacts) with TM2 and TM3 compared to morphine or DAMGO in β-arrestin2 stabilized with phosphorylated μOR (Mafi et al., 2020). Based on docking simulations, the protonated nitrogen ion of TRV130 formed electrostatic interactions with $Asp^{3.32}$ and through its ring structure formed interactions with $His^{6.52}$ (**Figure 1B**) (Cheng et al., 2018).

PZM21 interacts with the active μOR binding pocket by hydrogen bonds, hydrophobic interactions, and an ionic bond (Manglik et al., 2016). Podlewska and co-workers have compared PZM21 with fentanyl or morphine in docking and MD simulations in BU72 and DAMGO co-crystallized active structures (Podlewska et al., 2020). Interestingly, all compounds showed less stability in their orientations in the DAMGO co-crystallized conformation, especially morphine, meaning that their initial and final binding orientations were significantly different during the simulation. They also found that during simulation time, PZM21 had more contacts with $Asp^{3.32}$ in both crystal structures compared to fentanyl or morphine (Podlewska et al., 2020). Another recent study compared PZM21 to morphine in MD simulations and found that besides PZM21 interacting with key residues $Asp^{3.32}$ and $Tyr^{3.33}$ of TM3 (**Figure 1B**), similar to morphine, yet it strongly interacts with $Tyr^{7.43}$ of TM7 (**Figure 1B**), as indicated by a higher percentage of interaction fractions in H-bonds (Liao et al., 2021). Finally, Lee and co-workers have performed molecular docking with new potential biased μOR agonists, where they also compared these novel compounds to TRV-130 and PZM21 for control. Here, they found that TRV-130 and PZM21 failed to accomplish contact with $Val^{6.55}$ in contrast to the novel compounds, which is heavily involved with hydrophobic interactions (Lee et al., 2021).

LIGAND BINDING SIGNAL TRANSMISSION

The subtle changes in the ligand-binding pocket induced by the bound ligand trigger further delicate changes through a channel of residues within certain TM domains. These changes transmit the ligand-binding signal from the ligand-binding site to the cytoplasmic region of the receptor (Weng et al., 2017; Liao et al., 2021). Some of these groups of residues are generally termed as molecular switches and they are conserved across the GPCR family. Among these, the 3–7 lock switch, the NPxxY motif (Asn-Pro-Xaa-Xaa-Tyr), the tyrosine ($Tyr^{7.53}$) toggle switch, the $Trp^{6.48}$ rotamer toggle switch, ionic lock (or DRY motif, Asp-Arg-Tyr), or the transmission switch (or CWxP motif, Cys-Trp-Xaa-Pro) have been described to be altered in an agonist specific manner in the μOR and will be discussed in this section, among other related data. The role of these molecular switches has been described in detail in other studies (Lagerström and Schiöth, 2008; Nygaard et al., 2009; Chabbert et al., 2012; Trzaskowski et al., 2012; Marino et al., 2018; Filipek, 2019) and due to length limitations will not be discussed here.

A study demonstrated that the conformations of certain residues ($Met^{3.36}$ and $Gln^{2.60}$) were different compared to morphine and fentanyl bound states (**Figure 1C**) (Ricarte et al., 2021). These differences affected the $Asp^{3.32}$–$Tyr^{7.43}$ H-bonding (3–7 lock switch) (**Figure 1C**), which was stronger when fentanyl was present (indicated by higher H-bond occupancy values) (Ricarte et al., 2021). They also found that the conformational changes in the NPxxY motif were consistently induced in the more stable active-like state by fentanyl (Ricarte et al., 2021). These specific changes might explain the higher efficacy of fentanyl. Another study proposed that the N-aniline ring of fentanyl mediates μOR β-arrestin coupling through the $Met^{3.36}$ residue (de Waal et al., 2020). Additionally, a clear difference was shown in torsion angles of $Trp^{6.48}$ between morphine and fentanyl (**Figure 1C**) (Lipiński et al., 2019). Also, the frequency changes of the torsion angles of $Phe^{6.44}$ were considered the main difference between morphine and fentanyl. The same study revealed differences between morphine and fentanyl in the 3–7 lock switch and being tighter in the presence of morphine (**Figure 1C**) (Lipiński et al., 2019).

Sena et al. showed that morphine tends to drive the receptor toward increasing the distance in the 3–7 lock switch (**Figure 1C**) and found an important conformational change in TM5 when morphine was present (Sena et al., 2021). It is worth noting that MD simulations have been performed with morphine and a μOR splice variant lacking the complete TM1 (Majumdar et al., 2011,2012; Lu et al., 2015) where TM1 truncation results in the loss of key interactions that are necessary for morphine-induced μOR activation (Sader et al., 2018).

Huang and co-workers revealed an extensive network of polar interactions between the orthosteric binding pocket and the G-protein coupling interface, which rearranges upon receptor activation with BU72 (Huang et al., 2015). The NPxxY motif is also involved in this polar network and moves inward toward the TM5 upon activation (**Figure 1C**) (Huang et al., 2015). Later on, they found similar changes in the microswitches when DAMGO was bound to the μOR–G_i protein complex structure (Koehl et al., 2018).

Cheng and co-workers compared BU72 and TRV130, where the stability of $Asp^{3.32}$ was lower with TRV-130 compared to BU72 (**Figure 1C**) since the dominant torsion angle was ~ -12° and occupied ~23% of the simulation time in the presence of TRV-130 (BU72: ~28°, ~45%) (Cheng et al., 2018). A study analyzed the allosteric communication between the orthosteric binding pocket and the intracellular region of the μOR with TRV-130 compared to morphine (Schneider et al., 2016). According to contact probability calculations, TRV-130 only communicated with residues of the intracellular end of TM3 and there was no strong contact with residues at the end of TM6. Morphine allosterically regulated significant interactions with the intracellular ends of both TM3 and TM6. Additionally, the

network of side-chain interactions adjacent to TRV-130 was significantly smaller compared to morphine (Schneider et al., 2016). Also, when TRV-130 was bound, the residues in the EC2 and EC3 loops of the μOR formed a substantially extensive network of polar interactions when compared to morphine (Schneider et al., 2016). Kapoor and co-workers had found that more information is transferred across the receptor in TRV-130-bound μOR than in morphine-bound μOR based on transfer entropy analysis; for instance, the three extracellular loop regions are not involved entirely in any information transfer in the case of morphine (Kapoor et al., 2017).

Another study has found that morphine- and PZM21-activated network paths toward the intracellular end of TM6 were mostly identical, but the paths to the end of TM7 were evidently different (Liao et al., 2021). The same study also compared three key molecular switches, the ionic lock (DRY), transmission (CWxP), and Tyr toggle switches. Here, they found distance and rotational changes between morphine- and PMZ21-bound μOR, which affect the positions of TM5-7 (see later) (**Figure 1C**) (Liao et al., 2021). In another MD simulation, they compared TRV-130 and PZM21 with morphine, and one of the main differences was that the side chain of $Trp^{6.48}$ (**Figure 1C**) was reversed with a delay with PZM21 compared to morphine (300 vs. 50 ns) and that $Tyr^{7.43}$ side chain (**Figure 1C**) rotated with less fluctuation range compared to TRV-130-bound μOR (PZM21: 100°–175° vs. TRV-130: 100°–150°) (Zhao et al., 2020). These results also point to the low potency and lower bias effect of PZM21.

HIGHER-ORDER STRUCTURAL CHANGES, GLOBAL MOVEMENTS

With GPCRs, the subtle changes in the ligand-binding pocket and ligand binding signal transmission throughout the TM domains add up to large, global toggle switch movements of the TM domains (Nygaard et al., 2009; Venkatakrishnan et al., 2013). These movements are crucial in the receptor inactive–active conformation transition (Huang et al., 2015; Zhou et al., 2019). However, regarding the μOR, there are multiple data pointing out that agonists with different efficacies or functional selectivities trigger these large movements differently or to a different degree. Such data will be reviewed in this section.

A study comparing fentanyl and morphine showed that fentanyl selects for more upward conformations of TM3 than morphine (+0.6 Å vs +0.2 Å) (Ricarte et al., 2021). Additionally, both compounds are able to stabilize an active-like conformation of TM6 in simulations initiated from the activated state; however, only fentanyl can achieve the same when starting from the inactive state of the receptor. This difference may contribute to the greater efficacy of fentanyl relative to morphine.

In the case of BU72, upon activation, TM6 makes a large 10 Å outward movement and smaller inward movement of TM5 and TM7 (**Figure 1C**) (Huang et al., 2015). Complementing these data in the presence of a G-protein mimetic nanobody in solution-state NMR, a weak allosteric coupling was revealed between the agonist-binding pocket and the G-protein-coupling interface (TM5 and TM6) (Sounier et al., 2015), similar to that observed for the β2-adrenergic receptor (Manglik et al., 2015). Most interestingly, in the presence of BU72 or DAMGO alone, ICL1 and H8 showed larger conformational changes (**Figure 1C**) (indicated by larger spectral signals) compared to TM5 and TM6, suggesting that these domains might play a role in the initial interaction with the G-protein (Sounier et al., 2015).

Okude et al. studied the NMR signals from methionine residues of the μOR in the morphine-, DAMGO-, and TRV-130-bound states. They found that when morphine was bound, μOR exists in equilibrium between the closed and open conformations; in the DAMGO-bound state, the receptor mainly adopts the open conformation. Upon TRV-130 binding, μOR exists in equilibrium between the closed and open conformations; however, in such cases, the open conformation adopts a larger intracellular cavity (Okude et al., 2015). The study also demonstrated that the population of each open conformation defines the G-protein- and arrestin-mediated signaling levels in each ligand-bound state.

Kapoor et al. found that morphine-bound μOR motions involved the cytoplasmic ends of only TM6, TM3, and TM5 (**Figure 1C**). On the other hand, the TRV-130-bound μOR motions involved residues in TM1, TM2, TM3, TM5, TM7, and helix 8 (Kapoor et al., 2017). Also, TM6 bending and intra-helical backbone hydrogen bond rearrangement were only observed with morphine- but not with TRV-130-bound μOR (Kapoor et al., 2017).

Mafi and co-workers compared morphine, DAMGO, and TRV-130 in MD simulations with the β-arrestin2-stabilized active phosphorylated μOR (Mafi et al., 2020). Accordingly, in the presence of non-biased agonists, β-arrestin2 coupled to the phosphorylated μOR by forming more polar connections with ICL2 and either the ICL3 or the cytoplasmic region of TM6. In contrast, TRV-130 induced a reposition of TM6 in the cytoplasmic region of the μOR by forming more polar interactions with TM2 and TM3. This repositioning hinders β-arrestin2 from properly binding to the phosphorylated μOR.

PZM21 was bound to μOR, TM5-6 and TM7 showed a larger outward and less inward movement, respectively (**Figure 1C**) (Liao et al., 2021). Also, the further outward movement of TM5–7 of the PZM21-bound μOR created a larger cavity potentially favorable for G protein binding. Zhao et al. analyzed and compared the flexibility of the loop region of PZM21 with morphine and TRV-130, and they found that the protein root mean square fluctuation (RMSF) values of morphine- and PZM21-bound μOR in the ECL1-3 and ICL3 regions were significantly smaller than those of TRV130-bound μOR (Zhao et al., 2020).

DISCUSSION AND CONCLUSION

The introduction of the two active conformational structures of the μOR now allows a more precise analysis of ligand-specific changes in the receptor. Reviewing the increasing amount of the data regarding ligand-specific structural changes in μOR

activation, certain tendencies can be observed (**Table 1**; **Figure 1C**). The current data proved that ligand recognition largely depends on the structural properties of the ligand. The highlighted ligands in this review differ in terms of flexibility, H-bond capabilities, and energy landscapes (Podlewska et al., 2020; Vo et al., 2020; Giannos et al., 2021). For instance, morphine and fentanyl despite being in contact with similar residues (**Figure 1B**), the binding pose itself is significantly different since morphine is more rigid and compact, while fentanyl is more flexible with an elongated shape. On the other hand, BU72 and DAMGO structurally differ significantly and there is also a difference regarding the depth of their binding pose. However, the conformation of the active binding pocket is highly similar. In the case of biased agonists TRV-130 and PZM21, it seems that they accomplish stronger and/or more contact with the receptor compared to unbiased ligands.

There are significantly more differences than similarities when it comes to forwarding the ligand-binding signal to the intracellular regions of the receptor. There are subtle, but important ligand-specific changes within the molecular switches; for instance, the different torsion angles or distances between the involved residues (**Figure 1C**). As mentioned above, such minor changes might also explain the higher efficacy of fentanyl (Ricarte et al., 2021) or β-arrestin coupling (de Waal et al., 2020). Another interesting finding is that with PZM21 the difference in rotations of certain residues can be associated with its lower bias effect (Zhao et al., 2020). Such delicate changes induce larger-scale movements for the μOR, which eventually dictate the faith of the receptor's signaling pathway and possibly it's degree of desensitization. These larger movements in essence allow a physical barrier or a favorable position for either the G-protein or β-arrestins, depending on the bound ligand.

In conclusion, ligand-specific μOR activation is defined by the following: 1) distinct number and/or degree of residue contacts within the ligand-binding pocket; 2) ligand-specific subtle changes within the residues (with respect to torsion angles and distances) of the TM regions, and as a consequence 3) triggers large-scale movements, toggles in certain domains of the receptor defining the type of downstream signaling of the μOR, as well as the degree of receptor desensitization. Further mapping these steps might open new strategies to develop opioid agonists with reduced analgesic tolerance and other side effects.

AUTHOR CONTRIBUTIONS

FZ and MA-K performed the conceptualization. FZ constructed the figures and tables and performed the writing of the original draft. FZ, NE, KK, and MA-K performed the reviewing and editing of the manuscript.

FUNDING

This work was supported by the Hungarian Academy of Sciences "Bolyai János" Research Fellowship (BO/00476/20/5). Project no. FK_138389 and TKP2021-EGA-25 have been implemented with the support provided by the Ministry of Innovation and Technology of Hungary from the National Research, Development and Innovation Fund, financed under the FK_21 and TKP2021-EGA funding scheme.

REFERENCES

Allouche, S., Noble, F., and Marie, N. (2014). Opioid Receptor Desensitization: Mechanisms and its Link to Tolerance. *Front. Pharmacol.* 5, 280. doi:10.3389/fphar.2014.00280

Ballesteros, J. A., and Weinstein, H. (1995). "Integrated Methods for the Construction of Three-Dimensional Models and Computational Probing of Structure-Function Relations in G Protein-Coupled Receptors," in *Methods in Neurosciences*. Editor S.C. Sealfon (Cambridge, MA: Academic Press), 366–428. doi:10.1016/s1043-9471(05)80049-7

Brooks, B. R., Brooks, C. L., III, Mackerell, A. D., Jr., Nilsson, L., Petrella, R. J., Roux, B., et al. (2009). CHARMM: The Biomolecular Simulation Program. *J. Comput. Chem.* 30, 1545–1614. doi:10.1002/jcc.21287

Chabbert, M., Castel, H., Pele, J., Deville, J., Legendre, R., and Rodien, P. (2012). Evolution of Class A G-Protein-Coupled Receptors: Implications for Molecular Modeling. *Cmc* 19, 1110–1118. doi:10.2174/092986712799320600

Cheng, J.-x., Cheng, T., Li, W.-h., Liu, G.-x., Zhu, W.-l., and Tang, Y. (2018). Computational Insights into the G-Protein-Biased Activation and Inactivation Mechanisms of the μ Opioid Receptor. *Acta Pharmacol. Sin.* 39, 154–164. doi:10.1038/aps.2017.158

de Waal, P. W., Shi, J., You, E., Wang, X., Melcher, K., Jiang, Y., et al. (2020). Molecular Mechanisms of Fentanyl Mediated β-arrestin Biased Signaling. *PLoS Comput. Biol.* 16, e1007394. doi:10.1371/journal.pcbi.1007394

Dumitrascuta, M., Bermudez, M., Ballet, S., Wolber, G., and Spetea, M. (2020). Mechanistic Understanding of Peptide Analogues, DALDA, [Dmt1]DALDA, and KGOP01, Binding to the Mu Opioid Receptor. *Molecules* 25, 2087. doi:10.3390/molecules25092087

Feinberg, E. N., Farimani, A. B., Hernandez, C. X., and Pande, V. S. (2017). Kinetic Machine Learning Unravels Ligand-Directed Conformational Change of μ Opioid Receptor. *bioRxiv* 114, 170886. doi:10.1016/j.bpj.2017.11.359

Filipek, S. (2019). Molecular Switches in GPCRs. *Curr. Opin. Struct. Biol.* 55, 114–120. doi:10.1016/j.sbi.2019.03.017

Giannos, T., Lešnik, S., Bren, U., Hodošček, M., Domratcheva, T., and Bondar, A.-N. (2021). CHARMM Force-Field Parameters for Morphine, Heroin, and Oliceridine, and Conformational Dynamics of Opioid Drugs. *J. Chem. Inf. Model.* 61, 3964–3977. doi:10.1021/acs.jcim.1c00667

Huang, W., Manglik, A., Venkatakrishnan, A. J., Laeremans, T., Feinberg, E. N., Sanborn, A. L., et al. (2015). Structural Insights into M-Opioid Receptor Activation. *Nature* 524, 315–321. doi:10.1038/nature14886

Kapoor, A., Martinez-Rosell, G., Provasi, D., de Fabritiis, G., and Filizola, M. (2017). Dynamic and Kinetic Elements of M-Opioid Receptor Functional Selectivity. *Sci. Rep.* 7, 11255. doi:10.1038/s41598-017-11483-8

Kaserer, T., Lantero, A., Schmidhammer, H., Spetea, M., and Schuster, D. (2016). μ Opioid Receptor: Novel Antagonists and Structural Modeling. *Sci. Rep.* 6, 21548. doi:10.1038/srep21548

Katritch, V., Cherezov, V., and Stevens, R. C. (2013). Structure-Function of the G Protein-Coupled Receptor Superfamily. *Annu. Rev. Pharmacol. Toxicol.* 53, 531–556. doi:10.1146/annurev-pharmtox-032112-135923

Koehl, A., Hu, H., Maeda, S., Zhang, Y., Qu, Q., Paggi, J. M., et al. (2018). Structure of the M-Opioid Receptor-Gi Protein Complex. *Nature* 558, 547–552. doi:10.1038/s41586-018-0219-7

Lagerström, M. C., and Schiöth, H. B. (2008). Structural Diversity of G Protein-Coupled Receptors and Significance for Drug Discovery. *Nat. Rev. Drug Discov.* 7, 339–357. doi:10.1038/nrd2518

Lamim Ribeiro, J. M., Provasi, D., and Filizola, M. (2020). A Combination of Machine Learning and Infrequent Metadynamics to Efficiently Predict Kinetic

Rates, Transition States, and Molecular Determinants of Drug Dissociation from G Protein-Coupled Receptors. *J. Chem. Phys.* 153, 124105. doi:10.1063/5.0019100

Lee, J. H., Shon, S.-Y., Jeon, W., Hong, S.-J., Ban, J., and Lee, D. S. (2021). Discovery of μ,δ-Opioid Receptor Dual-Biased Agonists that Overcome the Limitation of Prior Biased Agonists. *ACS Pharmacol. Transl. Sci.* 4, 1149–1160. doi:10.1021/acsptsci.1c00044

Lemel, L., Lane, J. R., and Canals, M. (2020). GRKs as Key Modulators of Opioid Receptor Function. *Cells* 9, 2400. doi:10.3390/cells9112400

Liao, S., Tan, K., Floyd, C., Bong, D., Pino, M. J., and Wu, C. (2021). Probing Biased Activation of Mu-Opioid Receptor by the Biased Agonist PZM21 Using All Atom Molecular Dynamics Simulation. *Life Sci.* 269, 119026. doi:10.1016/j.lfs.2021.119026

Lipiński, P. F. J., Jarończyk, M., Dobrowolski, J. C., and Sadlej, J. (2019). Molecular Dynamics of Fentanyl Bound to μ-opioid Receptor. *J. Mol. Model.* 25, 144. doi:10.1007/s00894-019-3999-2

Lu, Z., Xu, J., Rossi, G. C., Majumdar, S., Pasternak, G. W., and Pan, Y.-X. (2015). Mediation of Opioid Analgesia by a Truncated 6-transmembrane GPCR. *J. Clin. Investig.* 125, 2626–2630. doi:10.1172/jci81070

Mafi, A., Kim, S.-K., and Goddard, W. A. (2020). Mechanism of β-arrestin Recruitment by the μ-opioid G Protein-Coupled Receptor. *Proc. Natl. Acad. Sci. U.S.A.* 117, 16346–16355. doi:10.1073/pnas.1918264117

Mahinthichaichan, P., Vo, Q. N., Ellis, C. R., and Shen, J. (2021). Kinetics and Mechanism of Fentanyl Dissociation from the μ-Opioid Receptor. *JACS Au* 1, 2208–2215. doi:10.1021/jacsau.1c00341

Maier, J. A., Martinez, C., Kasavajhala, K., Wickstrom, L., Hauser, K. E., and Simmerling, C. (2015). ff14SB: Improving the Accuracy of Protein S ide Chain and Backbone Parameters from ff99SB. *J. Chem. Theory Comput.* 11, 3696–3713. doi:10.1021/acs.jctc.5b00255

Majumdar, S., Grinnell, S., Le Rouzic, V., Burgman, M., Polikar, L., Ansonoff, M., et al. (2011). Truncated G Protein-Coupled Mu Opioid Receptor MOR-1 Splice Variants Are Targets for Highly Potent Opioid Analgesics Lacking Side Effects. *Proc. Natl. Acad. Sci. U.S.A.* 108, 19778–19783. doi:10.1073/pnas.1115231108

Majumdar, S., Subrath, J., Le Rouzic, V., Polikar, L., Burgman, M., Nagakura, K., et al. (2012). Synthesis and Evaluation of Aryl-Naloxamide Opiate Analgesics Targeting Truncated Exon 11-Associated μ Opioid Receptor (MOR-1) Splice Variants. *J. Med. Chem.* 55, 6352–6362. doi:10.1021/jm300305c

Manglik, A., Kim, T. H., Masureel, M., Altenbach, C., Yang, Z., Hilger, D., et al. (2015). Structural Insights into the Dynamic Process of β 2 -Adrenergic Receptor Signaling. *Cell.* 161, 1101–1111. doi:10.1016/j.cell.2015.04.043

Manglik, A., Kruse, A. C., Kobilka, T. S., Thian, F. S., Mathiesen, J. M., Sunahara, R. K., et al. (2012). Crystal Structure of the M-Opioid Receptor Bound to a Morphinan Antagonist. *Nature* 485, 321–326. doi:10.1038/nature10954

Manglik, A., Lin, H., Aryal, D. K., McCorvy, J. D., Dengler, D., Corder, G., et al. (2016). Structure-based Discovery of Opioid Analgesics with Reduced Side Effects. *Nature* 537, 185–190. doi:10.1038/nature19112

Manglik, A. (2020). Molecular Basis of Opioid Action: From Structures to New Leads. *Biol. Psychiatry* 87, 6–14. doi:10.1016/j.biopsych.2019.08.028

Mansour, A., Taylor, L. P., Fine, J. L., Thompson, R. C., Hoversten, M. T., Mosberg, H. I., et al. (1997). Key Residues Defining the Mu-Opioid Receptor Binding Pocket: a Site-Directed Mutagenesis Study. *J. Neurochem.* 68, 344–353. doi:10.1046/j.1471-4159.1997.68010344.x

Marino, K. A., Shang, Y., and Filizola, M. (2018). Insights into the Function of Opioid Receptors from Molecular Dynamics Simulations of Available Crystal Structures. *Br. J. Pharmacol.* 175, 2834–2845. doi:10.1111/bph.13774

Nygaard, R., Frimurer, T. M., Holst, B., Rosenkilde, M. M., and Schwartz, T. W. (2009). Ligand Binding and Micro-switches in 7TM Receptor Structures. *Trends Pharmacol. Sci.* 30, 249–259. doi:10.1016/j.tips.2009.02.006

Okude, J., Ueda, T., Kofuku, Y., Sato, M., Nobuyama, N., Kondo, K., et al. (2015). Identification of a Conformational Equilibrium that Determines the Efficacy and Functional Selectivity of the μ-Opioid Receptor. *Angew. Chem. Int. Ed.* 54, 15771–15776. doi:10.1002/anie.201508794

Pettersen, E. F., Goddard, T. D., Huang, C. C., Couch, G. S., Greenblatt, D. M., Meng, E. C., et al. (2004). UCSF Chimera?A Visualization System for Exploratory Research and Analysis. *J. Comput. Chem.* 25, 1605–1612. doi:10.1002/jcc.20084

Podlewska, S., Bugno, R., Kudla, L., Bojarski, A. J., and Przewlocki, R. (2020). Molecular Modeling of M Opioid Receptor Ligands with Various Functional Properties: PZM21, SR-17018, Morphine, and Fentanyl-Simulated Interaction Patterns Confronted with Experimental Data. *Molecules* 25, 4636. doi:10.3390/molecules25204636

Ricarte, A., Dalton, J. A. R., and Giraldo, J. (2021). Structural Assessment of Agonist Efficacy in the μ-Opioid Receptor: Morphine and Fentanyl Elicit Different Activation Patterns. *J. Chem. Inf. Model.* 61, 1251–1274. doi:10.1021/acs.jcim.0c00890

Sader, S., Anant, K., and Wu, C. (2018). To Probe Interaction of Morphine and IBNtxA with 7TM and 6TM Variants of the Human μ-opioid Receptor Using All-Atom Molecular Dynamics Simulations with an Explicit Membrane. *Phys. Chem. Chem. Phys.* 20, 1724–1741. doi:10.1039/c7cp06745c

Schneider, S., Provasi, D., and Filizola, M. (2016). How Oliceridine (TRV-130) Binds and Stabilizes a μ-Opioid Receptor Conformational State that Selectively Triggers G Protein Signaling Pathways. *Biochemistry* 55, 6456–6466. doi:10.1021/acs.biochem.6b00948

Sena, D. M., Cong, X., and Giorgetti, A. (2021). Ligand Based Conformational Space Studies of the μ-opioid Receptor. *Biochimica Biophysica Acta (BBA) - General Subj.* 1865, 129838. doi:10.1016/j.bbagen.2020.129838

Sounier, R., Mas, C., Steyaert, J., Laeremans, T., Manglik, A., Huang, W., et al. (2015). Propagation of Conformational Changes during μ-opioid Receptor Activation. *Nature* 524, 375–378. doi:10.1038/nature14680

Trzaskowski, B., Latek, D., Yuan, S., Ghoshdastider, U., Debinski, A., and Filipek, S. (2012). Action of Molecular Switches in GPCRs - Theoretical and Experimental Studies. *Cmc* 19, 1090–1109. doi:10.2174/092986712799320556

Venkatakrishnan, A. J., Deupi, X., Lebon, G., Tate, C. G., Schertler, G. F., and Babu, M. M. (2013). Molecular Signatures of G-Protein-Coupled Receptors. *Nature* 494, 185–194. doi:10.1038/nature11896

Vo, Q., Mahinthichaichan, P., Shen, J., and Ellis, C. (2021). How Mu-Opioid Receptor Recognizes Fentanyl. *Nat. Commun.* 12(1), 984. doi:10.1038/s41467-021-21262-9

Weis, W. I., and Kobilka, B. K. (2018). The Molecular Basis of G Protein-Coupled Receptor Activation. *Annu. Rev. Biochem.* 87, 897–919. doi:10.1146/annurev-biochem-060614-033910

Weng, W.-H., Li, Y.-T., and Hsu, H.-J. (2017). Activation-Induced Conformational Changes of Dopamine D3 Receptor Promote the Formation of the Internal Water Channel. *Sci. Rep.* 7, 12792. doi:10.1038/s41598-017-13155-z

Williams, J. T., Ingram, S. L., Henderson, G., Chavkin, C., von Zastrow, M., Schulz, S., et al. (2013). Regulation Ofμ-Opioid Receptors: Desensitization, Phosphorylation, Internalization, and Tolerance. *Pharmacol. Rev.* 65, 223–254. doi:10.1124/pr.112.005942

Zhao, Z., Huang, T., and Li, J. (2020). Molecular Dynamics Simulations to Investigate How PZM21 Affects the Conformational State of the μ-Opioid Receptor upon Activation. *Ijms* 21, 4699. doi:10.3390/ijms21134699

Zhou, Q., Yang, D., Wu, M., Guo, Y., Guo, W., Zhong, L., et al. (2019). Common Activation Mechanism of Class A GPCRs. *eLife* 8, e50279. doi:10.7554/eLife.50279

Conflict of Interest: The authors declare that the research was conducted in the absence of any commercial or financial relationships that could be construed as a potential conflict of interest.

Publisher's Note: All claims expressed in this article are solely those of the authors and do not necessarily represent those of their affiliated organizations, or those of the publisher, the editors, and the reviewers. Any product that may be evaluated in this article, or claim that may be made by its manufacturer, is not guaranteed or endorsed by the publisher.

pharmaceuticals

MDPI

Article

Pregabalin–Tolperisone Combination to Treat Neuropathic Pain: Improved Analgesia and Reduced Side Effects in Rats

Nariman Essmat [1,2], Anna Rita Galambos [1], Péter P. Lakatos [3], Dávid Árpád Karádi [1], Amir Mohammadzadeh [1], Sarah Kadhim Abbood [1], Orsolya Geda [3], Rudolf Laufer [3], Kornél Király [1], Pál Riba [1], Zoltán S. Zádori [1], Éva Szökő [3], Tamás Tábi [3,*] and Mahmoud Al-Khrasani [1,*]

[1] Department of Pharmacology and Pharmacotherapy, Semmelweis University, 4 Nagyvárad tér, H-1089 Budapest, Hungary; nariman.gomaa@phd.semmelweis.hu (N.E.); galambos.anna@phd.semmelweis.hu (A.R.G.); karadi.david_arpad@med.semmelweis-univ.hu (D.Á.K.); mohammadzadeh.amir@med.semmelweis-univ.hu (A.M.); abbood.sarah@phd.semmelweis.hu (S.K.A.); kiraly.kornel@med.semmelweis-univ.hu (K.K.); riba.pal@med.semmelweis-univ.hu (P.R.); zadori.zoltan@med.semmelweis-univ.hu (Z.S.Z.)

[2] Department of Pharmacology and Toxicology, Faculty of Pharmacy, Zagazig University, Zagazig 44519, Egypt

[3] Department of Pharmacodynamics, Semmelweis University, 4 Nagyvárad tér, H-1089 Budapest, Hungary; lakatos.peter.pal@semmelweis.hu (P.P.L.); geda.orsolya@semmelweis.hu (O.G.); laufer.rudolf@semmelweis.hu (R.L.); szoko.eva@semmelweis.hu (É.S.)

* Correspondence: tabi.tamas@semmelweis.hu (T.T.); al-khrasani.mahmoud@med.semmelweis-univ.hu (M.A.-K.); Tel.: +36-1-2104-411 (T.T.); +36-1-2104-416 (M.A.-K.)

Abstract: The current treatment of neuropathic pain (NP) is unsatisfactory; therefore, effective novel agents or combination-based analgesic therapies are needed. Herein, oral tolperisone, pregabalin, and duloxetine were tested for their antinociceptive effect against rat partial sciatic nerve ligation (pSNL)-induced tactile allodynia described by a decrease in the paw withdrawal threshold (PWT) measured by a dynamic plantar aesthesiometer. On day 7 after the operation, PWTs were assessed at 60, 120, and 180 min post-treatment. Chronic treatment was continued for 2 weeks, and again, PWTs were measured on day 14 and 21. None of the test compounds produced an acute antiallodynic effect. In contrast, after chronic treatment, tolperisone and pregabalin alleviated allodynia. In other experiments, on day 14, the acute antiallodynic effect of the tolperisone/pregabalin or duloxetine combination was measured. As a novel finding, a single dose of the tolperisone/pregabalin combination could remarkably alleviate allodynia acutely. It also restored the neuropathy-induced elevated CSF glutamate content. Furthermore, the combination is devoid of adverse effects related to motor and gastrointestinal transit functions. Tolperisone and pregabalin target voltage-gated sodium and calcium channels, respectively. The dual blockade effect of the combination might explain its advantageous acute analgesic effect in the present work.

Keywords: neuropathic pain; allodynia; tolperisone; pregabalin; duloxetine; CSF glutamate content; synaptosome; neuronal glutamate release

Citation: Essmat, N.; Galambos, A.R.; Lakatos, P.P.; Karádi, D.Á.; Mohammadzadeh, A.; Abbood, S.K.; Geda, O.; Laufer, R.; Király, K.; Riba, P.; et al. Pregabalin–Tolperisone Combination to Treat Neuropathic Pain: Improved Analgesia and Reduced Side Effects in Rats. *Pharmaceuticals* **2023**, *16*, 1115. https://doi.org/10.3390/ph16081115

Academic Editor: Sergio Marques Borghi

Received: 19 July 2023
Revised: 3 August 2023
Accepted: 4 August 2023
Published: 7 August 2023

1. Introduction

Neuropathic pain (NP) is a debilitating chronic condition that results from disease, trauma, or dysfunction affecting the somatosensory neurons. Several mechanisms are involved in the development of NP; mechanisms that alter the balance between operating excitatory and inhibitory neurotransmitters at the spinal cord level are of importance [1]. The current pharmacological lines of therapy for NP encompass different drugs. First-line treatments include gabapentinoids affecting the high voltage-activated calcium channels hosting α2δ-1 subunits that are localized on the excitatory neurons on the dorsal horn of the spinal cord, and antidepressants that are non-selective or selective inhibitors of serotonin and noradrenaline reuptake, such as amitriptyline or duloxetine, respectively.

The second-line treatments include the use of voltage-gated sodium channel inhibitors, such as topical lidocaine or drugs acting on other receptors, including tramadol, which simultaneously target both the noradrenergic and serotoninergic systems, yet activate opioid receptors [2,3]. The third-line treatments are strong opioids and subcutaneous botulinum toxin A. Furthermore, treatments include combination therapy, antiepileptic agents, selective serotonin reuptake inhibitors, NMDA receptor antagonists, and local capsaicin [3–7]. All the above-mentioned treatment approaches consist of different drugs of various pharmacodynamic targets, reflecting the complex nature of the pathophysiology of neuropathic pain [8–12]. Despite these treatment options, the current drugs used to treat NP cause side effects that result in dose escalation being practically impossible. To solve this problem, multimodal analgesia containing two or more analgesics at lower doses may provide additive or synergistic effects of increased efficacy, and decreased side effects compared to the single therapy. Several human studies have followed this strategy; among them is the combination of gabapentinoids with tricyclic antidepressants, such as nortriptyline or opioid analgesics, to manage post-herpetic neuralgia or painful diabetic polyneuropathy [13–15]. In these studies, the combination offers better analgesia as compared to the use of single-drug therapy. However, the adverse effects, such as dry mouth and constipation, among others, caused by the anticholinergic and opioid constituents of the combination were higher compared to gabapentinoids medication alone [16]. Another study showed that treating NP of diabetic patients with a combination composed of oxycodone and gabapentin did not worsen the commonly observed opioid-induced side effects, which supports the use of this combination for neuropathic pain control [17]. A discrepancy between studies has been reported regarding the analgesic effect of the combination of oxycodone and gabapentinoids, such as pregabalin, where a small dose of oxycodone has failed to enhance pregabalin's ability to relieve pain in patients with either painful diabetic neuropathy or post-herpetic neuralgia [18]. Numerous preclinical studies have also been carried out to evaluate the combination of different drugs that were used to manage human neuropathic pain. In neuropathic rats that underwent spinal nerve ligation, Matthews and Dickenson (2002) showed that, in contrast to morphine, gabapentin's inhibitory effect is increased in the dorsal horn neuronal response following its systemic administration [19], yet the response to morphine was diminished. The pregabalin–carbamazepine (sodium channel blocker) combination was found to produce a synergistic antiallodynic effect in the spinal nerve ligation model in rats. In this study, the antiallodynic effect was only seen when the drugs were combined in doses that exceeded ED75 values, although the side effects were not studied [20]. For more details on the analgesic and side effects of drug combinations being used to treat NP, see [21].

Tolperisone is a centrally acting muscle relaxant used clinically for various conditions, such as painful reflex muscle spasms and post-stroke spasticity [22,23]. Its mechanism of action has been suggested to include the blocking of sodium and calcium channels [24–26]. Recent research carried out by our group reported that acute oral tolperisone administration can induce a measurable acute antinociceptive effect against mechanical allodynia in neuropathic rats [27].

The present preclinical work includes a comparative study of drugs used to ameliorate human neuropathic pain by different mechanisms of action, such as pregabalin, duloxetine, and carbamazepine. A multimodal approach to manage NP has long been appreciated; thus, the present study also intended to explore the potential relevance of tolperisone in tactile allodynia treatment, particularly when combined with pregabalin, a combination that has not been tested before. In this regard, we hypothesized that the use of two mechanistically different analgesics, tolperisone (sodium channel blocker) with pregabalin (calcium channel blocker), at sub-analgesic doses may provide superior analgesia with a better adverse effect profile in tactile allodynia induced by partial sciatic nerve ligation or streptozotocin (STZ)-induced peripheral neuropathic pain in rats compared to each single drug to identify new combinational therapies for neuropathic pain treatment in future clinical trials. The study also includes experiments on the impact of the co-administration

of tolperisone and duloxetine on pSNL-induced NP. Finally, we assessed the motor and gastrointestinal side effects of the combination-based promising analgesic approach to treat NP.

2. Results

2.1. Chronic Treatment Is Essential for Both Tolperisone and Pregabalin to Alleviate Tactile Allodynia Evoked by Partial Sciatic Nerve Ligation (pSNL)

Figures 1 and 2 depict the effect of orally administered tolperisone or pregabalin (25, 50, and 100 mg/kg) in pSNL-induced tactile allodynia in rats on day 7 (single treatment), 14 (1 week treatment), and 21 (2 weeks treatment) after the operation at 60, 120, and 180 min. Tactile allodynia was indicated by a decrease in the rat paw withdrawal threshold (PWT) measured by a dynamic plantar aesthesiometer (DPA).

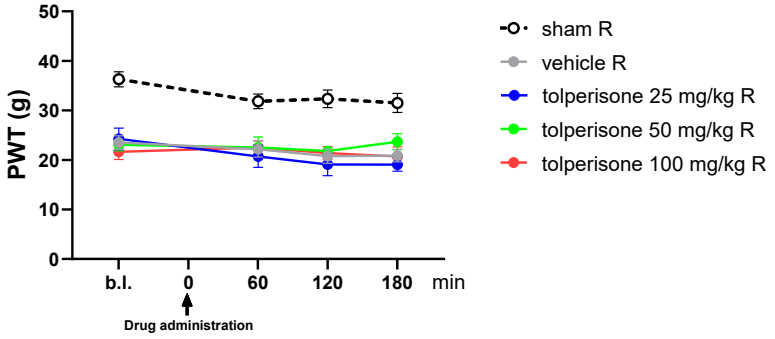

(**a**) Single treatment

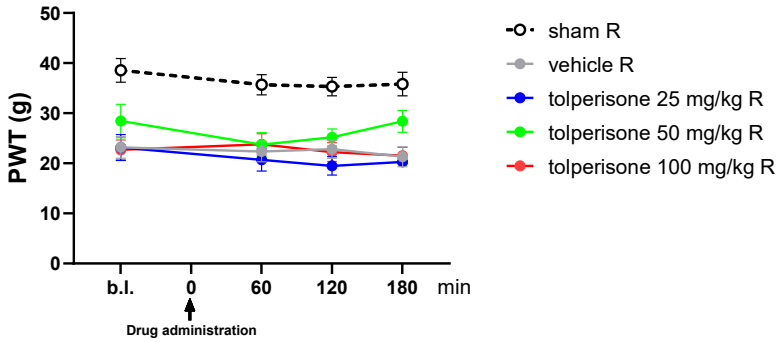

(**b**) One week treatment

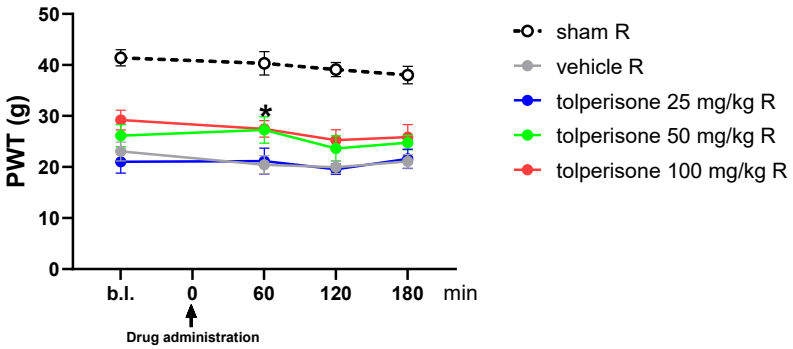

(**c**) Two weeks treatment

Figure 1. The antiallodynic effect of tolperisone on pSNL evoked allodynia. The PWTs were measured postoperatively on day 7 prior to and after a single treatment (panel (**a**)), on day 14 after 1 week of chronic treatment (panel (**b**)), and on day 21 after 2 weeks of chronic treatment (panel (**c**)). Tactile

allodynia was measured by DPA at 60, 120, and 180 min after oral treatment. Data are shown as the mean ± SEM of 8–13 animals per group. * $p < 0.05$ statistically significant compared to the vehicle-treated group at the indicated time points after treatment (two-way ANOVA followed by Dunnett's post-hoc test). Baseline (b.l.): was measured before the first treatment. Single treatment: was measured after acute administration on day 7 after the operation.

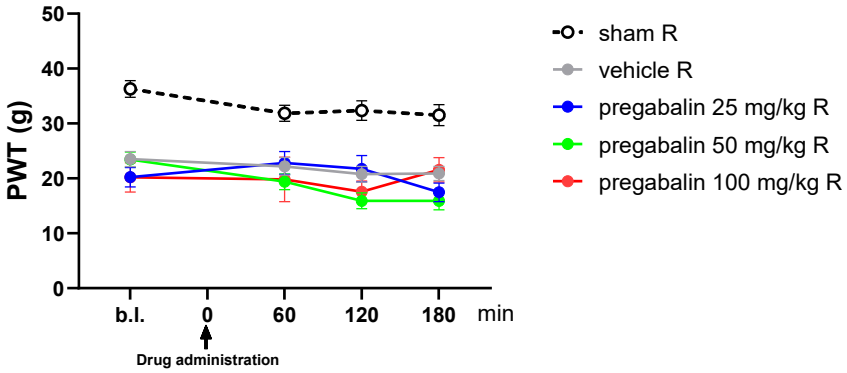

(**a**) Single treatment

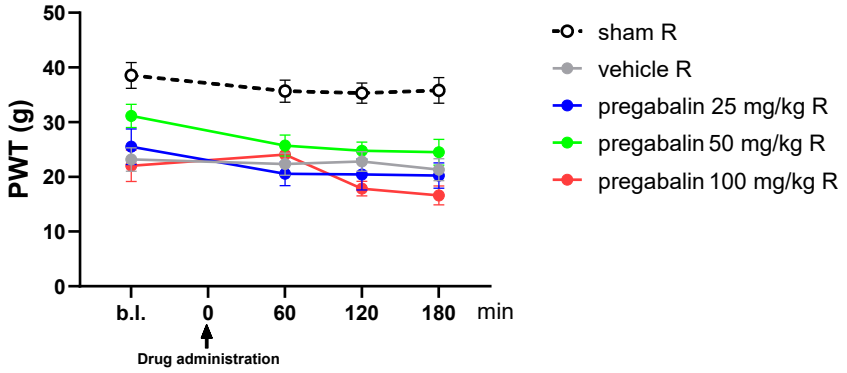

(**b**) One week treatment

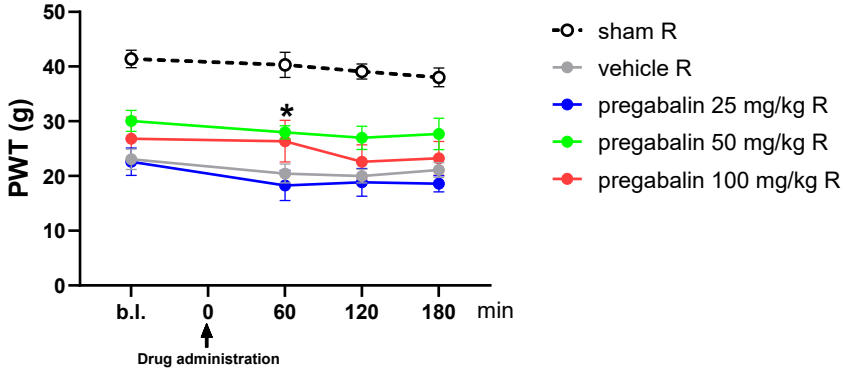

(**c**) Two weeks treatment

Figure 2. The antiallodynic effect of pregabalin on pSNL evoked allodynia. The PWTs were measured on day 7 prior to and after a single treatment (panel (**a**)), on day 14 (1 week treatment) (panel (**b**)), and on day 21 (2 weeks treatment) (panel (**c**)) after the operation. Tactile allodynia was measured by DPA at 60, 120, and 180 min after oral treatment. Data are shown as the mean ± SEM of 6–13 animals per group. * $p < 0.05$, statistically significant compared to the vehicle right (operated) paw at the indicated

time points after treatment (two-way ANOVA followed by Dunnett's post-hoc test). Baseline (b.l.): was measured before the first treatment. Single treatment: was measured after acute administration on day 7 after the operation.

In this series of experiments, we intended to measure the acute effect of oral (25, 50, and 100 mg/kg) tolperisone or pregabalin on the developed tactile allodynia of rats with pSNL on day 7, as well as of rats that were treated for 2 consecutive weeks (Figures 1 and 2). As shown in Figure 1a,b, oral test doses of tolperisone failed to produce a significant antiallodynic effect either after acute treatment or 1 week of chronic treatment, respectively. After 2 weeks of treatment, following oral administration, 100 mg/kg of tolperisone showed a significant effect against the developed tactile allodynia, 60 min after oral administration (Figure 1c) compared to the vehicle-treated group (two-way ANOVA: F (treatment group; 4, 45) = 25.41, $p < 0.0001$, Dunnett's post-hoc test: $p = 0.0260$).

Similar to tolperisone, pregabalin in test doses was ineffective in alleviating rat tactile allodynia following acute treatment or 1 week of chronic treatment (Figure 2a,b). However, 2 weeks of consecutive treatment with 50 mg/kg pregabalin significantly alleviated tactile allodynia 60 min after oral administration (two-way ANOVA: F (treatment group; 4, 39) = 23.91, $p < 0.0001$, Dunnett's post-hoc test: $p = 0.0080$) when compared to the vehicle-treated group (Figure 2c).

On the other hand, duloxetine in test doses was ineffective in alleviating rat tactile allodynia following acute or chronic treatment compared to vehicle-treated rats (Figure 3a–c).

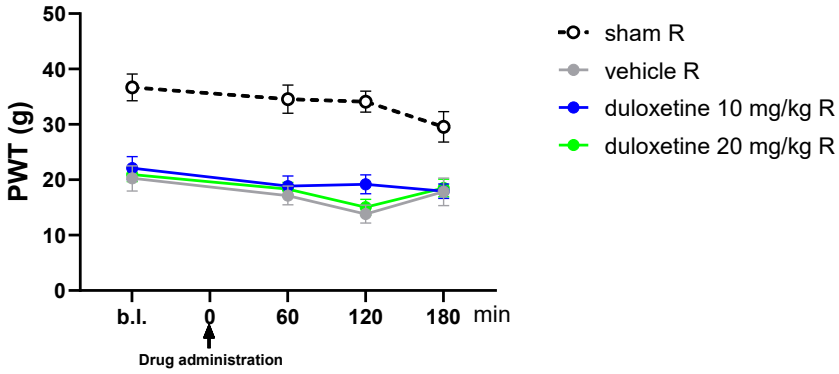

(**a**) Single treatment

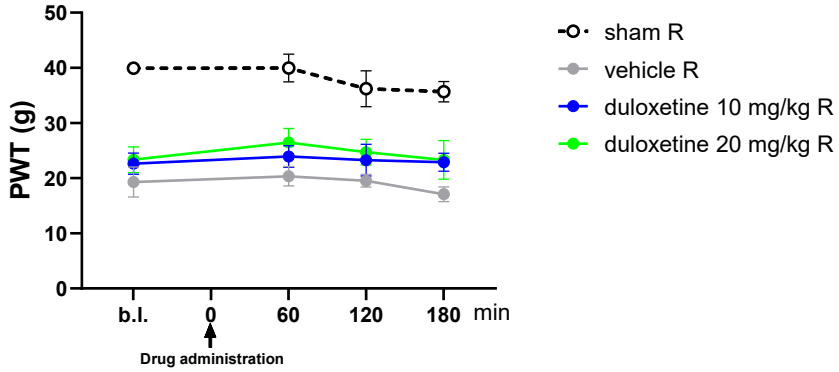

(**b**) One week treatment

Figure 3. *Cont.*

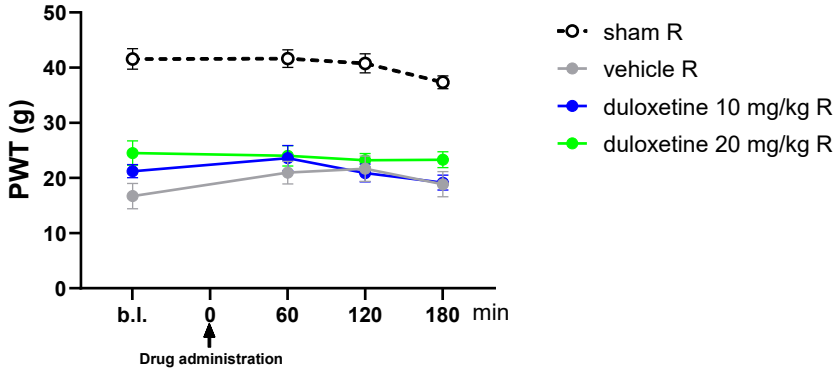

(**c**) Two weeks treatment

Figure 3. The antiallodynic effect of duloxetine on pSNL evoked allodynia. The PWTs were measured on day 7 prior to and after a single treatment (panel (**a**)), on day 14 (1 week treatment) (panel (**b**)), and on day 21 (2 weeks treatment) (panel (**c**)) after the operation. Tactile allodynia was measured by DPA at 60, 120, and 180 min after oral treatment. Data are shown as the mean ± SEM of 5–7 animals per group. $p < 0.05$, statistically significant compared to the vehicle right (operated) paw at the indicated time points after treatment (two-way ANOVA followed by Dunnett's post-hoc test). Baseline (b.l.): was measured before the first treatment. Single treatment: was measured after acute administration on day 7 after the operation.

2.2. Acute Oral Co-Administration of Tolperisone with Pregabalin but Not Duloxetine Alleviates Tactile Allodynia of Rats with Neuropathic Pain Evoked by pSNL

In this phase of the study, we followed a strategy of multimodal analgesia namely combining pregabalin and tolperisone. Thus, the pregabalin and tolperisone combination was investigated in animals showing allodynia two weeks after pSNL (Figure 4). As stated above, treatment with tolperisone or pregabalin at a dose of 25 mg/kg did not cause significant analgesic effects after either acute or chronic oral administration (Figures 1 and 2). Furthermore, Figure 4 showed that a single treatment with tolperisone (Figure 4a), pregabalin (Figure 4b), or duloxetine (Figure 4d) failed to induce significant effects in the PWTs of all treatment groups at 60, 120, and 180 min. Interestingly, pregabalin and tolperisone (25 mg + 25 mg) significantly alleviated the tactile allodynia of rats with NP at 120 min after acute oral administration compared to the vehicle (two-way ANOVA: F (treatment group; 4, 28) = 17.81, $p < 0.0001$, Dunnett's post-hoc test: $p = 0.0266$), tolperisone, or pregabalin-treated groups (Figure 4c). In contrast, the combination of tolperisone and duloxetine failed to attenuate the rat tactile allodynia following acute oral administration at the doses and time points indicated in Figure 4e.

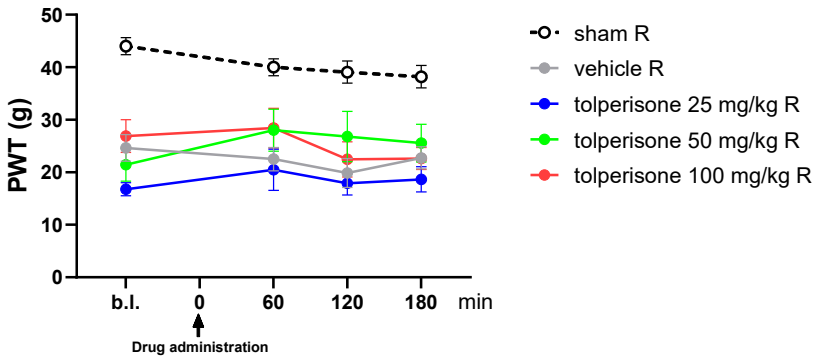

(**a**)

Figure 4. *Cont.*

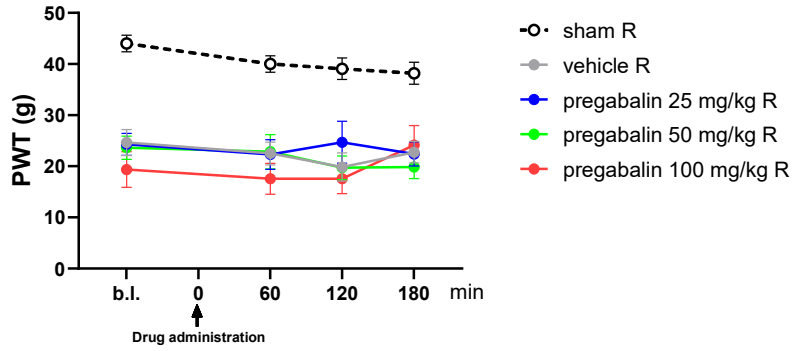

(**b**)

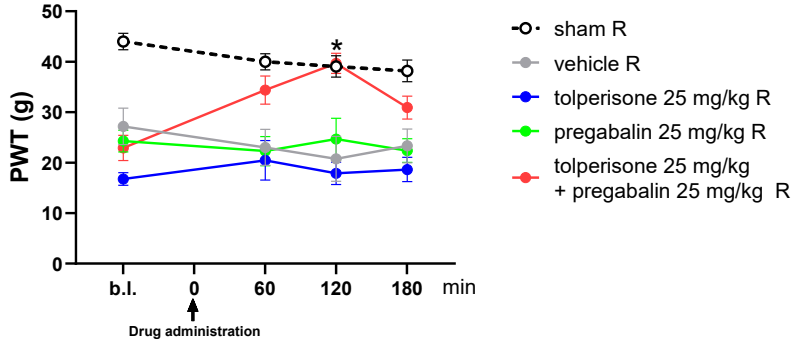

(**c**)

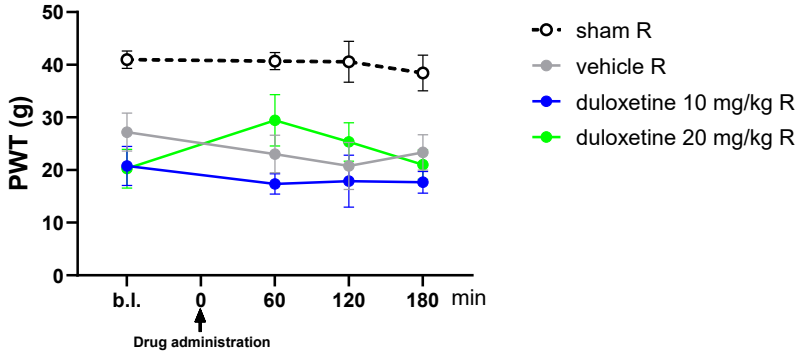

(**d**)

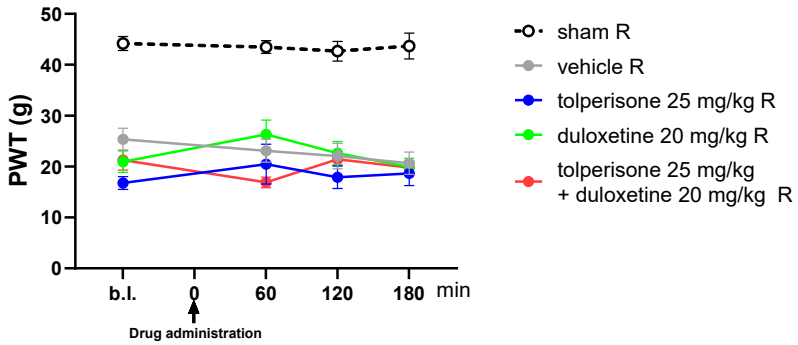

(**e**)

Figure 4. The acute antiallodynic effect of tolperisone (panel (**a**)), pregabalin (panel (**b**)), a combination of tolperisone and pregabalin (panel (**c**)), duloxetine (panel (**d**)), and a combination of tolperisone and

duloxetine (**e**) on the pSNL evoked allodynia. The PWT was measured on day 14 after the operation. Tactile allodynia was measured by DPA at 60, 120, and 180 min after acute oral treatment. Data are shown as the mean ± SEM of 6–8 animals (panel (**a**)), 8 animals (panel (**b**)), 5–8 animals (panel (**c**)), 4–5 animals (panel (**d**)), and 5–8 animals (panel (**e**)) per group. * $p < 0.05$, statistically significant compared to the vehicle right (operated) paw at the indicated time points after treatment (two-way ANOVA followed by Dunnett's post-hoc test). Baseline (b.l.): was measured before the treatment.

2.3. The Impact of Pregabalin and Tolperisone on Peripheral Neuropathic Pain of Diabetic Rats after Acute Administration

Based on the promising effect obtained in the mononeuropathic pain model, we extended our investigations to assess the antiallodynic effect of the tolperisone–pregabalin combination (25 and 25 mg/kg) in streptozotocin (STZ)-induced diabetic polyneuropathy. In accordance with our previous study [28], STZ treatment evoked a significant increase in the blood glucose level observed 72 h after 60 mg/kg STZ intraperitoneal injection compared to age-matched control animals that were maintained over the entire experiment (9 weeks), (see Figure A1a). Additionally, 3 weeks after STZ injection, the onset of tactile allodynia was indicated by a significant decrease in left and right PWTs that was maintained over the whole period (see Figure A1b). We determined the effect of the individual components of the combination (pregabalin and tolperisone both at 25 mg/kg), as well as the combination itself, 9 weeks following STZ treatment at 60 and 120 min after oral administration. Acute treatment with 25 mg/kg pregabalin produced a significant antiallodynic effect after 120 min (one-way ANOVA: $F(11, 31) = 7.167$, $p < 0.0001$, Dunnett's post-hoc test: $p = 0.0139$); however, tolperisone or the combination could induce only a tendentious effect (Figure 5). Significant changes between the body weight of diabetic rats and the nondiabetic age-matched animals were observed after 1 week and thereafter (see Figure A1c). In order to justify our results, weight-matched animals were also used in order to assess the impact of body weight on the PWT (see Figure A1d). Since the weight-matched animals showed a PWT similar to that of the age-matched animals at 9 weeks at all tested time points (see Figure A1e), the age-matched animals were used for comparison in this experiment.

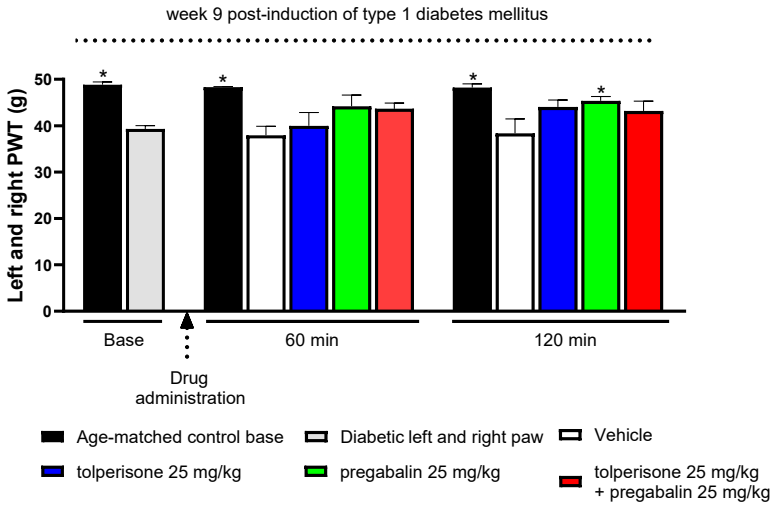

Figure 5. The acute antiallodynic effect of tolperisone and pregabalin on type 1 diabetes evoked tactile allodynia. The left and right PWT was measured in week 9 after diabetes induction. Tactile allodynia was measured by DPA at 60 and 120 min after acute oral treatment. Data are shown as the mean ± SEM of 3–5 animals per group. * $p < 0.05$, statistically significant compared to the vehicle-treated groups (one-way ANOVA followed by Dunnett's post-hoc test). The baseline was measured before treatment.

2.4. Effects of Acute Treatment with Tolperisone, Pregabalin, or their Combination on CSF Glutamate Content in Rats with pSNL-Induced Neuropathic Pain

Samples of cerebrospinal fluid (CSF) were taken from mono-neuropathic animals 14 days after pSNL operation, and their glutamate content was assessed by capillary electrophoresis. The vehicle treated mono-neuropathic animals showed a significant increase in the CSF glutamate concentration compared to the sham operated group (one-way ANOVA: $F(4, 64) = 6.435$, $p = 0.0002$, Dunnett's post-hoc test: $p = 0.0032$). Tolperisone, pregabalin, or their combination significantly inhibited the nerve injury induced elevation of the CSF glutamate content and normalized it to the level of the sham operated group (Figure 6).

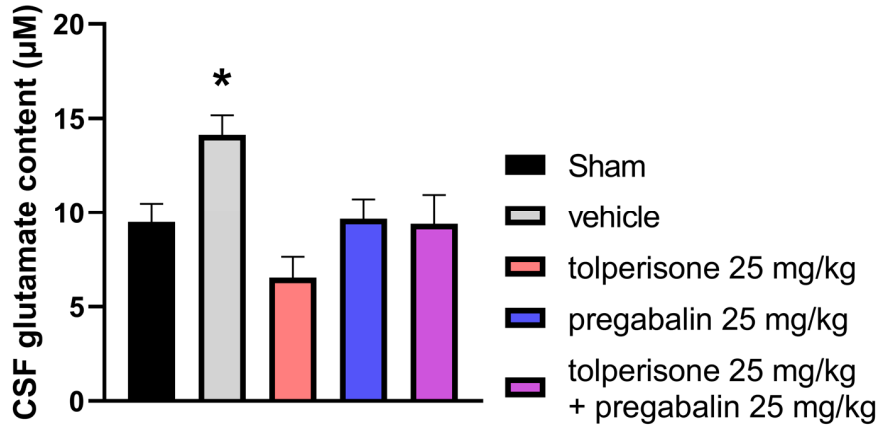

Figure 6. CSF glutamate content of mono-neuropathic (pSNL) and sham operated rats after acute treatment with orally administered tolperisone (25 mg/kg), pregabalin (25 mg/kg), or their combination (both at 25 mg/kg) on day 14 after pSNL operation. Data are shown as mean ± SEM of n = 4–21 animals per group. * $p < 0.05$ vs. other groups (one-way ANOVA followed by Dunnett's post-hoc test).

2.5. Effects of Treatment with Tolperisone, Pregabalin, or Their Combination on 4-Aminopyridine-Induced Glutamate Release from Rat Synaptosomes

The effect of tolperisone (100 µM), pregabalin (250 µM), or their combination on depolarization-induced glutamate release from rat brain synaptosomes was measured to better understand their probable mode of action. 4-aminopyridine, a K^+-channel inhibitor, was used to induce depolarization and subsequent neurotransmitter release [29]. 4-aminopyridine-induced transmitter release depends on the activation of sodium and calcium channels [30] and was blocked by tolperisone but not by pregabalin in accordance with our previous results [27]. Here, the combination was found to also significantly inhibit glutamate release induced by 4-aminopyridine (one-way ANOVA: $F(3, 24) = 8.686$, $p = 0.0004$, Dunnett's post-hoc test: 100 µM tolperisone, $p = 0.0012$; 100 µM tolperisone and 250 µM pregabalin, $p = 0.0016$, Figure 7).

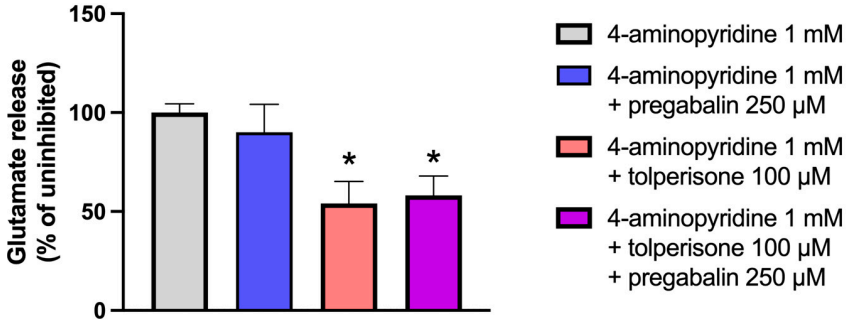

Figure 7. Effect of tolperisone (100 µM), pregabalin (250 µM), or their combination on glutamate release from rat brain synaptosomes induced by 1 mM 4-aminopyridine. Drugs were administered as

a pretreatment 20 min prior to stimulation. The concentration of released glutamate was measured 6 min after stimulation. All data points were normalized using the unstimulated, baseline release and presented as % of the stimulated glutamate release in the absence of test compounds (gray bar). All columns show the mean of glutamate release ± SEM in % in the indicated groups. * $p < 0.05$ vs. stimulated glutamate release by 1 mM 4-aminopyridine alone and treatment groups (one-way ANOVA followed by Dunnett's post-hoc test). In each treatment group, 4–13 parallel experiments were used.

2.6. The Impact of Pregabalin, Tolperisone, and Pregabalin/Tolperisone Combination on Motor Dysfunction and Coordination Imbalance in Naïve Rats

Acute oral pregabalin (50 and 100 mg/kg) but not tolperisone (100 and 150 mg/kg) treatments negatively influenced rats' motor coordination and balance, as indicated by a significant decrease in time to stay on a rotating rod (one-way ANOVA: F (13, 84) = 11.12, $p < 0.0001$, Dunnett's post-hoc test: 50 mg/kg, 60 min, $p = 0.0326$; 100 mg/kg, 60 min, $p = 0.0010$, 50 mg/kg; 120 min, $p < 0.0001$, 100 mg/kg; 120 min, $p < 0.0001$, Figure 8). On the other hand, pregabalin, at a dose of 25 mg/kg, did not elicit a change in rats' motor coordination and balance (Figure 8). The treatment with the combination of pregabalin and tolperisone (both at 25 mg/kg) failed to elicit alteration in rats' motor coordination and balance compared to the vehicle-treated group either 60 or 120 min after oral administration (Figure 8).

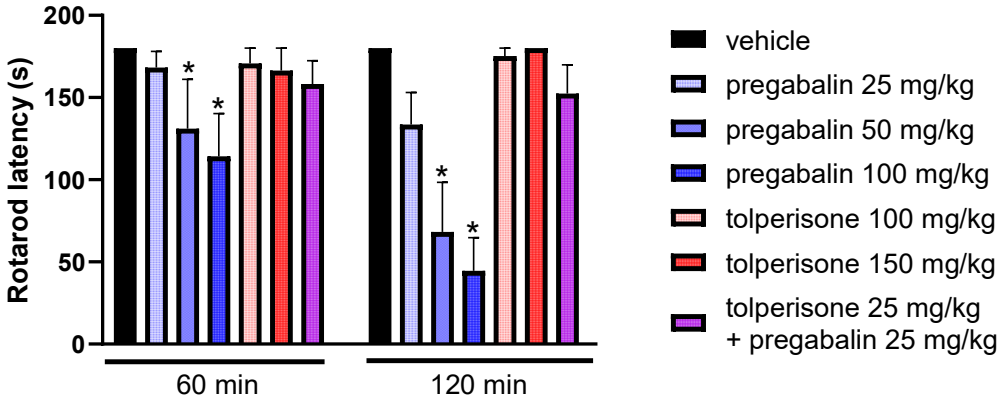

Figure 8. Effect of acute oral administration of tolperisone (100 and 150 mg/kg), pregabalin (25, 50, and 100 mg/kg), and the combination of tolperisone and pregabalin (both at 25 mg/kg) or vehicle at 60 and 120 min on motor coordination and balance of animals. Columns show the time latency in the rotarod assay. Data are shown as the mean ± SEM of 5–19 animals per group, measured at the peak effect of test compounds. * $p < 0.05$ statistically significant compared to the vehicle (one-way ANOVA followed by Dunnett's post-hoc test).

2.7. The Impact of Pregabalin, Tolperisone, and Pregabalin/Tolperisone Combination on Gastrointestinal (GI) Transit in Naïve Rats

Acute oral administration of tolperisone (25 and 50 mg/kg), pregabalin (25 mg/kg), and a combination of tolperisone and pregabalin (both at 25 mg/kg) failed to exhibit delays in the GI transit of a charcoal suspension in rats. However, acute pregabalin treatment with a dose of 50 mg/kg induced a moderate but significant delay in the GI transit of a charcoal suspension in rats compared to the vehicle (one-way ANOVA: F (5, 29) = 3.297, $p = 0.0177$, Dunnett's post-hoc test: $p = 0.0110$, Figure 9).

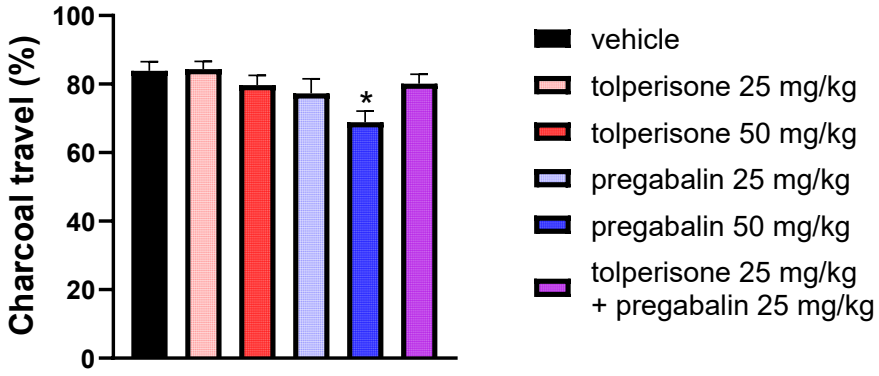

Figure 9. Effect of acute oral administration of tolperisone (25 and 50 mg/kg), pregabalin (25 and 50 mg/kg), and the tolperisone and pregabalin combination (both at 25 mg/kg) on the GI transit of naïve animals 30 min after a charcoal meal. Columns represent the charcoal travel (%) in the charcoal meal test. Data are shown as the mean ± SEM of 5–6 animals per group, measured at the peak effect of test compounds. * $p < 0.05$ statistically significant compared to the vehicle (one-way ANOVA followed by Dunnett's post-hoc test).

3. Discussion

It is of great clinical significance to develop a new medication or a novel combination treatment approach to treat NP. The difficulty in treating NP stems from the diversity of etiologies (injuries, illnesses, drugs, etc.) and the intricacy of the underlying mechanisms. All these factors contribute to the poor effects of the current mono or combination therapies to effectively manage NP symptoms. In this regard, the current therapeutic strategies of NP continue to be unsatisfactory because they have a low efficacy of pain inhibition, delayed onset of action, and deleterious adverse effects. Thus, an effective mono or combination therapy with a significant analgesic effect, fast onset of action, and a good safety profile is desperately needed [31,32]. In this context, the present study principally intended to investigate the antiallodynic effect of tolperisone compared to pregabalin or duloxetine as monotherapy. Of importance, the efficacy of combinations composed of either tolperisone with pregabalin or duloxetine was also studied in the same NP model. In our previous work, we have only shown that tolperisone or pregabalin alone acutely inhibit the developed mechanical allodynia. However, herein, we applied another measurement approach, namely DPA, which is designed to determine more localized tactile allodynia in a small dynamic range. Furthermore, the effect of long-term treatment was also assessed. Similar to our previous work, the possible mechanism for inhibiting tactile allodynia was also investigated. We have also extended our investigations to assess the impact of the tolperisone–pregabalin combination on another neuropathic pain type, polyneuropathic pain evoked by type 1 diabetes. Finally, the possible effect of the promising combination on motor coordination and balance as well as gastrointestinal transit was assessed.

Mono-neuropathic pain was induced by pSNL in rats based on the Seltzer method. In comparison studies, the evolution of the antiallodynic effect of test compounds was carried out acutely and on day 7 or 14 post-operation. In experiments intended to evaluate the effect of chronic treatments, the treatment was initiated on day 7 after the operation and was continued for 14 days, and the antiallodynic impact was assessed on the 14th and 21st days after the operation. The suitability of the time periods for undertaking the treatment and pain assessment based on the present and previous studies has established that pSNL evokes stable tactile allodynia within 1 week following nerve ligation and lasts for at least 4 weeks [33,34]. Herein, we used this rat model to show the effect of test compounds and combinations against developed tactile allodynia within the described test period; the investigation was started on day 7 and ended before day 28, enabling us to avoid factors that may disturb the quality and productivity of the study. The results obtained from the rat mono-neuropathic pain model indicate that acute tolperisone treatment failed to alleviate tactile allodynia. This ineffectuality was also seen following acute treatment with

pregabalin or duloxetine, two medications being used as first-line therapies for NP [35,36]. As already noted, the lack of an acute antiallodynic effect is in contrast with our previous results where mechanical allodynia was attenuated by acute tolperisone or pregabalin treatment, although the applied assay was different, as mentioned above [27]. To explain this, in our previous study, the antiallodynic effect of tolperisone or pregabalin was determined by the Randall–Selitto assay, which has been developed to measure the antinociceptive effect of test drugs on the pain thresholds evoked by mechanical pressure stimulation, although it can be considered a complement to cutaneous mechanical hyperalgesic assays [37]. On the other hand, we applied DPA, which is generally used to assess cutaneous mechanical hyperalgesia by applying filament stimuli to the plantar surfaces of the hind paws. It means that DPA likely detects tactile allodynia that needs long-term drug treatment to alleviate it. The difference between DPA and Randall–Selitto in terms of the dose of the drug administered was also observed previously by our group [38], namely, much higher analgesic doses are needed when DPA was used. Indeed, reports on the onset of the antiallodynic effect of pregabalin and duloxetine are contradictory [39–42]. For instance, applying a similar assay for at least 3 days was required for oral pregabalin to produce am antiallodynic effect in mice with NP evoked by cuffing the main branch of the sciatic nerve [43]. In addition, the analgesic assay, the route of administration, and particularly the type of NP are the main determinant factors in drawing a consensus about the analgesic effects of pregabalin and duloxetine, among others [15,44–48]. However, after chronic treatment, both tolperisone and pregabalin were able to elicit an antiallodynic effect. In fact, several preclinical and clinical studies have shown a similar lag time for pregabalin [49–51], but not for tolperisone. To the best of our knowledge, tolperisone has not been evaluated for potential analgesia in rats with preexisting tactile allodynia. This result raises a promising possibility for repurposing tolperisone for NP. With respect to duloxetine, despite the previous positive results, no significant antiallodynic effect could be measured either after acute or chronic oral treatment for 1 or 2 weeks [5]. Duloxetine is a serotonin and noradrenaline reuptake inhibitor; independent of its effect on depression, it alleviates allodynia in diabetic neuropathy. In this regard, spinal serotonin and noradrenaline play an important role in pain transmission. Pharmacological studies with serotonin and noradrenaline reuptake inhibitors have shown facilitatory or inhibitory effects on the descending serotonergic pathways that play a crucial role in neuropathic pain. This controversial or poor effect of serotonin has been attributed to the applied stimuli, the variable methods, and the timing of pain measurement [52,53].

Despite the discrepancy in the onset of action of the tested drugs, the essential finding of the present study is that the tolperisone/pregabalin, but not tolperisone/duloxetine, combination elicited a remarkable acute effect on the pSNL-induced allodynia at day 14 following operation. This result, to our best knowledge, is the first one to demonstrate the acute tactile antiallodynic efficacy of a low dose tolperisone–pregabalin combination in rat models of neuropathic pain. In addition, the effect of the combination was not associated with motor dysfunction or GI transit-related side effects. Indeed, the analgesic efficacy and safety of pregabalin alone or in combination with several drugs, but not with tolperisone, have been previously investigated in several clinical and preclinical studies for neuropathic pain treatment. Pregabalin and tolpersisone exert their analgesic effects against NP by inhibiting voltage-gated calcium channels hosting the α2-δ subunit and different voltage-dependent sodium channels, respectively [14,15,24,27]. Inhibition of these channels causes a reduction in calcium influx, neurotransmitter release, and, as a result, total neuronal excitability. It is worth noting that these channels are targets for first-line medications currently used to treat NP of different entities, including peripheral mononeuropathic pain among others [15,54–57]. In addition, tolperisone has been reported to inhibit muscle spasms with an advantageous side-effect profile; it is devoid of the central side effects of the other centrally acting skeletal muscle relaxants. This property encouraged us to investigate its effect once combined with pregabalin. Voltage-gated sodium channel blockers, such as carbamazepine, are among the medications that are

prescribed to treat NP [58,59]. The effect of carbamazepine either alone or combined with different drugs was studied in different neuropathic conditions. Fox et al. has reported that a single treatment with carbamazepine was ineffective against mechanical hyperalgesia or tactile allodynia in rats; however, it reversed mechanical hyperalgesia in guinea-pig NP evoked by pSNL [41,60]. This indicates that there is an overlap between the previously reported and present study regarding acute treatment with tolperisone or carbamazepine (see Figure A2a–d). With respect to the combination, it was shown that a gabapentin and carbamazepine combination induced synergistic analgesia compared to single drug administration, as indicated by high latency in the hot plate test in diabetic neuropathic rats [61]. Further, the pregabalin/carbamazepine combination was found to produce a synergistic antiallodynic effect in the rat spinal nerve ligation model. In fact, the antiallodynic effect was only seen when the drugs were combined in doses that exceeded the ED75 values, although, the side effects were not studied [20]. In fact, in our present study, the examined doses of tolperisone, pregabalin, or duloxetine that were shown to produce analgesia after chronic treatment are higher than the applied doses in the combination. It is worth noting that several preclinical and clinical studies have focused on the efficacy of carbamazepine, gabapentin, and pregabalin in managing trigeminal neuralgia, which is not the object of the present work [62–66]. Fortunately, the present study proceeded to identify combination therapy as having higher efficacy and fewer side effects. With respect to side effects, more than 50% of patients taking pregabalin experience considerable unwanted effects, most notably, excessive sedation [67]. Based on the above-mentioned literature of previous work and our present results, the tolperisone/pregabalin combination might be of clinical value, opening a possibility of repurposing.

It has been well established that rat NP evoked by peripheral nerve injury initiates both peripheral and central sensitization that concomitantly occurs with an imbalance between spinal excitatory and inhibitory systems [1]. An increase in spinal glutamate levels has been described as one of the major contributors to the mechanism responsible for the development of NP. Indeed, drugs that inhibit NMDA receptors are known to be among the effective management strategies for chronic pain [1,68]. Therefore, we also measured the CSF glutamate content, which was found to be increased in rats with NP. The inhibition of glutamatergic activity is one of the explanations proposed by researchers for the inhibition of mono and polyneuropathic pain [27,69–73]. However, the contribution of the glutamatergic system to the pathophysiology of NP is more complex than the simple thought of enhancing or decreasing the glutamatergic system.

We have also assessed the impact of the tolperisone–pregabalin combination on polyneuropathic pain evoked by type 1 diabetes. In this series of experiments, pregabalin has been shown to be a more efficacious analgesic than the combination that proved to be superior in mono-neuropathic pain, namely in the pSNL model. This effect of pregabalin was not surprising as several preclinical and clinical data support its effectiveness in diabetic neuropathy [74–76]. With respect to tolperisone, further future studies are needed to fully characterize its antiallodynic effect, but the present results suggest that it is most effective in nerve injury-induced NP, particularly when combined with pregabalin.

The major limitation of the present work was that in the diabetes-induced polyneuropathic pain model tolperisone, pregabalin, and their combination were only tested at a dose of 25 mg/kg, which was effective in nerve injury-induced mono-neuropathic pain. In fact, to have the full picture, future studies are needed to elucidate the antiallodynic effect of the test compounds at different doses and possible other mechanisms of action. Finally examining the effect of the combination following chronic treatment applied to the present and other animal models of NP would further justify the efficacy of the combination of tolperisone and pregabalin.

4. Materials and Methods

4.1. Animals

In the current study, 120–150 g male Wistar rats underwent partial sciatic nerve ligation (pSNL), and 170–200 g male Wistar rats were used for the rotarod assay and charcoal meal test to be matched with the operated animal's body weights on the test days. Animals were purchased from Toxi-Coop Zrt. (Budapest, Hungary) and housed in standard cages of up to 4 or 5 animals/cage based on their weights, maintained at a controlled temperature (20 ± 2 °C), light/dark cycle (12/12 h), and allowed free access to food and water in the local animal house of Semmelweis University, Department of Pharmacology and Pharmacotherapy (Budapest, Hungary). All procedures and housing conditions were performed according to the European Communities Council Directives (2010/63/EU), the Hungarian Act for the Protection of Animals in Research (XXVIII.tv. 32.§), and the local animal care committee (PEI/001/276-4/2013 and PE/EA/619-8/2018).

4.2. Chemicals

Tolperisone and pregabalin were kindly provided as a gift by Meditop Pharmaceuticals Ltd. (Budapest, Hungary). Streptozotocin (STZ), carbamazepine, and duloxetine were purchased from Sigma–Aldrich (St. Louis, MO, USA). From Sigma–Aldrich, hydroxy ethyl cellulose, as well as glutamate oxidase, horseradish peroxidase, and Amplex Red for glutamate release measurement were purchased (St. Louis, MO, USA). All compounds were stored and handled according to manufacturing procedures.

4.3. Experimental Protocols of the Animal Study

Experimental schedule 1 displays a schematic overview of the experimental techniques used in this work. Baseline measurements were carried out by DPA (dynamic plantar esthesiometer 37450; Ugo Basil, Gemonio, Italy) to evaluate paw withdrawal thresholds before the operation, and animals then underwent pSNL surgery (see Section 4.4). On day 7 after the operation, baseline measurements were taken once more to test the development of mechanical allodynia, and neuropathic rats were then treated with compounds or vehicles. Mechanical allodynia was tested once more at 60, 120, and 180 min after acute oral administration to investigate the acute antiallodynic effect of the test drugs. In the chronic experiments, rats were given daily treatments for 14 days to assess the chronic antiallodynic impact of the investigated compounds, and then DPA was carried out on days 14 and 21, respectively, after surgery.

In another set of animals, baseline measurements were carried out by DPA, and pSNL surgery was performed. On day 14 after the operation, baseline measurements were taken once more to test the development of mechanical allodynia, and neuropathic rats were then treated with compounds or vehicles. Mechanical allodynia was tested once more at 60, 120, and 180 min after acute oral administration to investigate the acute antiallodynic effect of the test drugs and their combinations (Experimental schedule 2).

Experimental schedule 1 (Scheme 1) shows the antiallodynic effects of pregabalin and tolperisone (both at 25, 50, and 100 mg/kg), carbamazepine (16.25, 32.5, and 65 mg/kg), and duloxetine (10 and 20 mg/kg) in rats that underwent partial sciatic nerve ligation evoked tactile allodynia measured by a DPA (dynamic plantar esthesiometer). In addition, the treatment day timeline and the precise intervals during the treatment days for DPA measurements are shown. Experimental schedule 2 shows the acute antiallodynic effects of pregabalin, tolperisone (both at 25, 50, and 100 mg/kg), their combination (25 mg and 25 mg), duloxetine (10 and 20 mg/kg), and the tolperisone and duloxetine combination (25 mg and 20 mg) in rats that underwent partial sciatic nerve ligation evoked tactile allodynia measured by DPA. The treatment day timeline and the precise intervals during the treatment days for DPA measurements are also shown.

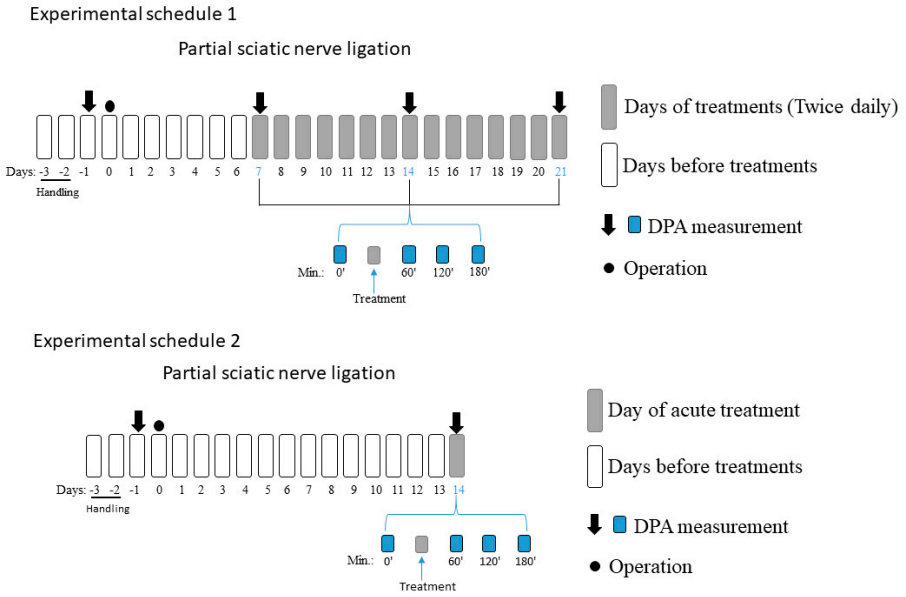

Scheme 1. Experimental schedule 1.

4.4. Partial Sciatic Nerve Ligation (pSNL)

This was performed as previously described [33,77] for partial ligation of the sciatic nerve (pSNL). In summary, pentobarbital (i.p., 60 mg/kg, in a volume of 2.5 mL/kg) was used to produce anesthesia on the day of the operation, and rats were then placed on a pillow at 30 °C. The right dorsal back was shaved, an incision was created, and the sciatic nerve was carefully exposed in an aseptic setting. A size 7-0 polypropylene wire was then used to tightly ligate the exposed nerve at the level of the thigh, ensuring that the dorsal 1/3 to 1/2 of the nerve thickness was ligated. The wound was then closed with two stiches. In the sham group (controls), the sciatic nerve was exposed but not ligated.

4.5. Assessment of Mechanical Allodynia

Mechanical allodynia, the main symptom of neuropathic pain, was measured using the DPA, as previously mentioned [28,77]. Handling was performed in the days preceding the beginning of the experiments to acclimatize the animals to the experimental conditions by putting them in the plastic cages of the experimental setup once a day. The paw withdrawal thresholds (PWTs) of the animals were measured in grams (g). PWT values were assessed following a 5 min cage acclimatization period for each measurement. According to the manufacturer's instructions, a metal filament with a diameter of 0.5 mm is raised alternately to the right and left hind paws (incrementation: 10 g/s, maximal force: 50 g). Three PWT measurements were performed on each paw, and the average of the three readings was calculated. For each animal, allodynia was defined as a 20% decrease in the average PWT value of the operated (right) paw compared to the unoperated (left) paw [28,38]. Measurements were performed in accordance with instructions in Section 4.3 or experimental schedules 1 and 2.

4.6. Treatment of Neuropathic Animals

The effects of pregabalin and tolperisone (both at 25, 50, and 100 mg/kg), duloxetine (10 and 20 mg/kg), and carbamazepine (16.25, 32.5, and 65 mg/kg) were investigated on day 7 after pSNL and assessments of allodynia began 60, 120, and 180 min after administration. The chronic treatments continued for 1–2 weeks, and again, assessment of the allodynia was determined on the day 14 and 21 after the operation. All drugs were administered twice per day in the chronic treatment experiments. In addition, the effects of pregabalin and tolperisone (both at 25, 50, and 100 mg/kg), duloxetine (10 and 20 mg/kg), the tolperisone and pregabalin combination (both at 25 mg/kg), and the tolperisone and

duloxetine combination (25 mg/kg and 20 mg/kg), as well as carbamazepine (16.25, 32.5, and 65 mg/kg), were investigated after a single oral dose on day 14 after pSNL. The solution of all drugs was prepared in 0.9% saline, except for carbamazepine, which was suspended in 1% hydroxyethyl cellulose solution. All drugs were administered in a volume of 5 mL/kg via an orogastric gavage.

4.7. Motor Function Test

The rotarod test (Rat Rotarod, Model 7750; Ugo Basile, Gemonio, Italy) was used to evaluate the effect of test drugs on motor coordination in naïve rats. One day prior to the experiment, animals were trained to stay on the rotating rod of the apparatus for 180 s (cut-off time) where the instrument's speed was adjusted to 16 rpm. On the following day, the acute effects of tolperisone (100 and 150 mg/kg), pregabalin (25, 50, and 100 mg/kg), and the tolperisone and pregabalin combination (both at 25 mg/kg), or vehicle, were tested after oral treatment at the time of the peak effect of the test drugs (60 and 120 min). The fall-off time, or the latency time, was recorded as an indication of motor coordination [10,78].

4.8. Determination of GastroIntestinal Peristalsis in Rats

The charcoal meal test was utilized to test the effect of tolperisone (25 and 50 mg/kg), pregabalin (25 and 50 mg/kg), or the tolperisone and pregabalin combination (both at 25 mg/kg) on gastrointestinal transit in rats after oral treatment [79]. In brief, naïve male Wistar rats were given free access to water and fasted for 18 h before the experiment. Drugs were administered, and 30 min later, an oral charcoal suspension (10% charcoal in 5% gum Arabic) in a volume of 2 mL/animal was given via oral gavage. After another 30 min, the rats were euthanized to take the whole small intestines. The charcoal travel distance was measured and compared to the whole small intestinal length.

4.9. Animal Model of Type 1 Diabetes-Induced Polyneuropathic Pain

For the STZ-induced type 1 diabetes model, male Wistar rats weighing 200–230 g were used. Animals were housed in a mesh-bottomed cage (type IV cage) that meets the EU's requirement. To induce diabetes, we used a single intraperitoneal injection of 60 mg/kg of STZ, freshly dissolved in cold distilled water (1–3 °C) right before injection to prevent any degradation [80,81]. Three days later, diabetes was confirmed by measuring the blood glucose level (>14 mmol/L) in the blood obtained from the tail vein using the Dcont Etalon blood glucose meter (Roche Diagnostics GmbH, Mannheim, Germany). The highest blood glucose level that may be measured using a blood glucose test is 33.3 mmol/L [82]. Every third week, the PWTs were measured and expressed in g. Each hind paw's PWT was measured three times alternatively. The average PWT values for each animal's two paws were then determined. Age-matched (i.e., animals with age-matched to diabetic ones) and vehicle-treated groups were utilized as controls. An animal was considered neuropathic when the PWT value decreased by at least 20% compared to age-matched animals [38].

4.10. Capillary Electrophoresis Analysis of CSF Glutamate Content

In our lab, a modified technique of capillary electrophoresis laser-induced fluorescence detection was established [83] for assessing the glutamate level in CSF samples. At 14 days after the pSNL, neuropathic and control rats were sacrificed with isoflurane. CSF samples were obtained by puncturing the cisterna magna, centrifuged at 2000× *g* and 4 °C for 10 min, and deproteinized by combining with two volumes of cold acetonitrile and centrifuging at 20,000× *g* for 10 min at 4 °C. Supernatants were derivatized using NBD-F (1 mg/mL final concentration) in 20 mM borate buffer pH 8.5 for 20 min at 65 °C. As an internal standard, 1 µM L-cysteic acid was utilized. A P/ACE MDQ Plus capillary electrophoresis system with a laser-induced fluorescence detector adjusted to 488 and 520 nm excitation and emission wavelengths, respectively (SCIEX, Framingham, MA, USA), was used to evaluate derivatized materials. Separations were performed in polyacrylamide-coated fused silica capillaries (i.d.: 75 µm, effective/total length: 40/50 cm) at 15 °C with a constant voltage of

−27 kV while using a 50 mM HEPES buffer pH 7.0 containing 6 mM 6-monodeoxy-6-mono (3-hydroxy) propylamino-β-cyclodextrin.

4.11. Glutamate Release from Synaptosomes

To examine the effects of tolperisone, pregabalin, or their combination on depolarization-evoked glutamate release, rat brain synaptosomes were prepared using a modified Modi et al. method [84]. In summary, animals were promptly decapitated, and their brains were separated and homogenized in a solution of 0.32 M sucrose and 4 mM HEPES (pH 7.4). After homogenate centrifugation (2 × 10 min, 1500× *g*, 4 °C), supernatants were collected and combined. After centrifuging the supernatant (2 × 10 min, 20,000× *g*, 4 °C), the pellet was resuspended in a buffer solution containing 4 mM HEPES, 0.32 M sucrose, 10% fetal bovine serum, and 10% dimethyl sulfoxide (DMSO), and stored at −80 °C until use. Glutamate release experiments were performed using a method described previously in our earlier publication [27].

On the experimental day, synaptosomal suspensions were defrosted, centrifuged (10 min, 20,000× *g*, 4 °C), and the pellet was resuspended in 10 mM HE-PES buffer containing 5.4 mM KCl, 130 mM NaCl, 0.9 mM $MgCl_2$, 1.3 mM $CaCl_2$, and 5.5 mM glucose (pH 7.4). The supernatant was collected from 10 mg synaptosomal suspensions centrifuged to an 8-well strip plate (15 min, 2500× *g*, 4 °C). Synaptosomes were equilibrated for 2 × 10 min at 37 °C before stimulation in HEPES buffer containing 40 µM DL-TBOA, a competitive, non-transportable blocker of excitatory amino acid transporters [23], to prevent glutamate reuptake. In the experiments, test drugs were added during the equilibration periods as pretreatment. After equilibration, a stimulation buffer containing 1 mM 4-aminopyridine was used to induce depolarization and subsequent glutamate release. Following stimulation, aliquots were taken at 8 min and stored at −20 °C until enzyme-linked fluorescent assay analysis.

4.12. Enzyme-Linked Fluorescent Assay of Glutamate Released from Synaptosomes

Glutamate release was measured using Glutamate Oxidase Assay Kit purchased from Sigma–Aldrich (St. Louis, MO, USA) using an enzyme-linked fluorescent assay. Briefly, the samples were mixed with a working solution containing glutamate oxidase (0.04 U/mL), horseradish peroxidase (0.125 U/mL), and Amplex Red (50 µM) (final concentrations), and fluorescent readings were performed after 30 min incubation at 37 °C. Excitation and emission wavelengths were 530 nm and 590 nm, respectively.

4.13. Statistical Analysis

GraphPad Prism 8.0 Software (San Diego, CA, USA), a statistical analysis program, was used to analyze the data. All data were presented as mean ± standard error of means (S.E.M.). All data were analyzed by one-way or two-way ANOVA followed by Dunnett's post-hoc test for multiple comparisons. Significant differences were considered if $p < 0.05$. ROUT analysis was performed to identify outliers, with a Q value = 0.5%

5. Conclusions

The current consensus from the present work is that the onset of action of pregabalin and tolperisone to produce an antiallodynic effect is 2 weeks after oral administration. We have demonstrated, for the first time, that the oral combination of tolperisone and pregabalin acutely produces analgesia against allodynia evoked by pSNL without motor or gastrointestinal transit-related adverse effects. Mechanistically, targeting both voltage-gated sodium and calcium channels could modulate the glutamatergic neurotransmission as reflected by the normalized neuropathy-induced elevation of the CSF glutamate content. The preclinical pharmacological characterization of existing and novel medications, or their combination, can provide clinical researchers with actionable and objective insights into developing or repurposing attitudes.

Author Contributions: Conceptualization, T.T., É.S. and M.A.-K.; formal analysis, N.E. and M.A.-K.; funding acquisition T.T., É.S. and M.A.-K.; investigation N.E., P.P.L., A.R.G., D.Á.K., A.M., S.K.A., O.G., R.L. and É.S.; methodology, N.E., Z.S.Z., T.T., É.S. and M.A.-K.; project administration, N.E., D.Á.K., A.R.G., P.P.L. and S.K.A.; resources, N.E., M.A.-K. and T.T.; supervision, M.A.-K.; validation, N.E., K.K. and P.R.; visualization, N.E.; writing—original draft, N.E. and M.A.-K.; writing—review and editing N.E., A.R.G., D.Á.K., S.K.A., K.K., R.L., T.T., Z.S.Z., É.S., P.R. and M.A.-K. All authors have read and agreed to the published version of the manuscript.

Funding: This work has been supported by the "Competitiveness and Excellence Cooperations" project (2018-1.3.1-VKE-2018-00030) provided by the National Research, Development, and Innovation Fund of Hungary, Hungary. D.Á.K. and A.R.G. were supported by "Semmelweis 250+ Excellence PhD Scholarship" (EFOP-3.6.3-VEKOP-16-2017-00009).

Institutional Review Board Statement: All housing and experiments were performed in accordance with the European Communities Council Directives (2010/63/EU), the Hungarian Act for the Protection of Animals in Research (XXVIII.tv. 32.§), and the local animal care committee (PEI/001/276-4/2013 and PE/EA/619-8/2018). Experimenters applied their best efforts to minimize the number of animals and their suffering.

Informed Consent Statement: Not applicable.

Data Availability Statement: Data is contained within the article.

Conflicts of Interest: The authors declare no conflict of interest.

Appendix A

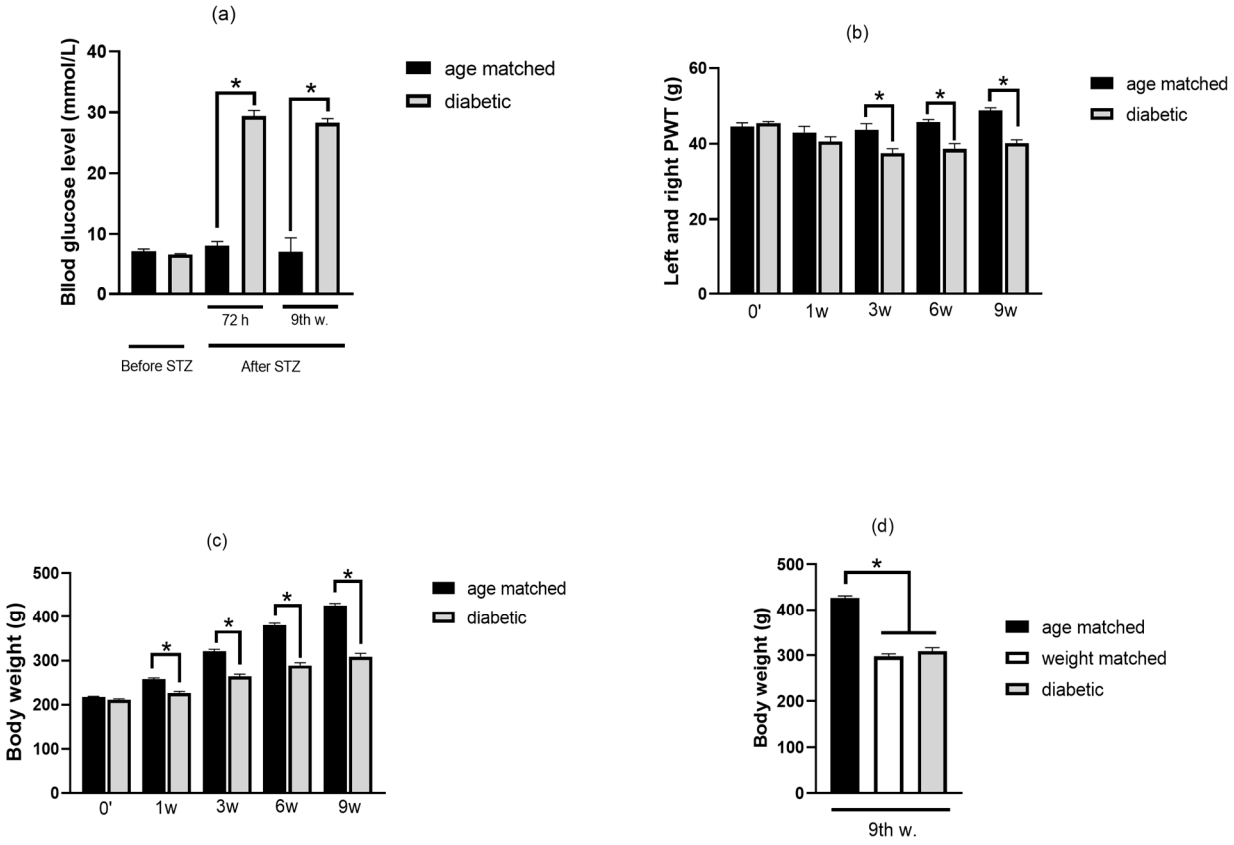

Figure A1. *Cont.*

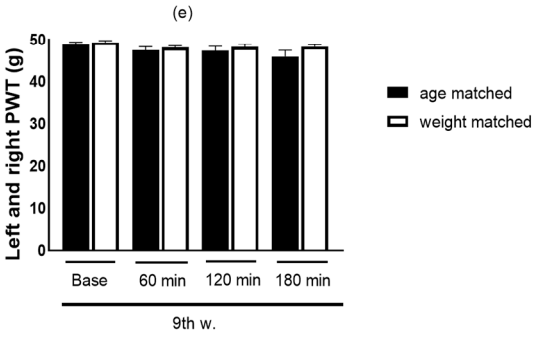

Figure A1. Blood glucose level (panel (**a**)), left and right PWT of age-matched and diabetic animals (panel (**b**)), the body weight of age-matched and diabetic animals (panel (**c**)), the body weight of age and weight-matched, and diabetic animals at 9 weeks (panel (**d**)), left and right PWT of age and weight-matched animals at 9 weeks (panel (**e**)). Data are shown as mean ± S.E.M. of 6 age-matched, 6 weight-matched, and 20 diabetic animals. * $p < 0.05$ statistically significant compared to the age-matched animals. Data were analyzed by unpaired *t*-test for panels (**a**–**c**) and (**e**) and one-way ANOVA followed by Dunnett's post-hoc test, panel (**d**).

Appendix B

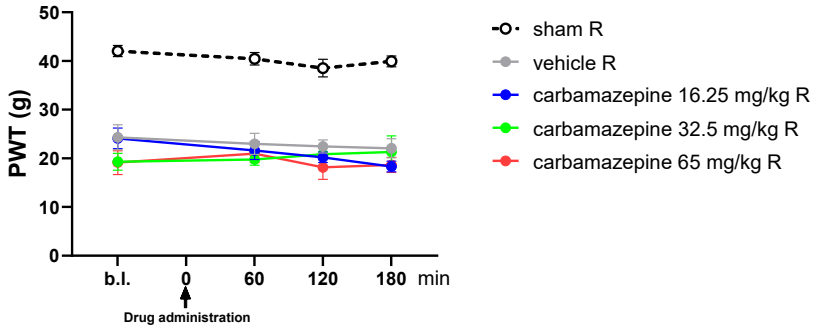

(**a**) Single treatment

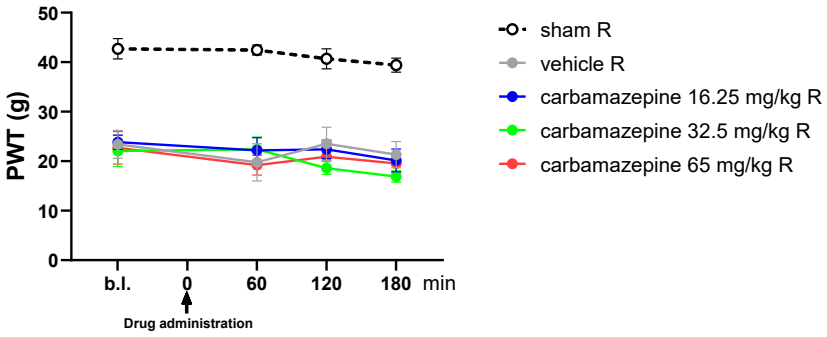

(**b**) One week treatment

Figure A2. *Cont.*

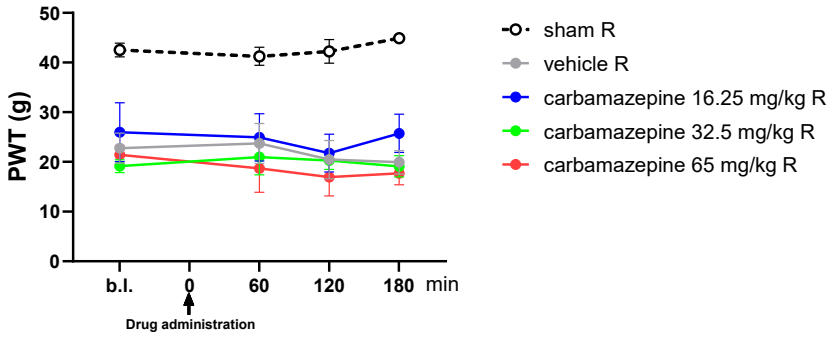

(**c**) Two weeks treatment

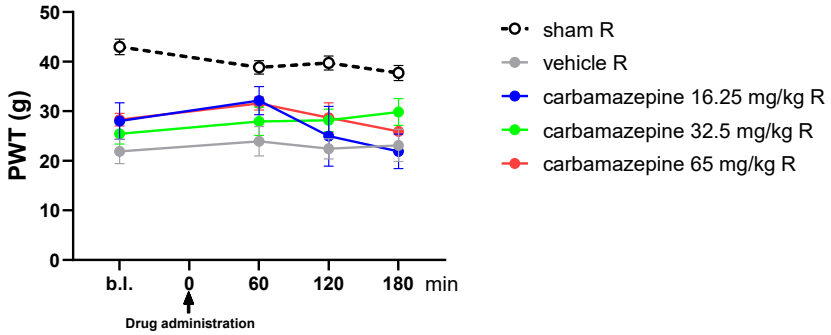

(**d**) 14th day

Figure A2. The antiallodynic effect of carbamazepine on pSNL evoked allodynia. The PWTs were measured on day 7 prior to and after a single treatment (panel (**a**)), on day 14 (1 week treatment) (panel (**b**)), on day 21 (2 weeks treatment) (panel (**c**)), and on day 14 after a single treatment (panel (**d**)) after the operation. Tactile allodynia was measured by DPA at 60, 120, and 180 min after oral treatment. Data are shown as the mean ± SEM of 6–7 animals (panels (**a**–**c**)) and 4–13 animals (panel (**d**)) in each group. $p > 0.05$, statistically not significant: treated groups versus the vehicle right (operated) paw at the indicated time points after treatment (two-way ANOVA followed by Dunnett's post-hoc test). Baseline (b.l.): was measured before the first treatment. Single treatment: was measured after acute administration on day 7 after the operation.

References

1. Al-Khrasani, M.; Mohammadzadeh, A.; Balogh, M.; Király, K.; Barsi, S.; Hajnal, B.; Köles, L.; Zádori, Z.S.; Harsing, L.G., Jr. Glycine transporter inhibitors: A new avenue for managing neuropathic pain. *Brain. Res. Bull.* **2019**, *152*, 143–158. [CrossRef]
2. Finnerup, N.B.; Sindrup, S.H.; Jensen, T.S. The evidence for pharmacological treatment of neuropathic pain. *Pain* **2010**, *150*, 573–581. [CrossRef]
3. Attal, N. Pharmacological treatments of neuropathic pain: The latest recommendations. *Rev. Neurol.* **2019**, *175*, 46–50. [CrossRef] [PubMed]
4. Alles, S.R.A.; Cain, S.M.; Snutch, T.P. *Pregabalin as a Pain Therapeutic: Beyond Calcium Channels*; Frontiers in Cellular Neuroscience; Frontiers Media S.A.: Lausanne, Switzerland, 2020; Volume 14.
5. Kremer, M.; Yalcin, I.; Goumon, Y.; Wurtz, X.; Nexon, L.; Daniel, D.; Megat, S.; Ceredig, R.A.; Ernst, C.; Turecki, G.; et al. A dual noradrenergic mechanism for the relief of neuropathic allodynia by the antidepressant drugs duloxetine and amitriptyline. *J. Neurosci.* **2018**, *38*, 9934–9954. [CrossRef] [PubMed]
6. Finnerup, N.B.; Attal, N.; Haroutounian, S.; McNicol, E.; Baron, R.; Dworkin, R.H.; Gilron, I.; Haanpää, M.; Hansson, P.; Jensen, T.S.; et al. Pharmacotherapy for neuropathic pain in adults: A systematic review and meta-analysis. *Lancet Neurol.* **2015**, *14*, 162–173. [CrossRef] [PubMed]
7. Pickering, G.; Martin, E.; Tiberghien, F.; Delorme, C.; Mick, G. Localized neuropathic pain: An expert consensus on local treatments. *Drug Des. Dev. Ther.* **2017**, *11*, 2709–2718. [CrossRef]

8. Meacham, K.; Shepherd, A.; Mohapatra, D.P.; Haroutounian, S. Neuropathic Pain: Central vs. Peripheral Mechanisms. *Curr. Pain Headache Rep.* **2017**, *21*, 28. [CrossRef]
9. Raffa, R.B.; Pergolizzi, J.V.; Tallarida, R.J. The Determination and Application of Fixed-Dose Analgesic Combinations for Treating Multimodal Pain. *J. Pain* **2010**, *11*, 701–709. [CrossRef]
10. Mohammadzadeh, A.; Lakatos, P.P.; Balogh, M.; Zádor, F.; Karádi, D.; Zádori, Z.S.; Király, K.; Galambos, A.R.; Barsi, S.; Riba, P. Pharmacological Evidence on Augmented Antiallodynia Following Systemic Co-Treatment with GlyT-1 and GlyT-2 Inhibitors in Rat Neuropathic Pain Model. *Int. J. Mol. Sci.* **2021**, *22*, 2479. [CrossRef]
11. Raffa, R.B.; Clark-Vetri, R.; Tallarida, R.J.; Wertheimer, A.I. Combination strategies for pain management. *Expert Opin. Pharmacother.* **2003**, *4*, 1697–1708. [CrossRef]
12. Raffa, R.B. Pharmacology of oral combination analgesics: Rational therapy for pain. *J. Clin. Pharm. Ther.* **2001**, *26*, 257–264. [CrossRef] [PubMed]
13. Gilron, I.; Bailey, J.M.; Tu, D.; Holden, R.R.; Jackson, A.C.; Houlden, R.L. Nortriptyline and gabapentin, alone and in combination for neuropathic pain: A double-blind, randomised controlled crossover trial. *Lancet* **2009**, *374*, 1252–1261. [CrossRef] [PubMed]
14. Verma, V.; Singh, N.; Singh Jaggi, A. Send Orders for Reprints to reprints@benthamscience.net Pregabalin in Neuropathic Pain: Evidences and Possible Mechanisms. *Curr. Neuropharmacol.* **2014**, *12*, 44–56. [CrossRef] [PubMed]
15. Field, M.J.; Cox, P.J.; Stott, E.; Melrose, H.; Offord, J.; Su, T.Z.; Bramwell, S.; Corradini, L.; England, S.; Winks, J.; et al. Identification of the α2-δ-1 subunit of voltage-calcium calcium channels as a molecular target for pain mediating the analgesic actions of pregabalin. *Proc. Natl. Acad. Sci. USA* **2006**, *103*, 17537–17542. [CrossRef]
16. Gilron, I.; Bailey, J.M.; Tu, D.; Holden, R.R.; Weaver, D.F.; Houlden, R.L. Morphine, gabapentin, or their combination for neuropathic pain. *N. Engl. J. Med.* **2005**, *352*, 1324–1334. [CrossRef] [PubMed]
17. Hanna, M.; O'Brien, C.; Wilson, M.C. Prolonged-release oxycodone enhances the effects of existing gabapentin therapy in painful diabetic neuropathy patients. *Eur. J. Pain.* **2008**, *12*, 804–813. [CrossRef]
18. Zin, C.S.; Nissen, L.M.; O'Callaghan, J.P.; Duffull, S.B.; Smith, M.T.; Moore, B.J. A randomized, controlled trial of oxycodone versus placebo in patients with postherpetic neuralgia and painful diabetic neuropathy treated with pregabalin. *J. Pain.* **2010**, *11*, 462–471. [CrossRef]
19. Matthews, E.A.; Dickenson, A.H. A Combination of Gabapentin and Morphine Mediates Enhanced Inhibitory Effects on Dorsal Horn Neuronal Responses in a Rat Model of Neuropathy. *Anesthesiology* **2002**, *96*, 633–640. [CrossRef]
20. Hahm, T.S.; Ahn, H.J.; Ryu, S.; Gwak, M.S.; Choi, S.J.; Kim, J.K.; Yu, J.M. Combined carbamazepine and pregabalin therapy in a rat model of neuropathic pain. *Br. J. Anaesth.* **2012**, *109*, 968–974. [CrossRef]
21. Balanaser, M.; Carley, M.; Baron, R.; Finnerup, N.B.; Moore, R.A.; Rowbotham, M.C.; Chaparro, L.E.; Gilron, I. Combination pharmacotherapy for the treatment of neuropathic pain in adults: Systematic review and meta-analysis. *Pain* **2022**, *164*, 230–251. [CrossRef] [PubMed]
22. Pratzel, H.G.; Alken, R.-G.; Ramm, S. Efficacy and tolerance of repeated oral doses of tolperisone hydrochloride in the treatment of painful reflex muscle spasm: Results of a prospective placebo-controlled double-blind trial. *Pain* **1996**, *67*, 417–425. [CrossRef] [PubMed]
23. Shimamoto, K. Glutamate transporter blockers for elucidation of the function of excitatory neurotransmission systems. *Chem. Rec.* **2008**, *8*, 182–199. [CrossRef]
24. Hofer, D.; Lohberger, B.; Steinecker, B.; Schmidt, K.; Quasthoff, S.; Schreibmayer, W. A comparative study of the action of tolperisone on seven different voltage dependent sodium channel isoforms. *Eur. J. Pharmacol.* **2006**, *538*, 5–14. [CrossRef] [PubMed]
25. Novales-Li, P.; Sun, X.-P.; Takeuchi, H. Suppression of calcium current in a snail neurone by eperisone and its analogues. *Eur. J. Pharmacol.* **1989**, *168*, 299–305. [CrossRef] [PubMed]
26. Quasthoff, S.; Pojer, C.; Mori, A.; Hofer, D.; Liebmann, P.; Kieseier, B.C.; Schreibmayer, W. No blocking effects of the pentapeptide QYNAD on Na^+ channel subtypes expressed in Xenopus oocytes or action potential conduction in isolated rat sural nerve. *Neurosci. Lett.* **2003**, *352*, 93–96. [CrossRef]
27. Lakatos, P.P.; Karádi, D.; Galambos, A.R.; Essmat, N.; Király, K.; Laufer, R.; Geda, O.; Zádori, Z.S.; Tábi, T.; Al-Khrasani, M.; et al. The Acute Antiallodynic Effect of Tolperisone in Rat Neuropathic Pain and Evaluation of Its Mechanism of Action. *Int. J. Mol. Sci.* **2022**, *23*, 9564. [CrossRef]
28. Balogh, M.; Zádor, F.; Zádori, Z.S.; Shaqura, M.; Király, K.; Mohammadzadeh, A.; Varga, B.; Lázár, B.; Mousa, S.A.; Hosztafi, S.; et al. Efficacy-Based Perspective to Overcome Reduced Opioid Analgesia of Advanced Painful Diabetic Neuropathy in Rats. *Front. Pharmacol.* **2019**, *10*, 347. [CrossRef]
29. Thesleff, S. Aminopyridines and Synaptic Transmission. *Neuroscience* **1980**, *5*, 1413–1419. [CrossRef]
30. Sánchez-Prieto, J.; Budd, D.C.; Herrero, I.; Vázquez, E.; Nicholls, D.G. Presynaptic receptors and the control of glutamate exocytosis. *Trends Neurosci.* **1996**, *19*, 235–239. [CrossRef]
31. Davis, M.P. What is new in neuropathic pain? *Support. Care Cancer* **2006**, *15*, 363–372. [CrossRef]
32. Gilron, I.; Max, M.B. Combination pharmacotherapy for neuropathic pain: Current evidence and future directions. *Expert Rev. Neurother.* **2005**, *5*, 823–830. [CrossRef]

33. Seltzer, Z.; Dubner, R.; Shir, Y. A novel behavioral model of neuropathic pain disorders produced in rats by partial sciatic nerve injury. *Pain* **1990**, *43*, 205–218. [CrossRef]
34. Pan, H.L.; Eisenach, J.C.; Chen, S.R. Gabapentin Suppresses Ectopic Nerve Discharges and Reverses Allodynia in Neuropathic Rats. *J. Pharmacol. Exp. Ther.* **1999**, *288*, 1026–1030. [PubMed]
35. Rodrigues, R.; Podestá, M.; Boralli, V. Animal Study Investigation of the Combination of Pregabalin with Duloxetine or Amitriptyline on the Pharmacokinetics and Antiallodynic Effect during Neuropathic Pain in Rats [Internet]. Available online: www.painphysicianjournal.com (accessed on 1 July 2021).
36. Sharma, U.; Griesing, T.; Emir, B.; Young, J.P. Time to Onset of Neuropathic Pain Reduction: A Retrospective Analysis of Data From Nine Controlled Trials of Pregabalin for Painful Diabetic Peripheral Neuropathy and Postherpetic Neuralgia [Internet]. Available online: www.americantherapeutics.com (accessed on 1 November 2010).
37. Santos-Nogueira, E.; Castro, E.R.; Mancuso, R.; Navarro, X.; TenBroek, E.M.; Yunker, L.; Nies, M.F.; Bendele, A.M.; Pottabathini, R.; Kumar, A.; et al. Randall-Selitto Test: A New Approach for the Detection of Neuropathic Pain after Spinal Cord Injury. *J. Neurotrauma* **2012**, *29*, 898–904. [CrossRef] [PubMed]
38. Király, K.; Kozsurek, M.; Lukácsi, E.; Barta, B.; Alpár, A.; Balázsa, T.; Fekete, C.; Szabon, J.; Helyes, Z.; Bölcskei, K.; et al. Glial cell type-specific changes in spinal dipeptidyl peptidase 4 expression and effects of its inhibitors in inflammatory and neuropatic pain. *Sci. Rep.* **2018**, *8*, 3490. [CrossRef] [PubMed]
39. Baron, R.; Mayoral, V.; Leijon, G.; Binder, A.; Steigerwald, I.; Serpell, M. Efficacy and safety of combination therapy with 5% lidocaine medicated plaster and pregabalin in post-herpetic neuralgia and diabetic polyneuropathy. *Curr. Med. Res. Opin.* **2009**, *25*, 1677–1687. [CrossRef]
40. Tesfaye, S.; Wilhelm, S.; Lledo, A.; Schacht, A.; Tölle, T.; Bouhassira, D.; Cruccu, G.; Skljarevski, V.; Freynhagen, R. Duloxetine and pregabalin: High-dose monotherapy or their combination? The "cOMBO-DN study"—A multinational, randomized, double-blind, parallel-group study in patients with diabetic peripheral neuropathic pain. *Pain* **2013**, *154*, 2616–2625. [CrossRef] [PubMed]
41. Fox, A.; Gentry, C.; Patel, S.; Kesingland, A.; Bevan, S. Comparative activity of the anti-convulsants oxcarbazepine, carbamazepine, lamotrigine and gabapentin in a model of neuropathic pain in the rat and guinea-pig. *Pain* **2003**, *105*, 355–362. [CrossRef]
42. Chincholkar, M. Analgesic mechanisms of gabapentinoids and effects in experimental pain models: A narrative review. *Br. J. Anaesth.* **2018**, *120*, 1315–1334. [CrossRef]
43. Kremer, M.; Yalcin, I.; Nexon, L.; Wurtz, X.; Ceredig, R.A.; Daniel, D.; Hawkes, R.A.; Salvat, E.; Barrot, M. The antiallodynic action of pregabalin in neuropathic pain is independent from the opioid system. *Mol. Pain* **2016**, *12*, 1744806916633477. [CrossRef]
44. Bender, G.; Florian, J.A.; Bramwell, S.; Field, M.J.; Tan, K.K.C.; Marshall, S.; DeJongh, J.; Bies, R.R.; Danhof, M. Pharmacokinetic–Pharmacodynamic Analysis of the Static Allodynia Response to Pregabalin and Sildenafil in a Rat Model of Neuropathic Pain. *Experiment* **2010**, *334*, 599–608. [CrossRef]
45. Ito, S.; Suto, T.; Saito, S.; Obata, H. Repeated Administration of Duloxetine Suppresses Neuropathic Pain by Accumulating Effects of Noradrenaline in the Spinal Cord. *Obstet. Anesth. Dig.* **2018**, *126*, 298–307. [CrossRef] [PubMed]
46. Tanenberg, R.J.; Irving, G.A.; Risser, R.C.; Ahl, J.; Robinson, M.J.; Skljarevski, V.; Malcolm, S.K. Duloxetine, Pregabalin, and Duloxetine Plus Gabapentin for Diabetic Peripheral Neuropathic Pain Management in Patients with Inadequate Pain Response to Gabapentin: An Open-Label, Randomized, Noninferiority Comparison. *Mayo Clin. Proc.* **2011**, *86*, 615–626. [CrossRef]
47. Lee, B.-S.; Jun, I.-G.; Kim, S.-H.; Park, J.Y. Intrathecal Gabapentin Increases Interleukin-10 Expression and Inhibits Pro-Inflammatory Cytokine in a Rat Model of Neuropathic Pain. *J. Korean Med. Sci.* **2013**, *28*, 308–314. [CrossRef] [PubMed]
48. Park, H.J.; Joo, H.S.; Chang, H.W.; Lee, J.Y.; Hong, S.H.; Lee, Y.; Moon, D.E. Attenuation of neuropathy-induced allodynia following intraplantar injection of pregabalin. *Can. J. Anaesth.* **2010**, *57*, 664–671. [CrossRef]
49. Freynhagen, R.; Strojek, K.; Griesing, T.; Whalen, E.; Balkenohl, M. Efficacy of pregabalin in neuropathic pain evaluated in a 12-week, randomised, double-blind, multicentre, placebo-controlled trial of flexible- and fixed-dose regimens. *Pain* **2005**, *115*, 254–263. [CrossRef]
50. Sabatowski, R.; Gálvez, R.; Cherry, D.A.; Jacquot, F.; Vincent, E.; Maisonobe, P.; Versavel, M. Pregabalin reduces pain and improves sleep and mood disturbances in patients with post-herpetic neuralgia: Results of a randomised, placebo-controlled clinical trial. *Pain* **2004**, *109*, 26–35. [CrossRef]
51. Mangaiarkkarasi, A.; Rameshkannan, S.; Meher Ali, R. Effect of gabapentin and pregabalin in rat model of taxol induced neuropathic pain. *J. Clin. Diagn. Res.* **2015**, *9*, FF11–FF14. [CrossRef] [PubMed]
52. Rahman, W.; Suzuki, R.; Webber, M.; Hunt, S.P.; Dickenson, A.H. Depletion of endogenous spinal 5-HT attenuates the behavioural hypersensitivity to mechanical and cooling stimuli induced by spinal nerve ligation. *Pain* **2006**, *123*, 264–274. [CrossRef]
53. Suzuki, R.; Rahman, W.; Hunt, S.P.; Dickenson, A.H. Descending facilitatory control of mechanically evoked responses is enhanced in deep dorsal horn neurones following peripheral nerve injury. *Brain Res.* **2004**, *1019*, 68–76. [CrossRef]
54. Bauer, C.S.; Nieto-Rostro, M.; Rahman, W.; Tran-Van-Minh, A.; Ferron, L.; Douglas, L.; Kadurin, I.; Ranjan, Y.S.; Fernandez-Alacid, L.; Millar, N.S.; et al. The increased trafficking of the calcium channel subunit α2δ-l to presynaptic terminals in neuropathic pain is inhibited by the α2δ ligand pregabalin. *J. Neurosci.* **2009**, *29*, 4076–4088. [CrossRef]

55. Dib-Hajj, S.D.; Fjell, J.; Cummins, T.R.; Zheng, Z.; Fried, K.; LaMotte, R.; Black, J.A.; Waxman, S.G. Plasticity of sodium channel expression in DRG neurons in the chronic constriction injury model of neuropathic pain. *Pain* **1999**, *83*, 591–600. [CrossRef]
56. Murai, N.; Sekizawa, T.; Gotoh, T.; Watabiki, T.; Takahashi, M.; Kakimoto, S.; Takahashi, Y.; Iino, M.; Nagakura, Y. Spontaneous and evoked pain-associated behaviors in a rat model of neuropathic pain respond differently to drugs with different mechanisms of action. *Pharmacol. Biochem. Behav.* **2016**, *141*, 10–17. [CrossRef] [PubMed]
57. Pancrazio, J.J.; Kamatchi, G.L.; Roscoe, A.K.; Lynch, C., III. Inhibition of Neuronal Na Channels by Antidepressant Drugs. *J. Pharmacol. Exp. Ther.* **1998**, *284*, 208–214. [PubMed]
58. Jo, S.; Bean, B.P. Sidedness of carbamazepine accessibility to voltage-gated sodium channels. *Mol. Pharmacol.* **2014**, *85*, 381–387. [CrossRef]
59. Sanchez-Larsen, A.; Sopelana, D.; Diaz-Maroto, I.; Perona-Moratalla, A.; Gracia-Gil, J.; García-Muñozguren, S.; Palazón-García, E.; Segura, T. Assessment of efficacy and safety of eslicarbazepine acetate for the treatment of trigeminal neuralgia. *Eur. J. Pain* **2018**, *22*, 1080–1087. [CrossRef] [PubMed]
60. Chogtu, B.; Dhar, S.; Himabindu, P.; Bairy, K. Comparing the efficacy of carbamazepine, gabapentin and lamotrigine in chronic constriction injury model of neuropathic pain in rats. *Int. J. Nutr. Pharmacol. Neurol. Dis.* **2013**, *3*, 34. [CrossRef]
61. Al-Mahmood, S.M.A.; Abdullah, S.T.B.C.; Ahmad, N.N.F.N.; Bin Mohamed, A.H.; Razak, T.A. Analgesic synergism of gabapentin and carbamazepine in rat model of diabetic neuropathic pain. *Trop. J. Pharm. Res.* **2016**, *15*, 1191. [CrossRef]
62. Magnus, L. Nonepileptic uses of gabapentin. *Epilepsia* **1999**, *40* (Suppl. 6), S66–S72. [CrossRef]
63. Obermann, M.; Yoon, M.S.; Sensen, K.; Maschke, M.; Diener, H.; Katsarava, Z. Efficacy of Pregabalin in the Treatment of Trigeminal Neuralgia. *Cephalalgia* **2007**, *28*, 174–181. [CrossRef]
64. Taylor, J.C.; Brauer, S.; Espir, M.L.E. Long-term treatment of trigeminal neuralgia with carbamazepine. *Postgrad. Med. J.* **1981**, *57*, 16–18. [CrossRef] [PubMed]
65. Taheri, A.; Marani, S.F.; Khoshbin, M.; Beygi, M. A retrospective review of efficacy of combination therapy with pregabalin and carbamazepine versus pregabalin and amitriptyline in treatment of trigeminal neuralgia. *Anaesth. Pain Intensive Care* **2019**, *19*, 8–12.
66. Prisco, L.; Ganau, M.; Bigotto, F.; Zornada, F. Trigeminal neuralgia: Successful antiepileptic drug combination therapy in three refractory cases. *Drug Health Patient Saf.* **2011**, *3*, 43–45. [CrossRef]
67. Gooch, C.; Podwall, D. The diabetic neuropathies. *Neurologist* **2004**, *10*, 311–322. [CrossRef]
68. D'Mello, R.; Dickenson, A.H. Spinal cord mechanisms of pain. *Br. J. Anaesth.* **2008**, *101*, 8–16. [CrossRef] [PubMed]
69. Chen, S.R.; Samoriski, G.; Pan, H.L. Antinociceptive effects of chronic administration of uncompetitive NMDA receptor antagonists in a rat model of diabetic neuropathic pain. *Neuropharmacology* **2009**, *57*, 121–126. [CrossRef] [PubMed]
70. Chaplan, S.R.; Malmberg, A.B.; Yaksh, T.L. Efficacy of Spinal NMDA Receptor Antagonism in Formalin Hyperalgesia and Nerve Injury Evoked Allodynia in the Rat. *J. Pharmacol. Exp. Ther.* **1997**, *280*, 829–838.
71. Eisenberg, E.; Lacross, S.; Strassman, A.M. The clinically tested N-methyl-D-aspartate receptor antagonist memantine blocks and reverses thermal hyperalgesia in a rat model of painful mono-neuropathy. *Neurosci. Lett.* **1995**, *187*, 17–20. [CrossRef]
72. Mao, J.; Price, D.D.; Hayes, R.L.; Lu, J.; Mayer, D.J.; Frenk, H. Intrathecal treatment with dextrorphan or ketamine potently reduces pain-related behaviors in a rat model of peripheral mononeuropathy. *Brain Res.* **1993**, *605*, 164–168. [CrossRef]
73. Suzuki, R.; Matthews, E.A.; Dickenson, A.H. Comparison of the Effects of MK-801, Ketamine and Memantine on Responses of Spinal Dorsal Horn Neurones in a Rat Model of Mononeuropathy [Internet]. Available online: www.elsevier.nl/locate/pain (accessed on 1 March 2001).
74. Richter, R.W.; Portenoy, R.; Sharma, U.; Lamoreaux, L.; Bockbrader, H.; Knapp, L.E. Relief of painful diabetic peripheral neuropathy with pregabalin: A randomized, placebo-controlled trial. *J. Pain* **2005**, *6*, 253–260. [CrossRef]
75. Lesser, H.; Sharma, U.; LaMoreaux, L.; Poole, R.M. Pregabalin relieves symptoms of painful diabetic neuropathy: A randomized controlled trial. *Neurology* **2004**, *63*, 2104–2110. [CrossRef] [PubMed]
76. Li, J.; Chen, X.; Lu, X.; Zhang, C.; Shi, Q.; Feng, L. Pregabalin treatment of peripheral nerve damage in a murine diabetic peripheral neuropathy model. *Acta Endocrinol.* **2018**, *14*, 294–299. [CrossRef] [PubMed]
77. Balogh, M.; Varga, B.K.; Karádi, D.; Riba, P.; Puskár, Z.; Kozsurek, M.; Al-Khrasani, M.; Király, K. Similarity and dissimilarity in antinociceptive effects of dipeptidyl-peptidase 4 inhibitors, Diprotin A and vildagliptin in rat inflammatory pain models following spinal administration. *Brain Res. Bull.* **2019**, *147*, 78–85. [CrossRef] [PubMed]
78. Hanlon, K.E.; Vanderah, T.W. Constitutive Activity at the Cannabinoid CB1 Receptor and Behavioral Responses. *Methods Enzym.* **2010**, *484*, 3–30.
79. Zádor, F.; Balogh, M.; Váradi, A.; Zádori, Z.S.; Király, K.; Szűcs, E.; Varga, B.; Lázár, B.; Hosztafi, S.; Riba, P.; et al. 14-O-Methylmorphine: A Novel Selective Mu-Opioid Receptor Agonist with High Efficacy and Affinity. *Eur. J. Pharmacol.* **2017**, *814*, 264–273. [CrossRef] [PubMed]
80. Courteix, C.; Bardin, M.; Chantelauze, C.; Lavarenne, J.; Eschalier, A. Study of the sensitivity of the diabetes-induced pain model in rats to a range of analgesics. *Pain* **1994**, *57*, 153–160. [CrossRef]
81. Rajaei, Z.; Hadjzadeh, M.-A.; Nemati, H.; Hosseini, M.; Ahmadi, M.; Shafiee, S. Antihyperglycemic and Antioxidant Activity of Crocin in Streptozotocin-Induced Diabetic Rats. *J. Med. Food* **2013**, *16*, 206–210. [CrossRef] [PubMed]
82. Courteix, C.; Eschalier, A.; Lavarenne, J. Streptozocin-induced diabetic rats: Behavioural evidence for a model of chronic pain. *Pain* **1993**, *53*, 81–88. [CrossRef] [PubMed]

83. Jakó, T.; Szabó, E.; Tábi, T.; Zachar, G.; Csillag, A.; Szökő, E. Chiral analysis of amino acid neurotransmitters and neuromodulators in mouse brain by CE-LIF. *Electrophoresis* **2014**, *35*, 2870–2876. [CrossRef]
84. Modi, J.; Prentice, H.; Wu, J.-Y. Preparation, Stimulation and Other Uses of Adult Rat Brain Synaptosomes. *Bio-Protocol* **2017**, *7*, e2664. [CrossRef]